PNL-5750 Pt. 3
UC-11

17

Pacific Northwest Laboratory Annual Report for 1985 to the DOE Office of Energy Research

Part 3 Atmospheric Sciences
February 1986

Prepared for the U.S. Department of Energy
under Contract DE-AC06-76RLO 1830

Pacific Northwest Laboratory
Operated for the U.S. Department of Energy
by Battelle Memorial Institute

Battelle

DISCLAIMER

PACIFIC NORTHWEST LABORATORY
operated by
BATTELLE
for the
UNITED STATES DEPARTMENT OF ENERGY
under Contract DE-AC06-76RLO 1830

Printed in the United States of America
Available from
National Technical Information Service
United States Department of Commerce
5285 Port Royal Road
Springfield, Virginia 22161

NTIS Price Codes
Microfiche A01

Printed Copy

Pages	Price Codes
001-025	A02
026-050	A03
051-075	A04
076-100	A05
101-125	A06
126-150	A07
151-175	A08
176-200	A09
201-225	A010
226-250	A011
251-275	A012
276-300	A013

PNL-5750 PT 3
UC-11

Pacific Northwest Laboratory Annual Report for 1985 to the DOE Office of Energy Research

Part 3 Atmospheric Sciences

C. E. Elderkin and Staff Members
of Pacific Northwest Laboratory

February 1986

Prepared for
the U.S. Department of Energy
under Contract DE-AC06-76RLO 1830

Pacific Northwest Laboratory
Richland, Washington 99352

PREFACE

This 1985 annual report from Pacific Northwest Laboratory (PNL) to the Department of Energy (DOE) describes research in environment, health, and safety conducted during fiscal year 1985. The report again consists of five parts, each in a separate volume.

The five parts of the report are oriented to particular segments of our program. Parts 1 to 4 report on research performed for the DOE Office of Health and Environmental Research in the Office of Energy Research. Part 5 reports progress on all research performed for the Assistant Secretary for Environment, Safety and Health. In some instances, the volumes report on research funded by other DOE components or by other governmental entities under interagency agreements. Each part consists of project reports authored by scientists from several PNL research departments, reflecting the multidisciplinary nature of the research effort.

The parts of the 1985 Annual Report are:

Part 1: Biomedical Sciences		
	Program Manager - J. F. Park	D. L. Felton, Report Coordinator and Editor
Part 2: Environmental Sciences		
	Program Manager - R. E. Wildung	R. E. Wildung, Report Coordinator C. M. Novich, Editor
Part 3: Atmospheric Sciences		
	Program Manager - C. E. Elderkin	C. E. Elderkin, Report Coordinator E. L. Owczarski, Editor
Part 4: Physical Sciences		
	Program Manager - L. H. Toburen	L. H. Toburen, Report Coordinator J. E. Danko, Editor
Part 5: Overview and Assessment		
	Program Manager - L. G. Faust	L. G. Faust, Report Coordinator R. W. Baalman, Editor

Activities of the scientists whose work is described in this annual report are broader in scope than the articles indicate. PNL staff have responded to numerous requests from DOE during the year for planning, for service on various task groups, and for special assistance.

Credit for this annual report goes to many scientists who performed the research and wrote the individual project reports, to the program managers who directed the research and coordinated the technical progress reports, to the editors who edited the individual project reports and assembled the five parts, and to Ray Baalman, editor in chief, who directed the total effort.

A highlight this past year was the appointment of a Scientific Advisory Committee. Honoring us by accepting our invitation to serve on the committee are:

Dr. Franklin I. Badgley	University of Washington
Dr. Leo K. Bustad	Washington State University
Dr. Franklin Hutchinson	Yale University
Dr. Albert W. Johnson	San Diego State University
Dr. J. Newell Stannard	University of Rochester University of California, San Diego

W. J. Bair, Manager
S. Marks, Associate Manager
Environment, Health and Safety
Research Program

Previous reports in this series:

Annual Report for

1951	W-25021, HW-25709
1952	HW-27814, HW-28636
1953	HW-30437, HW-30464
1954	HW-30306, HW-33128, HW-35905, HW-35917
1955	HW-39558, HW-41315, HW-41500
1956	HW-47500
1957	HW-53500
1958	HW-59500
1959	HW-63824, HW-65500
1960	HW-69500, HW-70050
1961	HW-72500, HW-73337
1962	HW-76000, HW-77609
1963	HW-80500, HW-81746
1964	BNWL-122
1965	BNWL-280; BNWL-235, Vol. 1-4; BNWL-361
1966	BNWL-480, Vol. 1; BNWL-481, Vol. 2, Pt. 1-4
1967	BNWL-714, Vol. 1; BNWL-715, Vol. 2, Pt. 1-4
1968	BNWL-1050, Vol. 1, Pt. 1-2; BNWL-1051, Vol. 2, Pt. 1-3
1969	BNWL-1306, Vol. 1, Pt. 1-2; BNWL-1307, Vol. 2, Pt. 1-3
1970	BNWL-1550, Vol. 1, Pt. 1-2; BNWL-1551, Vol. 2, Pt. 1-2
1971	BNWL-1650, Vol. 1, Pt. 1-2; BNWL-1651, Vol. 2, Pt. 1-2
1972	BNWL-1750, Vol. 1, Pt. 1-2; BNWL-1751, Vol. 2, Pt. 1-2
1973	BNWL-1850, Pt. 1-4
1974	BNWL-1950, Pt. 1-4
1975	BNWL-2000, Pt. 1-4
1976	BNWL-2100, Pt. 1-5
1977	PNL-2500, Pt. 1-5
1978	PNL-2850, Pt. 1-5
1979	PNL-3300, Pt. 1-5
1980	PNL-3700, Pt. 1-5
1981	PNL-4100, Pt. 1-5
1982	PNL-4600, Pt. 1-5
1983	PNL-5000, Pt. 1-5
1984	PNL-5500, Pt. 1-5

FOREWORD

The goals of atmospheric research at Pacific Northwest Laboratory (PNL) are to describe and predict the nature and fate of atmospheric contaminants and to develop an understanding of the atmospheric processes contributing to their distribution on local, regional, and continental scales. In 1985, this research has examined the transport and diffusion of atmospheric contaminants in areas of complex terrain, summarized the field studies and analyses of dry deposition and resuspension conducted in past years, and begun participation in a large, multilaboratory program to assess the precipitation scavenging processes important to the transformation and wet deposition of chemicals composing "acid rain."

The description of atmospheric research at PNL is organized in terms of the following study areas:

- Atmospheric Studies in Complex Terrain
- Dispersion, Deposition, and Resuspension of Atmospheric Contaminants
- Processing of Emissions by Clouds and Precipitation (PRECP).

Atmospheric Studies in Complex Terrain

Air pollution in mountainous regions is a particularly difficult problem because of the complexity of meteorological conditions over spatial scales ranging from individual valleys to systems of many valleys and ridges of a region, and the diurnal coupling/decoupling phenomena between air in individual valleys and the regional convective boundary layer. This study area has coordinated research activities in the areas of boundary layer meteorology, transport and dispersion of contaminated air parcels, and the transformation and removal of atmospheric contaminants in mountainous terrain settings. This coordination attempts to integrate theoretical analysis, model development, and the results of carefully designed field experiments. The improved understanding of transport and diffusion in complex terrain gained through this collaborative approach will allow the development of assessment models that can be applied with greatly improved reliability in the siting of energy-producing facilities in the western United States.

Dispersion, Deposition, and Resuspension of Atmospheric Contaminants

Dispersion, deposition, and resuspension processes are linked intimately with the dynamics of the boundary layer. The former two processes act to reduce air concentrations of gaseous and particulate material while the latter process acts to increase air concentrations of particulate material, particularly in the large particle size classes. In many energy development areas, all three processes are important in determining the effective residence times of potentially hazardous particles in the atmosphere. The activities in this study area in 1985 were focused on summarizing the results of past field studies and further development of mathematical modeling of the phenomena involved.

Processing of Emissions by Clouds and Precipitation (PRECP)

The PRECP program was a new undertaking for DOE in 1985. PRECP is a multilaboratory effort to improve understanding of the phenomena that are important in acid rain. Ultimately, understanding of these processes will contribute to the implementation of effective control strategies. Personnel at PNL are primarily responsible for advances in understanding of precipitation scavenging; activities in 1985 were principally in the conduct of two field studies–APRIL and PRESTORM. Data obtained from these experiments are now being analyzed and will be used to increase the realism of regional-scale "acid rain" numerical models being developed elsewhere as part of the National Acid Precipitation Assessment Program.

This report describes the progress in FY 1985 in each of these areas. A divider page summarizes the goals of each area and lists, as bulleted items, project titles that support research in each area.

CONTENTS

PREFACE iii
FOREWORD v
ATMOSPHERIC STUDIES IN COMPLEX TERRAIN
Atmospheric Diffusion in Complex Terrain
Airflow Visualization Using Oil Fog Photography in a Deep Canyon
M. M. Orgill and J. M.Thorp 3

Coupling/Decoupling of Synoptic and Valley Circulations
Processing of Meteorological and Surface Energy Budget Data from the 1984 ASCOT Experiment, *M. M. Orgill, K. J. Allwine, R. I. Schreck, and C. D. Whiteman.* . 7
Nocturnal Vertical Velocity Profiles in a Mountain Valley, *C. D. Whiteman* 9

Atmospheric Boundary Layer Studies
The Occurrence of Nocturnal Slope Flow During the 1980 Geysers Field Study, *T. W. Horst* 11
The Downslope Development of Slope Flow, *T. W. Horst and J. C. Doran* 13
Numerical Flow Simulations for Land-Water-Land Trajectories, *J. C. Doran* 15

DISPERSION, DEPOSITION AND RESUSPENSION OF ATMOSPHERIC CONTAMINANTS
Dry Deposition and Resuspension
Deposition Velocities of Uranine Particles to the Hanford Diffusion Grid, *G. A. Sehmel* 19
Dry Deposition: A Review of PNL Research, *W. R. Barchet* 24
Resuspension Research with Tracers at PNL, *G. A. Sehmel* 30

PROCESSING OF EMISSIONS BY CLOUDS AND PRECIPITATION
Processing of Emissions by Clouds and Precipitation
The PRECP Program: PNL's Contribution to the DOE's Multilaboratory Study of the Processing of Emissions by Clouds and Precipitation, *W. G. N. Slinn, et al.* 37
PNL's Contributions to the PRECP-I (APRIL) Field Studies, *K. M. Busness, M. T. Dana, W. E. Davis, W. G. N. Slinn, and J. M. Thorp* 44
PNL's Contributions to PRECP-II (PRE-STORM), *D. S. Daly, M. T. Dana, A. C. D. Leslie, C. G. Lindsey, and W. G. N. Slinn* 54
Analyses of Precipitation Chemistry Data from the MAP3S and APN Networks, *M. T. Dana and R. C. Easter* 64

PUBLICATIONS 71
PRESENTATIONS 73
AUTHOR INDEX 75
ORGANIZATION CHART 77
DISTRIBUTION Distr-1

Atmospheric Studies in Complex Terrain

ATMOSPHERIC STUDIES IN COMPLEX TERRAIN

- **Atmospheric Diffusion in Complex Terrain**
- **Coupling/Decoupling of Synoptic and Valley Circulations**
- **Atmospheric Boundary Layer Studies**

Major reserves of fossil fuels are located in regions of complex terrain. As the use of these fuels as an energy source increases, the emission of air contaminants, such as sulfur and nitrogen compounds, trace metals, and fugitive dust produced by the combustion, conversion, and extraction of these fuels, will increase also. The analysis of the fate of these pollutants is particularly difficult in mountainous terrain. However, the improved understanding of transport and diffusion in complex terrain gained through these studies will allow the development of environmental assessment models that can be applied with greatly improved reliability to the siting of energy- producing facilities in the western United States.

The atmospheric diffusion research activities at PNL in FY 1985 are related primarily to the multilaboratory Atmospheric Studies in Complex Terrain (ASCOT) program. Data from ASCOT field programs in the Geysers geothermal area in California and in the Brush Creek valley in western Colorado are being analyzed. The purpose of these analyses is to develop models accounting for the transport and dispersion of air contaminants under nocturnal meteorological conditions.

• Atmospheric Diffusion in Complex Terrain

Objectives of this study are:

To contribute to the development of multilaboratory long-range technical plans for studying the dispersion and transport of pollutants over complex landforms.

To collect and analyze field data as input and confirmation data for model prediction and for describing transport and diffusion phenomena in complex terrain.

To develop models of the transport and diffusion of pollutants over various complex terrain landforms during different phases of the diurnal cycle.

AIRFLOW VISUALIZATION USING OIL FOG PHOTOGRAPHY IN A DEEP CANYON

M. M. Orgill and J. M. Thorp

One task of the 1984 ASCOT field program was an airflow visualization experiment where an oil fog smoke tracer was used to document the behavior of drainage flows in Pack Canyon and Brush Creek valley in Colorado (Figure 1). The purpose of the experiments was threefold: 1) to determine visually how a nighttime drainage flow from a ridge enters into a tributary canyon and the main valley; 2) to study the flow interactions and resultant diffusion; and 3) to visualize the tributary mass flux contribution to the main valley drainage flow. Some preliminary results were presented by Orgill and Thorp in 1985.

The photographic data base has been catalogued and two photographic albums of the pictures have been organized. One of these albums has been sent to the Lawrence Livermore National Laboratory (LLNL) as part of the ASCOT data base. The photographic data base has been examined for characteristics of the nighttime flow patterns within Pack Canyon. A generally consistent smoke behavior pattern was observed with some variations dependent on the ambient wind over the valley, the drainage flow from the northern and southern gullies of Pack Canyon, and the main drainage flow in Brush Creek valley. The smoke behavior patterns were described in the article by Orgill and Thorp (1985).

The smoke behavior patterns are now being studied in relation to coincident meteorological measurements made by Argonne National Laboratory (ANL) and other groups. The ANL team had a tethered balloon system and a high-frequency minisodar. These systems were located 150 m down the slope from the juncture of the northern and southern gullies of Pack Canyon. The tethered balloon system made an ascent about every 90 min and collected temperature, humidity, and wind information up to 800 m or more. The minisodar, which measured the radial component of the wind, was usually pointed up or down the canyon at various elevation angles. An LLNL team operated wind and turbulence sensors on 6-m towers at three locations: two sites on the northwest-facing slope of Pack Canyon, and one site on a southwest-facing slope in Brush Creek valley near the Pack Canyon entrance.

The tethered balloon and minisodar data provided an opportunity to examine the complex meteorological conditions within Pack Canyon. Generally, a three-layered structure was observed, but large deviations took place within the lower layers on a time scale of abut 10 min. Figure 2 is an idealized schematic of the flow and temperature conditions observed in Pack Canyon. For most of the nights, a surface-based stable layer prevailed up to between 20 to 80 m above the ANL site. Temperature increased at about 6°C per 100 m. Above this layer the temperature profile was approximately isothermal. Although the temperature profiles did not vary greatly during the night, the wind speeds and directions were quite variable above the lower stable layer (20 to 80 m). The airflow in the lower stable layer was in the expected downslope direction approximately 50% of the time. Shallow slope winds and some of the ridge drainage winds probably contributed to the shallow surface drainage flow exiting Pack Canyon. Between 100 and 200 m, the variable winds in this region corresponded to

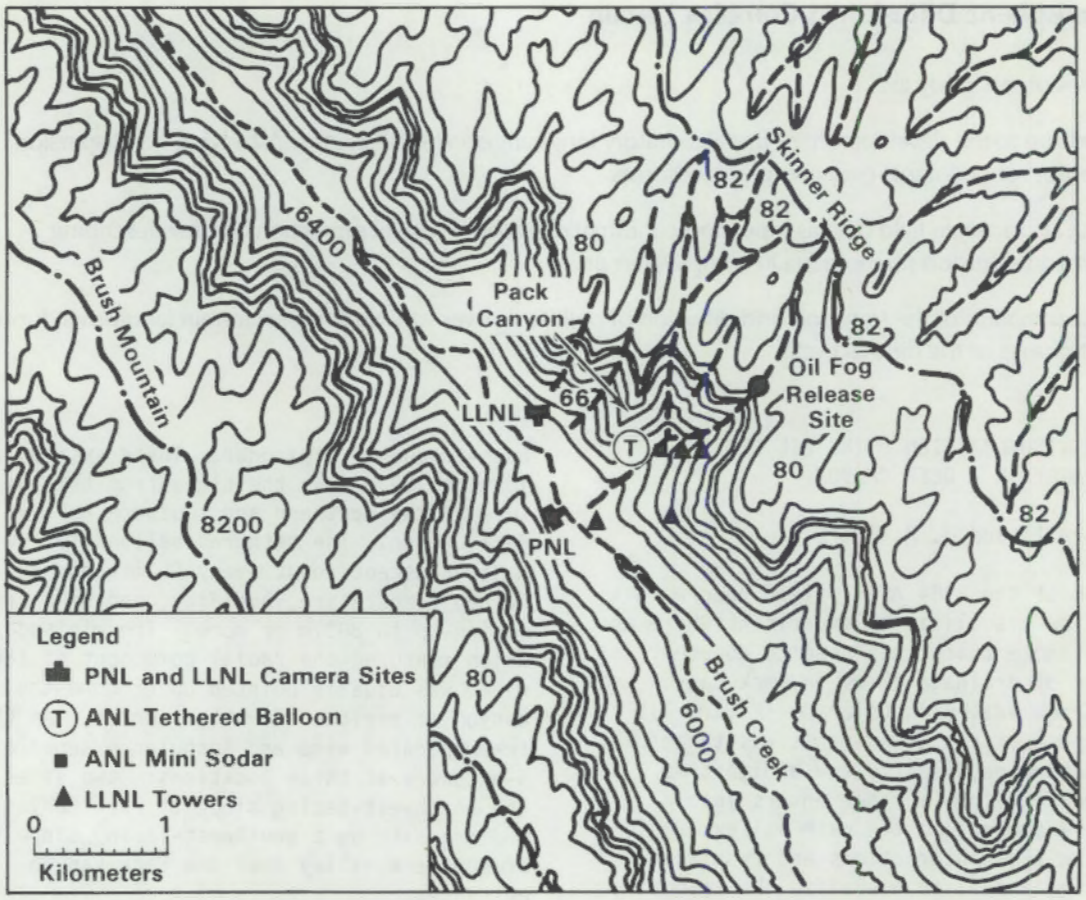

FIGURE 1. Topographic Map of Pack Canyon and Brush Creek Valley, Colorado.

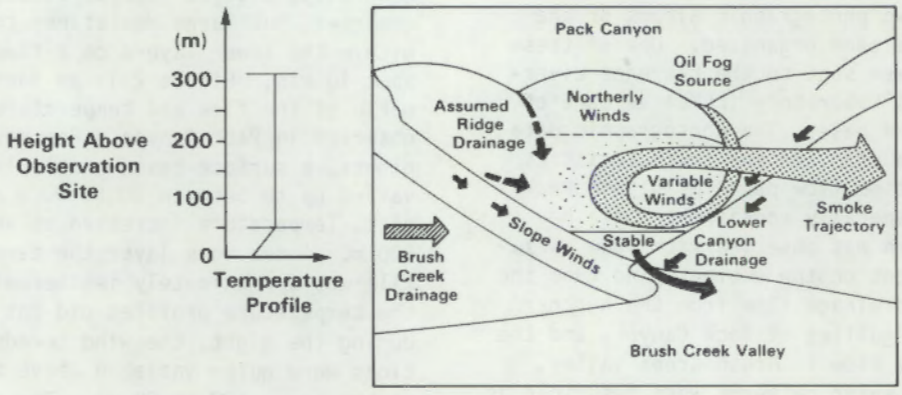

FIGURE 2. Schematic of Flow and Temperature Conditions Observed in Pack Canyon.

the region of the canyon where the smoke tracer began to diffuse rapidly after descending from the southern gully and cliff. After it diffused, the smoke was transported out of Pack Canyon as an elevated layer 90 to 300 m above the valley floor of Brush Creek.

The results of this smoke visualization study point to three conclusions: 1) the ridge drainage flow enters the canyon and the main valley at elevated levels; 2) interactions beween various drainage flows result in rapid diffusion of the smoke tracer; 3) the tributary mass flux contribution to the main valley drainage flow consists of a small lower-level mass flux and a larger higher-level mass flux (Orgill, Thorp and Coulter 1985).

Future work will be directed toward estimating the Pack Canyon mass flux and obtaining the perfluorocarbon tracer data and other meteorological data to continue further analysis of the Pack Canyon drainage and its interaction with the main drainage in Brush Creek valley.

References

Orgill, M. M., and J. M. Thorp. 1985. "Photography of Smoke Tracers in a Valley." In Pacific Northwest Laboratory Annual Report for 1984 to the DOE Office of Energy Research, Part 3, Atmospheric Sciences. PNL-5500 PT3, Pacific Northwest Laboratory, Richland, Washington.

Orgill, M. M., J. M. Thorp, and R. M. Coulter. 1985. "Interaction of Sub-Mesoscale Flows in Complex Terrain during Nocturnal Drainage Conditions." Paper presented at the 7th Symposium on Turbulence and Diffusion, November 12-15, 1985, Boulder, Colorado.

• Coupling/Decoupling of Synoptic and Valley Circulations

Objectives of this study are:

To conduct experiments to investigate and model mass and energy budgets that control the development and breakup of nocturnal valley circulations and their interactions with synoptic flow.

To develop simple predictive models for the coupling and decoupling of valley circulations from the overlying synoptic flows, and to use these models to produce improved environmental assessment models for complex terrain areas.

To provide scientific and technical support to the U.S. Department of Energy's Atmospheric Studies in Complex Terrain (ASCOT) program.

PROCESSING OF METEOROLOGICAL AND SURFACE ENERGY BUDGET DATA FROM THE 1984 ASCOT EXPERIMENT[a]

M. M. Orgill, K. J. Allwine, R. I. Schreck, and C. D. Whiteman

One activity in the 1984 ASCOT field program in Brush Creek valley in western Colorado was the installation and operation of five energy balance (Bowen ratio) stations. These stations were operated continuously for a period of 3 weeks with the assistance of Drs. Leo Fritschen and James Simpson of the University of Washington (UW). Measurements obtained from these stations will ultimately form the basis for calculating the energy budget of the valley atmosphere. A description of the instrumentation, the sites where the stations were installed, and a preliminary examination of radiation and energy balance data for one day, September 30, have been reported (Orgill and Whiteman 1985, Fritschen et al. 1985, and Simpson et al. 1985).[b] An extensive examination of the basic data was carried out in FY 1985.

The procedure used for examining and processing the basic data is shown in Figure 1. Program RAWCON was written in FORTRAN using

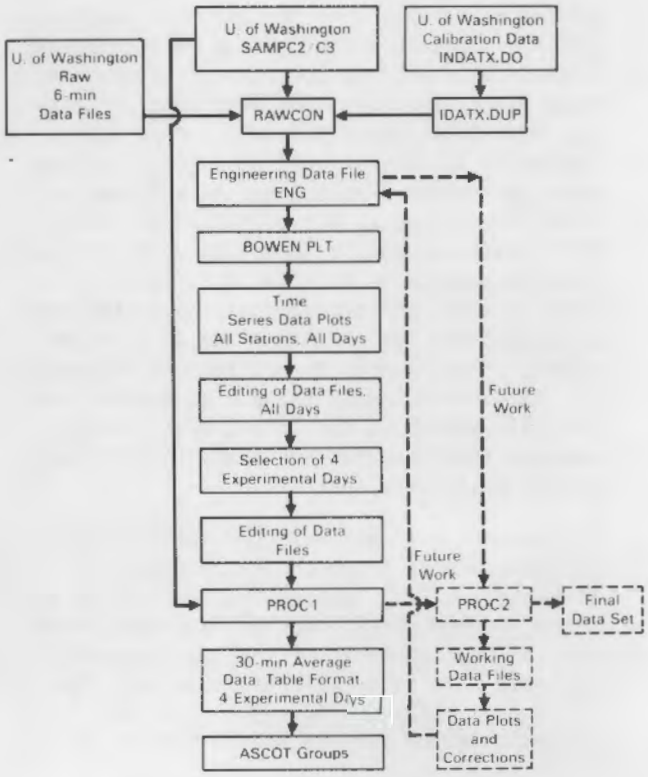

FIGURE 1. Data Processing Procedure for Obtaining Surface Energy Budget Data.

portions of the UW BASIC program SAMPC2. This program read the original 6-min-averaged raw data files, converted the data to engineering units using the appropriate calibration data files for each station, and developed an engineering units data file. Each input file contains data for one entire day at a single site. Program BOWENPLT was developed to read the output files from

(a) This work is a joint effort of the Atmospheric Diffusion in Complex Terrain and the Coupling/Decoupling of Synoptic and Valley Circulations programs.

(b) Whiteman, C. D., M. M. Orgill, K. J. Allwine, R. I. Schreck, L. J. Fritschen and J. R. Simpson. 1985. "Summary Data from PNL-UW Bowen Ratio Stations for Experiments 1, 3, 4, and 5: September-October, 1984." Letter data report distributed to ASCOT participants.

RAWCON and create time series plot files for 16 measured parameters. These plot files were plotted for the five Bowen ratio stations for the days September 16 through 30 and October 1 through 6. These time series plots were examined visually for data errors with the aid of field notes. A complete operational log was developed for the five stations that showed when operational problems were encountered, when data were missing, and when stations were operating properly.

The next step was to select four experimental days (days 1, 3, 4, and 5) and edit the data for all five stations for these days. The edited data files were processed by program PROC1 using portions of the UW BASIC program SAMPC3; this program computed 12 parameters, made 30-min averages, and organized the output data in a format suitable for printing. Tables of 30-min-averaged data for 12 parameters were then produced and distributed to other investigators who participated in the ASCOT multilaboratory experiment. Missing or suspicious data were marked by asterisks. Table 1 lists the experimental days that were processed and Table 2 lists the data parameters. These tables do not include estimates of the surface energy balance parameters such as soil, sensible, and latent heat fluxes, because this requires additional processing of the basic data set.

Future work will evaluate the soil, sensible, and latent heat fluxes. This work is in progress and will require the development of a new program (PROC2) to generate additional data files. Further editing and correction of these data files will be required. The final corrected data files will be used to investigate the surface energy balance of the Brush Creek valley and its effect on the meteorology of the valley.

TABLE 1. Experiments

Experiment No.	Period of Observations (Time MST/Date)
1	0000 9/19 - 2400 9/20
3	0000 9/25 - 2400 9/26
4	0000 9/27 - 2400 9/28
5	0000 9/29 - 2400 9/30

TABLE 2. Parameters in Data Tables

Qn	Net radiation (W/m^2)
Kdn	Downward solar radiation (W/m^2)
Kup	Reflected solar radiation (W/m^2)
Ldn	Downward longwave radiation (W/m^2)
Lup	Upward longwave radiation (W/m^2)
D	Diffuse radiation (W/m^2)
Gf	Soil hear flux from hear flow transducer at 10 cm, (W/m^2)
Tsoil	Average soil temperature in the 0- to 10-cm layer, (°C)
Ta	Air temperature at approximately 1-m height, (°C)
Tw	Wet bulb temperature at approximately 1-m height, (°C)
U	Wind speed at approximately 2 m (m/s)
Udir	Wind direction at approximately 2 m (deg. true)

References

Fritschen, L. J., J. R. Simpson, C. D. Whiteman, and M. M. Orgill. 1985. "Energy Balance Stations in a Deep Colorado Valley: ASCOT 84." In Proceedings, 17th Conference on Agriculture and Forest Meteorology, pp. 1-3. American Meteorological Society, Boston, Massachusetts.

Orgill, M. M., and C. D. Whiteman. 1985. "Surface Energy Budget Components over a Complex Terrain Area." In Pacific Northwest Laboratory Annual Report for 1984 to the DOE Office of Energy Research, Part 3, Atmospheric Sciences. PNL-5500 PT3, Pacific Northwest Laboratory, Richland, Washington.

Simpson, J. R., L. J. Fritschen, C. D. Whiteman, and M. M. Orgill. 1985. "Energy Balance in a Deep Colorado Valley: ASCOT 84." In Proceedings, 17th Conference on Agriculture and Forest Meteorology, pp. 8-11. American Meteorological Society, Boston, Massachusetts.

Whiteman, C. D., L. J. Fritschen, J. R. Simpson, and M. M. Orgill. 1985. "Radiation Balance in a Deep Colorado Valley: ASCOT 84." In Proceedings, 17th Conference on Agriculture and Forest Meteorology, pp. 4-7. American Meteorological Society, Boston, Massachusetts.

NOCTURNAL VERTICAL VELOCITY PROFILES IN A MOUNTAIN VALLEY

C. D. Whiteman

In the summer of 1982, the multilaboratory ASCOT program conducted a set of meteorological and atmospheric tracer studies in the Brush Creek valley of Colorado. A large number of wind soundings were made at hourly intervals in the 650-m-deep valley from a set of sites located at different points along the axis of the 25-km-long valley (Figure 1). Of particular interest were soundings taken during a 7-h period on the night of July 30-31, 1982, when winds in the valley had reached a near-steady state. These data allow, for the first time, the calculation of averaged nocturnal profiles of vertical velocity in a valley under conditions of steady-state mountain winds. The calculation of vertical velocities relates to a number of practical problems, including the prediction of air pollution transport and diffusion in deep valleys. In the following article, the method for making such calculations is summarized and results illustrated using data from three sites in the Brush Creek valley.

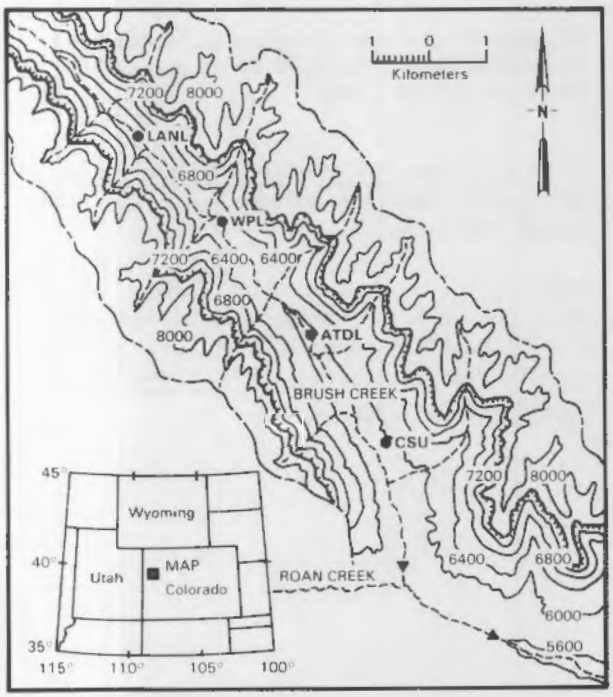

FIGURE 1. Topographic Map of the Lowest 10 km of Colorado's Brush Creek Valley Showing the Locations of Tethersonde Wind Profiling Sites (LANL, WPL, CSU, and ATDL). The boundaries of the watershed drainage are shown as a dash-dot line. A spiked line indicates the location of a line of cliffs making up the valley "rim." Contour interval = 400 ft.

Method

The method (Whiteman and Barr 1985) relies on the principle of conservation of mass applied to the mass of air within a valley. A balloon tethered at a site located at the middle of the valley floor measures the mean down-valley component of flow during a nighttime period of steady winds. The wind sounding is assumed to be representative of the valley's entire cross section, from sidewall to sidewall. Using this assumption, we can calculate the flux of air mass through the valley cross section as a function of height on the cross section. An estimate of the mean vertical velocity at any height can be made when wind observations are available from two or more cross sections. The basic principle involved is that when a larger flow of air goes through one cross section than goes through the adjacent cross section, additional air must enter the volume between the two cross sections. In a simply shaped valley without tributaries, this additional air must sink into the volume from above. The vertical velocity of this sinking air can be calculated from the equation

$$W_H = \frac{\Delta F_H}{\Delta X \, \Delta Y_H}$$

where W_H is the mean subsidence rate between two cross sections at a given height H, ΔX is the distance between the two cross sections, ΔY_H is the valley width at height H, and ΔF_H is the difference in mass flux between the two cross sections accumulated up to height H. The value ΔF_H is calculated using the formula:

$$\Delta F_H = \int_0^H \int_{Y_L(z)}^{Y_R(z)} \rho(z) \, [U_2(z) - U_1(z)] \, dy \, dz$$

where U_1 and U_2 are the down-valley components of wind speed at the two cross sections, ρ is air density, and Y_L and Y_R are the cross-valley coordinates of the left and right sidewalls of the valley.

Results

Observations in Colorado's Brush Creek valley show that vertical profiles of down-valley wind speed do not change significantly with down-valley distance (Whiteman and Barr 1984). However, because the valley widens appreciably, the atmospheric mass flux through cross sections increases with down-valley distance. This increase in mass flux requires that mass sink into the valley from above. If all the mass sinks into the valley from above, profiles of vertical velocity would resemble those shown in Figure 2. Maximum subsidence rates of 0.10 to 0.15 m/s occur at the level of the Brush Creek valley "rim"; the subsidence rates decrease to zero near the valley floor and decrease more rapidly above the valley rim.

Further Work

The calculated profiles of nocturnal vertical velocity have raised questions concerning the basic physics of valley flows, since sinking motions in the valley atmosphere strongly affect the energy and momentum budgets of a valley. These budgets tell us how energy is transferred in the valley atmosphere, thus affecting the development of valley wind systems and temperature inversion structure. These, in turn, strongly affect the transport and diffusion of pollutants released in the valley atmosphere. Further work will investigate the mass, thermal energy, and momentum budgets of the Brush Creek valley, using data from the 1982 and 1984 ASCOT experiments and numerical models.

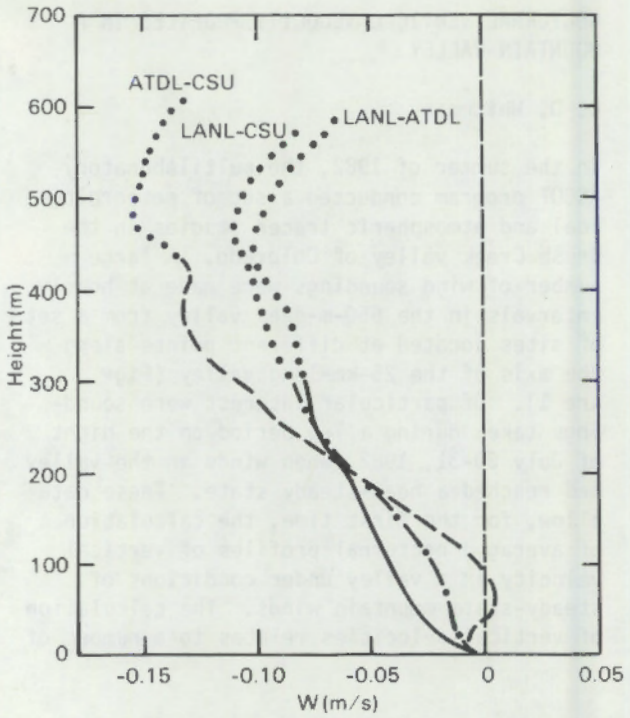

FIGURE 2. Vertical Velocity Profiles Calculated Between the Cross Sections Shown for the Period from 2200 to 0500 MST on July 30-31, 1982.

References

Whiteman, C. D., and S. Barr. 1984. "Atmospheric Mass Budget for a Deep, Narrow Valley in Colorado." In Conference Volume: Third Conference on Mountain Meteorology, pp. 61-64. American Meteorological Society, Boston, Massachusetts.

Whiteman, D. C., and S. Barr. 1985. "Atmospheric Mass Transport by Along-Valley Wind Systems in a Deep Valley." Paper accepted for publication by J. Climate and Applied Meteorology.

• Atmospheric Boundary Layer Studies

Objectives of this study are:

To determine experimentally the mean and turbulence characteristics of gravity controlled slope and valley flows.

To develop appropriate analytical, numerical, and graphical representations of the principal features of such flows.

To describe features of pollutant transport and diffusion in slope and valley winds.

To formulate and verify economical predictive models for these features.

THE OCCURRENCE OF NOCTURNAL SLOPE FLOW DURING THE 1980 GEYSERS FIELD STUDY

T. W. Horst

During the September 1980 ASCOT field study in the Geysers Geothermal Resource Area of northern California, PNL operated a micrometeorological profile tower, 60-m high, at a site known as Unit 19. This site was on the southeast slope of Cobb Mountain, 670 m below the summit and midway between Anderson and Gunning creeks. The surrounding topography is a broad bowl with several convergent drainage systems. During the period September 11 through 25, 1980, data were collected continuously from the Unit 19 tower, which was instrumented to measure winds and temperatures at 8 levels, a soil temperature profile, net radiation, and short wave radiation. On 7 of the 14 nights, these tower measurements were supplemented by regular tethered balloon ascents to measure ambient wind, temperature and humidity profiles to 500 m above the surface. One of the purposes of these measurements was to investigate the occurrence of nocturnal slope flow.

Nocturnal drainage winds begin when air adjacent to a sloped surface flows down the slope because it is cooled more, and is therefore denser than the free air at the same elevation. The best slope flows occur on calm nights with clear skies. Drainage winds cannot occur without cooling of the air near the slope, which is principally caused by radiational cooling of the surface and a resultant downward transport of heat from the adjacent air. The formation of a strong surface inversion, and development of well-defined downslope flow, is inhibited by either cloudy skies that reduce the radiational cooling of the surface or by a strong ambient wind that reduces the strength of the inversion by mixing the cooling over a much greater depth. Strong winds can also disrupt, or mask, the drainage by dominating the near-surface flow even in the presence of an apparently adequate inversion.

Periods of good slope flow are identified by the presence of the surface-based inversion and a well-defined maximum in the downslope wind component at a height of roughly one-half the depth of the inversion. Since the Geysers topography is not a simple tilted plane, the effective downslope direction was determined by the wind direction during cases of obviously good drainage. During good slope flow at Unit 19, the wind direction near the center of the katabatic layer was very steady and close to 325°, the azimuth of the summit of Cobb Mountain relative to Unit 19. Correspondingly, the wind direction shifted noticeably from the downslope direction when slope flow was disrupted.

Each hour of Unit 19 tower data from one hour after sunset until sunrise was classified as good, fair, or no drainage depending on the relationship of the wind direction near the center of the katabatic layer, ϕ, to the downslope direction. Good drainage was defined by $310° < \phi < 340°$ with a one-hour mean direction $\bar{\phi}$ close to 325°, and fair drainage had $290° < \phi < 360°$ with $310° < \bar{\phi} < 340°$. Out of 156 hours of nocturnal data, good drainage occurred almost one-fourth of the time, and about half of the time there was no drainage at all.

The occurrence of slope flow had the expected dependence on inversion strength (the temperature difference between the top of the inversion and the air at the surface) and ambient wind speed. All but one hour of good drainage and 76% of all drainage occurred when the strength of the surface-based inversion at the Unit 19 site was greater than 7°C, 89% of all drainage occurred with an inversion strength greater than 6°C, and no drainage occurred with an inversion strength less than 4°C. The dependence on ambient wind speed was investigated with ridge-top winds measured at Unit 13, 250 m above Unit 19. These winds were available for the entire ASCOT field study and were generally similar to (but in a few cases greater than) those obtained with the tethered balloon profile system at Unit 19. For example, 92% of the good drainage and 82% of all drainage occurred with winds at Unit 13 less than 5 m/s, all of the good drainage and 93% of all drainage occurred with winds less than 6 m/s, and no drainage occurred with winds above 7 m/s. There was little apparent correlation between ambient wind direction and the occurrence of slope flow.

The relative influence of inversion strength and ambient wind speed on the occurrence of slope flow was quantified by considering the momentum equation, integrated through the depth of the katabatic layer. Good slope flow occurs or does not occur, depending on whether the buoyancy deficit or the external horizontal pressure gradient is the dominant forcing term. The ratio of these two terms is a dimensionless number S

$$S = \frac{g}{\theta_o} \frac{\tan\alpha}{fUZ_i} \int_o^{Z_i} d \, dn$$

where

g = gravitational acceleration
θ_o = ambient potential temperature
α = slope angle
d = the temperature deficit near the slope, $\theta - \theta_o$
n = the coordinate normal to the slope
Z_i = the depth of the inversion
f = the Coriolis parameter
U = wind speed at Unit 13.

Here the external pressure gradient has been approximated by assuming that the wind at Unit 13 is in geostrophic balance. Figure 1 shows the observed dependence of slope flow occurrence at Unit 19 on S. Slope flow never occurred for S less than 9, while for S greater than 9 slope flow occurred 75% of the time and good slope flow occurred 37% of the time. Above S=33, slope flow always occurred and 91% of the time it was good slope flow. Above S=67, good slope flow always occurred.

These results need to be tested at other sites before they can be generalized. Further, it should be noted that S is diagnostic rather than prognostic, because of its dependence on the strength and depth of the surface inversion. Since the net radiation drives the surface cooling, a prognostic parameter might use that quantity to replace the inversion characteristics.

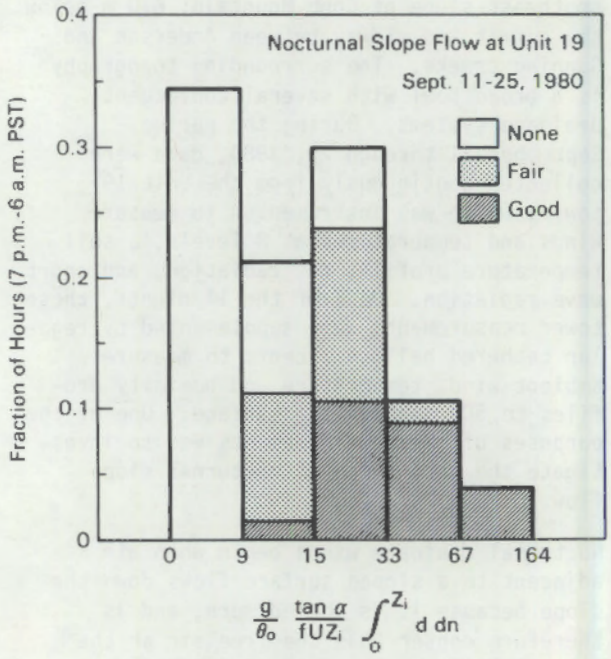

FIGURE 1. Dependence on S of slope flow occurrence at Unit 19.

THE DOWNSLOPE DEVELOPMENT OF SLOPE FLOW

T. W. Horst and J. C. Doran

Observations of nocturnal slope flow have been made at a site on Rattlesnake Mountain near Richland, Washington, that closely approximates a tilted plane. Rattlesnake Mountain is a ridge 15 km in length, and the measurement site is uniform for about 2 km in the cross-slope direction. The vegetation is 20- to 30-cm-high bunchgrass and scattered sagebrush with heights of 1 to 1.5 m. Temperature and wind profiles were measured from 3 towers that were located at vertical distances of 69, 151, and 229 m below the top of the ridge. Towers A and B were on a uniform slope of 21° extending from nearly the top of the ridge to a point 170 m below the top. Tower C was located below this change of slope, on a slope of about 8°. Four nights of good drainage flow data from the summers of 1980 and 1981 have been analyzed in detail (Horst and Doran 1982), and this data base was supplemented in 1983 with three additional nights of good data from Towers A and B.

Ellison and Turner (1959) showed that the depth of buoyancy-driven slope flow grows with downslope distance by entrainment of ambient fluid into the slope flow. The development of katabatic flow with distance down the slope is particularly evident from the wind and temperature profiles measured on Rattlesnake Mountain. In most cases of good slope flow, the inversion generally deepened with increasing downslope distance and the total buoyancy deficit (proportional to the area under the temperature profile, see Equation 3 below) increased monotonically with downslope distance. There was usually, but not always, an increase of the maximum downslope wind speed, the height of the wind maximum, and the total depth of downslope flow. Figure 1 gives an example of these features during the morning of July 3, 1981, when the ambient wind had both upslope and cross-slope components of 1-2 m/s.

Models that treat the katabatic flow as a single layer define integral scales by predicting vertically averaged properties such as

$$Uh = \int_0^H u \, dn \qquad (1)$$

and

$$U^2h = \int_0^H u^2 \, dn \qquad (2)$$

(Ellison and Turner 1959, Manins and Sawford 1979). Here u is the downslope component of the wind, n is the coordinate normal to the slope, and H is a height above the influence of the katabatic flow, where the ambient wind is assumed to be zero. Equations 1 and 2, then, define integral wind speed and height scales, U and h. Although the interpretation of the momentum depth, h, is often uncertain because the ambient wind is seldom light enough to neglect its contribution to the integrals, data for low ambient wind cases at both the Cobb Mountain and Rattlesnake Mountain sites suggest that the momentum depth is comparable to the depth of the surface inversion.

Doran and Horst (1983) proposed an alternate integral depth, h', that depends only on the temperature profile and is defined by

$$Dh' = \int_0^H d \, dn \qquad (3)$$

and

$$Dh'^2 = \int_0^H d \, n \, dn \qquad (4)$$

where D is an integral temperature deficit and in this case H is the height at which the temperature deficit, d, equals zero. These integrals are generally less ambiguous than Equations 1 and 2 because, unlike u, d is defined to be zero near the top of the katabatic layer. Observations suggest that h' is roughly one-fourth of the inversion depth.

Manins and Sawford's (1979) model of slope flow predicts that with neutral ambient stratification the integral depths h and h' will increase linearly with downslope distance, s, the integral temperature deficit D will decrease with the 1/3 power of s, and the integral wind speed scale, U, will increase with the 1/3 power of s. For small

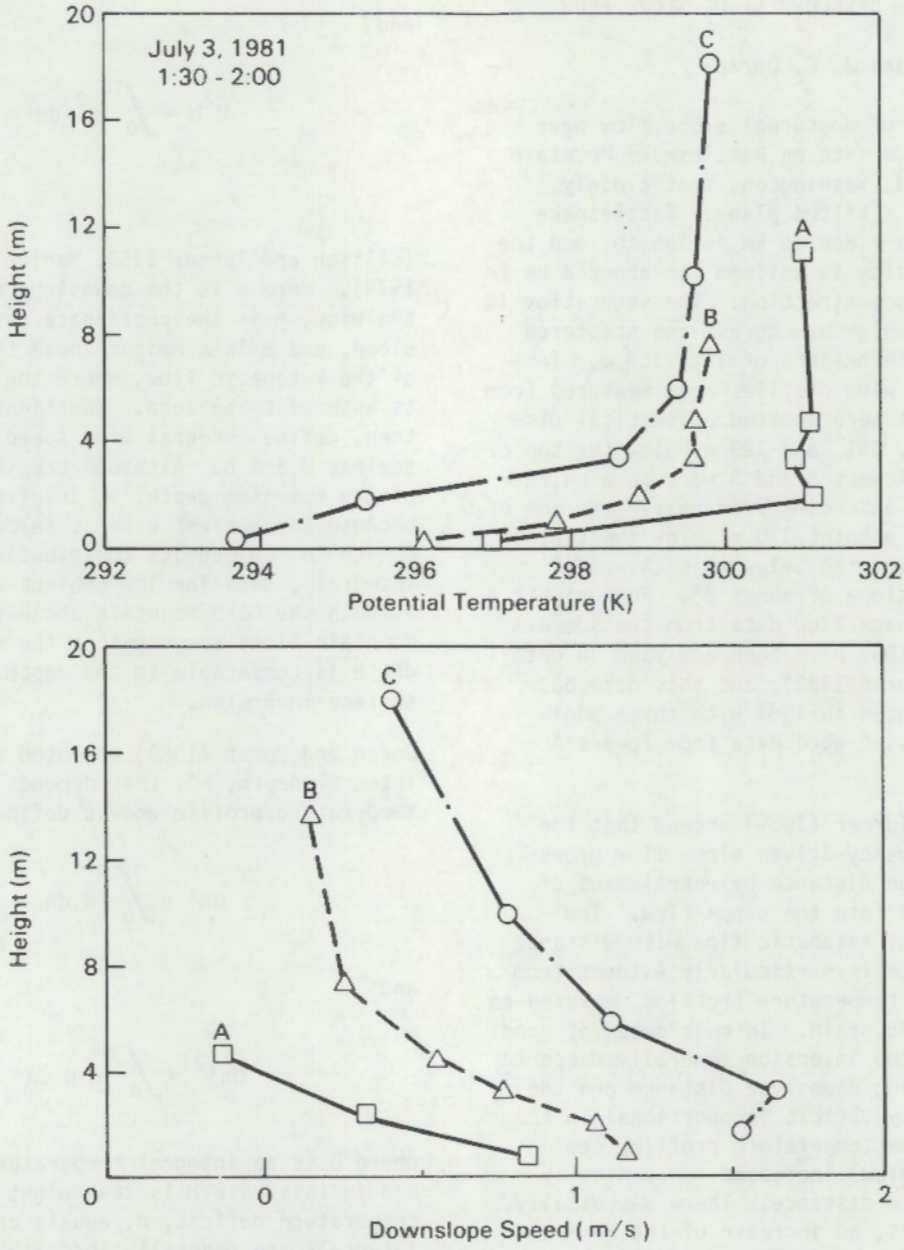

FIGURE 1. Wind and Temperature Profiles from Rattlesnake Mountain Towers A, B, and C, July 3, 1981: a) Temperature Profiles; b) Downslope Speed Profiles.

downslope distances, they predict that the development of slope flow with stable ambient stratification will be similar to that for neutral stratification. Beyond a scaling distance s_*, however, the depth will increase at a faster rate, the temperature deficit will decrease at a faster rate, and the wind speed will increase at a slower rate.

The rate of downslope development was determined for the constant slope portion of the Rattlesnake Mountain site, and the results are shown in the last column of Table 1.

The observed exponents are consistent with Manins and Sawford's (1979) model predictions

TABLE 1. Downslope Development of Slope Flow, ∂ in $X/\partial \ln s$

X	Manins and Sawford (1979) Neutral	Manins and Sawford (1979) Stable	Rattlesnake Mountain Towers A and B
h	1	1.08	0.97 (0.3 to 1.5)
h'	1	1.08	1.17 (0.6 to 1.9)
U	1/3	0.25	0.11 (-0.1 to 0.4)
D	-1/3	-0.62	-0.49 (-0.2 to -1.0)

for stable ambient stratification. For the Rattlesnake Mountain observations, 330 m is a minimum value for s_*, while the slope distances for Towers A and B are 190 and 420 m, respectively. Thus the growth to Tower A is expected to be that for neutral stratification, while that between Towers A and B is predicted to depart from the simple power laws. If we make the assumption that Tower B is located at $s = s_*$, Manins and Sawford's model predicts the values found in Table 1 for stable ambient stratification. These values are reasonably close to the observations. In particular, the predicted deviations from the power laws for neutral ambient stratification are of the same sign and magnitude as observed. This agreement supports the basic assumption of Manins and Sawford's model that slope flow wind and temperature profiles are self-similar.

References

Doran, J. C., and T. W. Horst. 1983. "Observations of Drainage Winds on a Simple Slope." In Proceedings of the Sixth AMS Symposium on Turbulence and Diffusion. American Meteorological Society, Boston, Massachusetts.

Ellison, T. H., and J. S. Turner. 1959. "Turbulent Entrainment in Stratified Flows." J. Fluid Mech. 6:423-448.

Horst, T. W., and J. C. Doran. 1982. Simple Nocturnal Slope Flow Data from the Rattlesnake Mountain Site. PNL-4406/ASCOT-82-5, Pacific Northwest Laboratory, Richland, Washington.

Manins, P. C., and B. L. Sawford. 1979. "A Model of Katabatic Winds." J. Atmos. Sci. 36:619-630.

NUMERICAL FLOW SIMULATIONS FOR LAND-WATER-LAND TRAJECTORIES[a]

J. C. Doran

In the spring of 1984, a cooperative Nordic mesoscale dispersion experiment was carried out across the Øresund, the sound between Denmark and Sweden. An extensive network of meteorological instrumentation was deployed to determine ambient wind and temperature fields, and SF_6 was used as a tracer for the dispersion. The data from that experiment are currently being processed and archived, and are expected to be available to the public sometime after the spring of 1986. The emphasis of the experiment was to study modifications of the wind and the diffusion of material crossing a water surface between two land masses of widely different roughness lengths. Tracer releases were carried out during the day, so that the sea surface temperature was generally colder than the land.

In the summer of 1985, the author visited the Risø National Laboratory at Roskilde, Denmark. As part of a model development program, one of the days of the Øresund experiment (June 5, 1984) was chosen for study, and numerical simulations were made of the wind and temperature fields for the time of the tracer release. The model used was a two-dimensional version of the Colorado State University Hydrostatic Mesoscale Model, developed by R. A. Pielke and his collaborators (McNider and Pielke 1984). The model has been extensively described in the literature; only slight modifications were required for these studies, e.g., a variable roughness length was assigned over Denmark, ranging from 80 cm over the Copenhagen region to 11 cm near Risø.

There have been several analytical studies of the modification of wind fields over discontinuities in roughness length, but these have been limited to neutral conditions. Moreover, the sea breeze problem has been studied extensively, and the thermal circulations responsible for these winds are well known.

(a) This work is a cooperative effort of the Boundary Layer, the Atmospheric Diffusion in Complex Terrain, and the Coupling/Decoupling of Synoptics and Valley Circulations programs.

However, in the June 5 case, the winds over the Øresund were relatively strong, and the classical sea breeze circulations were not observed because the thermal forcing was insufficient to overcome the ambient winds.

The numerical simulations revealed several interesting features. If the land surfaces are not heated and an essentially neutral temperature profile is maintained in the first few hundred meters above the surface, the results are consistent with expectations about the effects on the wind of changes in roughness length. Specifically, the winds in the first few hundred meters accelerate as they pass from Sweden over the Øresund, and decelerate as they subsequently pass over Denmark. The winds over Denmark are slower than those over Sweden because of larger surface roughness.

If the land surfaces are heated after sunrise, the situation becomes more complicated. An unstable layer now develops over the land, while a shallow stable layer forms over the water. Close to the surface, the winds passing over the water initially accelerate as they encounter the smoother surface. However, farther from shore the stable layer deepens and intensifies. The vertical transport of momentum from above is then insufficient to balance the frictional drag at the surface, and the winds decelerate as they continue over the Øresund. Above the shallow stable layer, this effect is much weaker and the deceleration is not as pronounced.

Preliminary comparisons with data suggest that this near-surface deceleration effect is, in fact, observed. Measurements were not made sufficiently close to the Swedish shore to reveal the initial acceleration, so corroborating evidence is not available for this area. A more detailed discussion of the results of the numerical simulation with observations must await the release of the data for general use. However, the utility of the model in situations such as that simulated was demonstrated, and additional insight has been provided for a situation in which the balance between two competing mechanisms, frictional drag from below and turbulent transport from above, varies with stability.

Reference

McNider, R. T., and R. A. Pielke. 1984. "Numerical Simulation of Slope and Mountain Flows." J. Clim. and Appl. Meteor. 23(10):1441-1453.

Dispersion, Deposition and Resuspension of Atmospheric Contaminants

DISPERSION, DEPOSITION, AND RESUSPENSION OF ATMOSPHERIC CONTAMINANTS

- **Dry Deposition and Resuspension**

The concentration of contaminant species in air is governed by the rate of imput from sources, the rate of dilution or dispersion as a result of atmospheric turbulence, and the rate of removal by wet and dry deposition. Once on the surface, contaminants also may be resuspended, depending on meteorological and surface conditions. An understanding of these processes is necessary for accurate prediction of exposures of hazardous or harmful contaminants to humans, animals, and crops.

At PNL, several research programs have focused attention on removal processes and resuspension for about 15 years. This year marked a time for summarizing the results of past studies with the purpose of identifying areas where further analysis is needed and completing analysis of research from previous years.

In the field, plume dispersion and plume depletion by dry deposition have been studied using tracers. A unique application of tracer technology at PNL has been the simultaneous release of depositing and nondepositing tracers. Dry deposition has been investigated for particles of both respirable and inhalable sizes. Resuspension has also been studied using tracers and contaminated surfaces and in a wind tunnel. The objective of the resuspension studies was to develop and verify models for predicting the airborne concentrations of contaminants over areas with surface contamination, develop resuspension rate predictors for downwind transport, and develop predictors for resuspension input to the food chain.

• Dry Deposition and Resuspension

Objectives of this study are:

To develop model predictors for dry deposition velocities as a function of pollutant and deposition surface properties and atmospheric variables.

To investigate dry deposition velocities in field and wind tunnel experiments using tracers (including multiple tracers) to obtain area-averaged dry deposition removal rates.

To develop model predictors for resuspension rates (and resulting airborne concentrations) of radionuclides and long-lived toxic chemical contaminants as a function of time, atmospheric and mechanical stresses, contaminant properties, and contaminated surface variables.

To investigate resuspension processes in field experiments using tracers and contaminated surfaces, including the investigation of long-time (weathering) effects on resuspension by evaluating airborne concentrations from aged radionuclide sources.

To investigate detailed resuspension processes by evaluating airborne concentrations in wind tunnel experiments.

DEPOSITION VELOCITIES OF URANINE PARTICLES TO THE HANFORD DIFFUSION GRID

G. A. Sehmel

Dry and wet deposition, processes that are active in the transport and removal of air pollutants, operate over different time and space scales. Although wet deposition can rapidly remove pollution, wet removal is intermittent in both space and time. Dry deposition may be of equal or greater importance for cleansing the atmosphere since dry deposition is continuous in both time and space; also, the fact that dry deposition reduces concentrations at respiration height is of great importance in estimating health effects. However, our ability to predict dry deposition is limited. Although dry deposition has been evaluated in many experiments, results have not been generalized for area-average deposition.

This article presents further development of results of dry deposition experiments conducted in 1984. The experiments were conducted at night using the Hanford diffusion grid for measuring area-averaged removal rates during moderately stable to near-neutral conditions. Two simultaneous experiments took place: in one, sponsored by the Environmental Protection Agency (EPA), and conducted by Doran and Horst (1985), the tracers were zinc sulfide (ZnS) and non-depositing sulfur hexafluoride (SF_6) gas; in the other, sponsored by the DOE, the particulate tracers uranine ($Na_2C_{20}H_{10}O_5$) and lithium carbonate (Li_2CO_3) were used. The objective of the study was to investigate dry deposition for tracer particles of nearly monodisperse diameters from tracer particle/gas ratios.

Experimental Conditions and Procedures

Experimental conditions described here are the vegetative canopy and tracer particle sizes; procedures for tracer release, tracer sampling, and sample analysis are also described. Meteorological data collected and analyzed by Doran and Horst (1985) were used in calculating deposition velocities.

Canopy

The deposition fetch was 3.2 km in length between the tracer release locations and the last sampling arc at 3200 m. The terrain was generally flat with a vegetative canopy consisting of desert grasses and 1- to 2-m high sagebrush.

Tracer Sizes

The emphasis in the DOE experiments was to determine effects of tracer particle diameter

on area-average dry deposition velocities. Since dry deposition velocities are a function of particle diameter, an essential constraint on tracer particle generation was that tracer particle diameter be reasonably monodisperse in particle size. The ideal geometric standard deviation for the monodispersed particles would be less than about 1.2. The further constraint of producing large quantities of tracer required considerable development in tracer generation technology.

The uranine and Li_2CO_3 tracer particles were released from water-alcohol solutions using two spinning disc generators. These generators were modified paint sprayers (Sehmel and Hodgson 1984) that were operated at rotation speeds of 17,500 and 38,000 rpm respectively for uranine and Li_2CO_3 tracers. After droplet generation, droplet size distributions were truncated by design in order to obtain more monodispersed size particles; that is, in generating the Li_2CO_3 particles, large droplets were removed by impaction onto a cylinder concentric with the particle generator, and in generating the uranine particles, small droplets were removed by using satellite removal air.

To determine the tracer size characteristics, tracers were generated in the inlet of a wind tunnel and were pulled slowly through the wind tunnel to allow time for evaporation before sampling. Size distributions for tracer particle diameters were evaluated with an optical particle counter that had fine discrimination as a function of particle diameter. Mass-median diameters and geometric standard deviations are estimated at the 50% cutoff diameter of the particle size distributions. It is emphasized that these are estimates since the size distributions were not log-normal. Also, mass-average particle diameters were calculated from mass concentration (mg/m^3) and the number concentration (m^{-3}).

Size characteristics for all three tracer particles are summarized in Table 1. As planned, the smallest tracer particles were Li_2CO_3, with a mass median diameter of 1.5 to 1.7 µm. The uranine tracer particles were larger, with a mass median diameter of 4.4 to 5.1 µm. The ZnS tracer particles were the largest, with a mass median diameter from 4.8 to 8.0 µm (Doran and Horst 1985). Although none of the tracer particles are monodispersed in size, there are significant differences in the size and geometric standard deviation of each tracer.

TABLE 1. Tracer Particle Size Characteristics for Assumed Log-Normal Mass Distributions

Tracer	Mass Average Diameter, µm	Mass Median Diameter, µm	Geometric Standard Deviation
Li_2CO_3	0.8 to 1.0	1.5 to 1.7	1.9 to 2.2
Uranine	1.4 to 2.6	4.4 to 5.1	1.7
ZnS		4.8 to 8.0	1.8 to 2.4

Tracer Release

Quantities of tracers released are shown in Table 2. The average quantities of particle tracer released were 0.11 g for lithium, 18 g for uranine, and 830 g for ZnS. Larger quantities are desirable for uranine and lithium tracers in order to reduce signal-to-noise ratios caused by uncertainties in backgrounds for filters.

All four tracers were released within a distance of 11 m with some lateral separation between release sites along a line oriented from north to south. The Li_2CO_3 tracer particles were released from the most northern release site. The separation between the Li_2CO_3 and uranine release sites was 2 m. The SF_6 tracer gas was released 8 m south of the uranine release site. The separation between the SF_6 and ZnS release sites was less than 1 m. The tracer release height was 2 m for ZnS and SF_6 releases. The uranine and Li_2CO_3 tracer particles were released at a height of 2.3 m the first night and 2.1 m the remaining experimental nights.

The visual appearances of the tracer plumes were different, and these differences affected the initial conditions for downwind transport and diffusion; that is, immediately after release, plume dispersion was controlled by the operating characteristics of tracer generators, rather than by meteorology. The maximum observed plume width for uranine tracer particles was about 0.3 to 0.6 m, and the plume could be seen for about

TABLE 2. Summary of Tracer Quantities Released

Release		Quantity of Tracer Released, g			
Date	Duration, min	Li_2CO_3 Tracer	Uranine Tracer	ZnS Tracer	SF_6 Tracer
May 18	30	0.104	17.16	1062	1633
May 26	30	0.132	17.25	842	1043
June 5	30	0.137	17.37	792	1293
June 12	30	0.112	17.30	840	1134
June 24	22	0.069	14.6	634	930
June 27	30	0.128	24.15	822	1087

6 m. The maximum observed plume width for Li_2CO_3 tracer particles appeared wider, about 1 to 1.3 m, and the plume could be seen for about 3 m.

Tracer Sampling

Tracer gas was sampled with sampling bags, and tracer particles were sampled with filters. Tracer particles were collected using open-faced membrane filters, 4.1 cm in diameter, exposed to the air. Anisokinetic sampling errors for these filters can be estimated (Sehmel 1967). The true concentrations are expected to be within 10% of the measured concentrations.

Tracers were collected downwind at a height of 1.5 m along five sampling arcs of approximately 90° sectors each. The arcs were at 100, 200, 800, 1600, and 3200 m downwind of the tracer release location. The sampling density for particles was much greater than it was for the SF_6 gas. The spacings between sample bags for SF_6 tracer gas were 8°, 4°, 4°, 2°, and 3°, respectively. The spacings between filter samples for particle tracers were 2° for the first three arcs, and 1° for the 1600- and 3200-m arcs.

In addition to these surface samples, tracers were sampled as a function of height at two locations. Samplers were mounted on towers at heights from 0.2 to 24.8 m at the 106° and 122° azimuths of the 1600 m arc.

Sample Analysis

Chemical analyses for uranine and Li_2CO_3 tracer particles were done after ZnS analyses were completed. Since both of these tracers are water soluble, they were removed from the filters by extraction with water: 7 ml of water were added to a vial containing a filter and the vial was vibrated for 1 hour. Most of the ZnS particles were removed by subsequent settling and decanting about 5 ml of the supernatant liquid into a centrifuge tube, centrifuging for 20 min, and using a syringe to withdraw about 4 ml of the clear liquid. Any ZnS particles remaining in suspension were removed by forcing the liquid in the syringe through a 5-μm glass-fiber prefilter and a 0.05-μm membrane filter. This liquid was analyzed fluorimetrically for uranine and by graphite-furnace atomic absorption for Li_2CO_3.

Dry Deposition Velocity Calculations

Deposition velocities were calculated using the surface depletion approach. Descriptions of the surface depletion approach, assumptions to describe the plumes before the first sampling arc, and exposure calculations follow.

Surface Depletion

The theoretical basis for calculating dry deposition velocities from surface depletion of an airborne plume of depositing and non-depositing tracers has been described by Horst (1977) and Doran and Horst (1985). Dry deposition velocities are calculated from crosswind integrated concentrations near ground level. The area-average dry deposition velocity is

$$\overline{v}_d = \frac{(Q_d/Q_o)_h \, \overline{C}^y_o(x,z_d,h) - \overline{C}^y_d(x,z_d,h)}{\int_0^x \overline{C}^y_d(x',z_d,h)\ (1/Q_o)\ \overline{C}^y_o(x-x',z_d,h=0)\ dx'} . \quad (1)$$

Equation 1 was tested with smaller downwind increments, until the deposition velocity was independent of smaller increments. Crosswind-integrated exposures (CWIE), rather than crosswind-integrated concentrations, are experimentally determined and used in Equation 1; CWIEs are required since sampling pumps were working before, during, and after the tracer plume passed a sampling site. Airborne exposures, E, are evaluated for both particle and SF_6 tracers; i.e.,

$$E = \int_0^t C \, dt \ . \qquad (2)$$

To evaluate the area-average dry deposition velocity, $\overline{v}_d$, from Equation 1, CWIEs are measured and estimated between sampling arcs as a function of downwind distance x. The CWIEs between arcs were represented by logarithmic interpolation between each sampling arc.

Assumptions Before First Arc

Several assumptions are made to describe the plumes for the 100-m distance between the release and the first sampling arc. Assumptions are the same as those used by Doran and Horst (1985). A Gaussian plume was assumed.

The significance of these assumptions depends on the magnitude of the deposition velocity and on how rapidly plume characteristics near the source are controlled by meteorological dispersion. Near the source, plume characteristics are controlled initially by the operating characteristics of the tracer release systems for each tracer. That is, tracer release systems can result in narrow or wide plumes before plume dispersion is controlled by meteorological dispersion. This initial dispersion is not described in the analysis; rather, meteorology-controlled dispersion is assumed for a point source at the release location.

Exposure Calculations

The CWIEs were calculated using linear interpolation between exposures at each azimuth. Conceptually, interpolation procedures are simple, but in practice assumptions are needed since some sampling pumps malfunctioned and filter backgrounds are variable. Some variability is caused by meandering of the tracer plume since the direction of the nocturnal drainage winds was not constant on some nights.

Source-strength normalized exposures, E/Q, have units of s/m^3. After a background of 14 ppt/v is subtracted for SF_6, the source-normalized exposure is calculated from the average SF_6 gas concentration in each sampling bag:

$$E/Q_0 = \overline{C} \, (t_2 - t_1)/Q, \qquad (3)$$

where $\overline{C}$ is the measured concentration in a sampling bag and $t_2 - t_1$ is the sampling time for filling the bag. For particles the exposure is calculated from the mass of tracer, M, on the filter:

$$M = \int_0^t e \, C \, F \, dt, \qquad (4)$$

where e is the isokinetic correction factor for nonisokinetic sampling and F is the sampling flow rate. After background is subtracted for particles, the source-normalized exposure is

$$E/Q_d = M/(e \, F \, Q) \ . \qquad (5)$$

Results

Area-average dry deposition velocities for uranine tracer particles are listed in Table 3 as a function of experiment date and sampling arc. The notation S/N means that uranine signal-to-noise from background filter samples may be too small for accurately calculating CWIEs.

Dry deposition velocities are reasonably consistent with distance for all arcs (i.e., differences by factors of unity, not orders of magnitude). This is important for checking the validity of assumptions. The assumptions required for calculating deposition velocities for the first 100 m are also utilized for calculating deposition velocities for the last 100 m.

Deposition velocities are calculated from airborne exposures. For a point source release, one expects CWIEs to be maximum for the SF_6 tracer gas. This is true for both the uranine and ZnS tracer particles, but not

TABLE 3. Area-Averaged Deposition Velocities for Uranine Tracer Particles

Arc (m)	Range of Deposition Velocities (cm/s) for Uranine Tracer Particles Dependent on Assumed Range of Uranine Concentrations for Filter Background					
	May 18	May 26	June 5	June 12	June 24	June 27
100	1.3	0.5 to 0.5	0.9 to 0.9	1.4 to 1.4	1.2 to 1.2	1.9 to 1.9
200	2.8	0.5 to 0.6	2.8 to 2.8	0.9 to 0.9	0.3 to 0.4	1.1 to 1.2
800	0.7	S/N 0.2 to 0.5	2.3 to 2.7	1.2 to 1.3	1.0 to 1.4	0.4 to 1.1
1600	4.3	S/N 1.7 to 2.1	S/N -0.6 to 0.1	1.0 to 1.3	0.6 to 1.7	S/N
3200	NA	S/N	NA	S/N 2.2 to 2.5	S/N	S/N
Summary:						
Range of V_d Not S/N	0.7 to 4.3	0.5 to 0.6	0.9 to 2.8	0.9 to 1.4	0.3 to 1.7	0.4 to 1.9

S/N = Uranine signal to noise concentrations from filter background samples may be too small for accurately calculating cross-wind integrated concentrations. Data analysis is continuing.
NA = Not applicable since filter samples were destroyed during analysis for ZnS concentrations.

true for the Li_2CO_3 tracer particles. Exposures for these smallest tracer particles exceeded exposures for SF_6 and remained large with increasing distance. The explanation may be in the different initial conditions for the tracer release for both particles and gas.

Conclusions

Experiments were conducted using Li_2CO_3 and uranine tracer particles released simultaneously with the ZnS tracer particles permitting the simultaneous investigation of dry deposition for three different particle diameters. The three mass-median tracer particle diameters are 1.5 to 1.7, 4.4 to 5.1, and 4.8 to 8.8 μm. Results could be analyzed further for effects of uncertainties in filter background and uncertainties introduced by inoperative sampling pumps.

However, data interpretation is complicated by unanticipated differences in exposures for the four tracers, including the nondepositing SF_6 tracer gas. Exposure results for both uranine and ZnS tracer particles support the concept that CWIEs for dry depositing particles are less than exposures for nondepositing SF_6 tracer gas. In contrast, however, at 100 m, CWIEs for Li_2CO_3 particles tended to be greater than for the nondepositing SF_6 tracer gas. It is believed that high exposures for Li_2CO_3 were caused by the different initial conditions for the tracer plumes at the tracer release sites.

Based on the data for this experiment, it is suggested that more emphasis be placed on tracer release characteristics in any future experiment. In future experiments, all tracers should be uniformly mixed while airborne within a holding chamber, and then co-released through a common tracer-release exit port or manifold.

References

Doran, J. C., and T. W. Horst. 1985. "An Evaluation of Gaussian Plume-Depletion Models with Dual-Tracer Field Measurements." Atmos. Environ. 19:939-951.

Horst, T. W. 1977. "A Surface Depletion Model for Deposition from a Gaussian Plume." Atmos. Environ. 11:41-46.

Sehmel, G. A. 1967. "Errors in the Subisokinetic Sampling of an Air Stream." Ann. Occup. Hyg. 10:73-78.

Sehmel, G. A., and W. H. Hodgson. 1984. "Generation of Nearly Monodispersed Particles for Dry Deposition Field Experiments." In Pacific Northwest Laboratory Annual Report for 1983 to the DOE Office of Energy Research: Part 3 - Atmospheric Sciences. PNL-5000-3, pp. 41-42, Pacific Northwest Laboratory, Richland, Washington.

DRY DEPOSITION: A REVIEW OF PNL RESEARCH

W. R. Barchet

Over the last 15 years PNL has conducted research on dry deposition in several areas. This year a summary of the research carried out at PNL on dry deposition was prepared for the DOE. This article is a capsule overview of that summary.

Dry deposition research at PNL was motivated by the potential health hazard posed by the release of radioactive materials from operations involving nuclear materials and by fallout from atmospheric nuclear weapons tests. Deposition and retention of radioactive particles in ducts, tubes, particle samplers and delivery lines, on surfaces in the open air, and on lung passageways needed to be quantified to properly assess the risk of human exposure to nuclear materials in the environment. The range of materials for which dry deposition was a concern gradually broadened to include gases and particles released by all energy production processes.

Research on dry deposition at PNL can be categorized into three broad areas: 1) laboratory studies, 2) theoretical and numerical modeling, and 3) field studies. The research program of the Dry Deposition and Resuspension project focused primarily on the laboratory and field experimental aspects of dry deposition, whereas other research programs dealt with the theoretical and numerical modeling aspects. This capsule summary emphasizes the laboratory and field experiment results on particle dry deposition velocities.

Wind Tunnel Studies

The starting point for the PNL dry deposition program was the work being done in the late 1960s and early 1970s on particle deposition in ducts and tubes. These studies were expanded to a single-pass, variable-speed, wind tunnel (see Figure 1) in which deposition to a variety of surfaces could be studied (Sehmel and Schwendiman 1970). The range of surface types and wind speeds studied in this tunnel over the period from 1960 to 1985 is shown in Table 1.

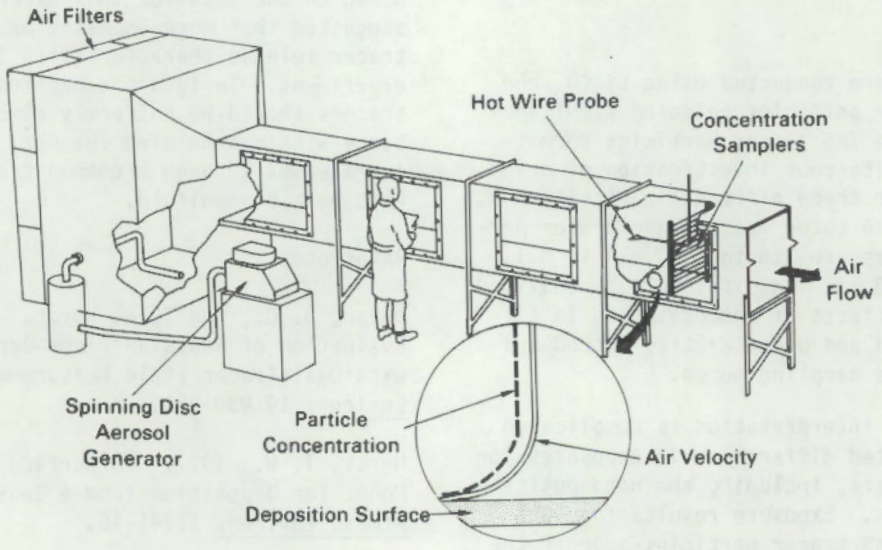

FIGURE 1. Diagram of the PNL Single Pass Wind Tunnel Used to Study Particle Dry Deposition (Sehmel, Hodgson, and Sutter 1974).

TABLE 1. Surface Types and Characteristics Used in the PNL Wind Tunnel

Surface Type	Characteristic Height or size cm	Range of Parameters in Experiments			
		u, m/s	u_*, cm/s	z_o, cm	d, cm
Brass shim	Smooth	2.2-13	11-73	0.004	
Plastic grass	0.7 tall	2.2-13	19-144	0.13-0.34	
Plastic trees[(a)]	7-9 tall	2.2-13			
Crushed gravel					
Clear chip	0.47-1.59 diam.	2.4-16.4	22-133	0.13-0.18	0.48-0.81
Railroad ballast	3.8-5.1 diam. 5 deep	1.6-17	15-107	0.3-0.6	
River rock	1.2-2.5 diam. ~4.8 deep	1-14	30-83	0.046-1.2	0-3.8
Water	2.5 waves 2.2 deep	2.2-13.8	11-122	0.002-0.1	

(a) Fetch inadequate to establish boundary layer, u_* and z_o not calculated.

Experiments conducted in this wind tunnel, largely using monodisperse uranine particles (Sehmel 1967), investigated the influence of surface roughness, wind speed, surface orientation (ceiling versus floor), and surface stickiness (clean, smooth brass versus petroleum-jelly-coated brass), on dry deposition. In order to examine the role of the surface in deposition, the laboratory results were expressed as a deposition velocity applicable to a height only 1 cm above the surface. This constraint makes the wind tunnel deposition velocities independent of large-scale vertical transport processes. The results of these experiments are shown in Figure 2 as a function of particle diameter. This figure illustrates the minimum in deposition velocity for particles in the 0.1- to 1-μm-diameter range expected from theory and the marked dependence of deposition on the characteristics of the surface. For instance, deposition velocities to plastic grass (squares) are two orders of magnitude greater than deposition velocities to water for submicrometer particles, but velocities are nearly equal for particles larger than 3 μm in diameter.

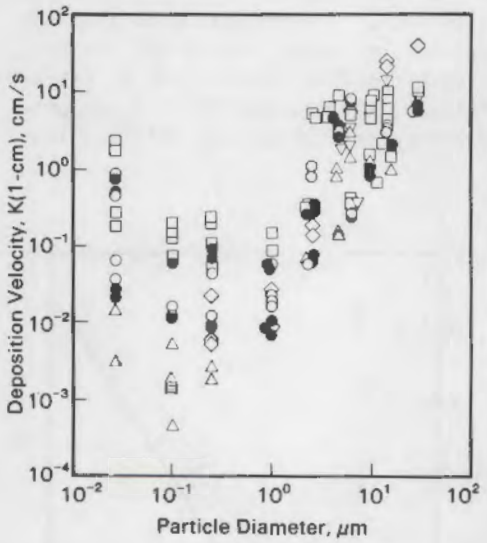

FIGURE 2. Deposition Velocities, K(1-cm), Measured in the Wind Tunnel for Uranine Particles. Symbols identify surface type: square = plastic grass, up-triangle = clean brass, down-triangle = coated brass, + = small gravel, x = crushed rock, and diamond = water. There are 275 points in the data base.

Deposition Velocity Modeling

An important component to the wind tunnel studies was the synthesis of the laboratory results into an empirical model of deposition velocities that could be scaled to natural conditions. Sehmel and Hodgson (1975, 1977, 1980) and Sehmel (1976, 1984) devised several models, based on the accumulated wind tunnel data, to enable other researchers to estimate

particle deposition velocities. The parameters used to scale the model are the dimensionless Schmidt and Stokes numbers along with the friction velocity, surface roughness length, and particle diameter. These parameters largely represent the atmospheric transport processes that bring the depositing particles to the surface. The dependence of the deposition velocity on particle diameter and surface roughness for the most recent model (Sehmel 1984) is shown in Figure 3 for a constant friction velocity of 30 cm/s. Figure 4 illustrates that although the model explains much of the variability of the deposition velocity and is, as such, a useful tool for predicting deposition velocities, the parameters of the regression are incapable of quantifying the influence of the unique features of the individual surfaces studied on particle deposition.

It is clear from the empirical modeling work that models of dry deposition must include parameters that represent the characteristics of the surface. Theoretical work by Slinn (1976, 1982) on canopy models has led to models that describe the surface in terms of filtration factors, canopy wind speed profiles, and canopy collection efficiencies.

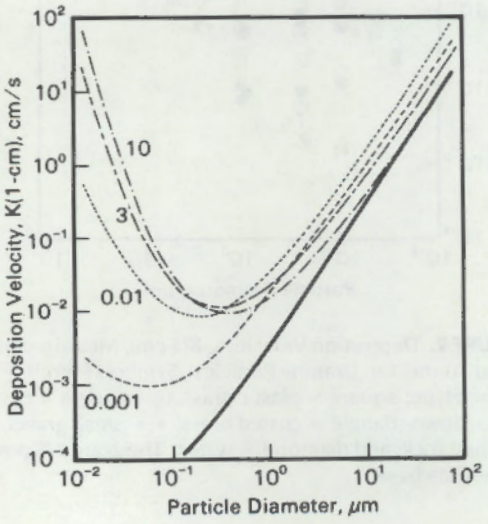

FIGURE 3. Dry Deposition Velocities at 1 cm Predicted by Model of Sehmel (1984) for $u_* = 30$ cm/s and a Particle Density of 1.0 g/cm^3; Surface Roughness (cm) is Shown as Parameter by Curve. Solid line is the gravitational settling speed.

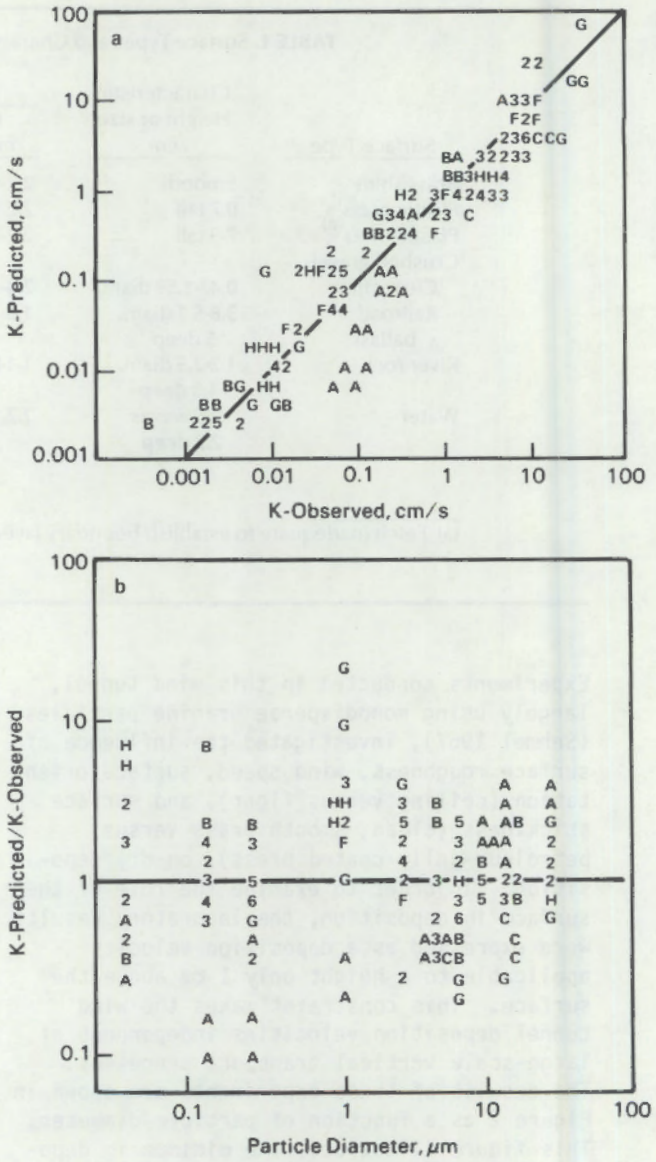

FIGURE 4. Deposition Velocities, K(1-cm), Predicted by Sehmel (1984) Empirical Model Compared to Observed Values (a) and the Ratio of Predicted to Observed Value (b) as a Function of Particle Diameter. Letters Denote Surface Type: A = Plastic Grass, B = Uncoated Brass, C = Coated Brass, F = Small Gravel, G = Water, H = Crushed Rock. Numbers indicate multiple points at same location. There are 275 points in the data base.

These parameters are difficult, if not impossible, to reliably determine for any particular canopy. Nevertheless, as shown in Figure 5, Slinn's (1982) model mimics the deposition data shown in Figure 2 quite

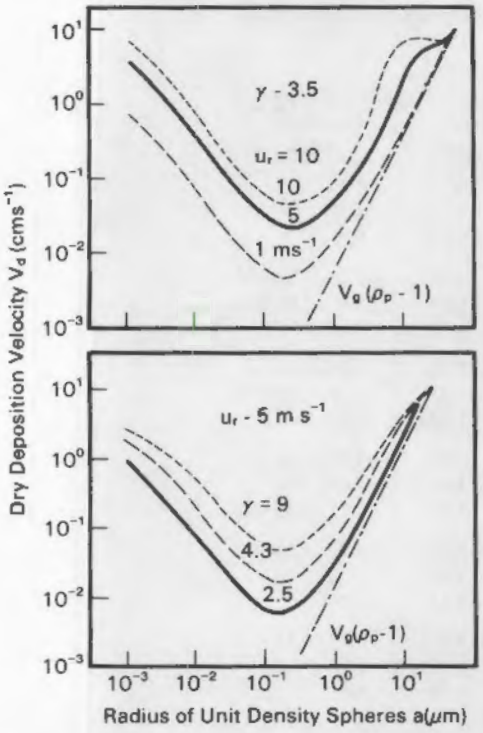

FIGURE 5. Deposition Velocity, V_d, Predicted by Canopy Model of Slinn (1982) as a Function of Particle Size and (a) Wind Speed and (b) Canopy Profile Parameter.

well. Unfortunately, little progress has been made in quantifying these parameters for natural canopies.

Field Studies

At the same time the wind tunnel studies of particle dry deposition were being carried out, field studies into plume dispersion and depletion were being conducted on the Hanford Site. A mass balance approach was often used to interpret these dispersion experiments and to determine the apparent depletion of the plume by dry deposition. However, Nickola and Clark (1975), after designing, conducting, and analyzing many such experiments, came to the conclusion that achieving a mass balance in any experiment was to a considerable extent fortuitous and that other approaches were needed to examine plume depletion. Nickola and Clark (1974) proposed measuring the dispersion of both a depositing tracer and a nondepositing tracer to determine plume depletion. As a result of their pioneering work, dual tracers became an accepted approach in the study of dry deposition.

However, early work with the dual-tracer approach yielded much the same information as the mass balance approach: a reliable measure of the fraction of material deposited out of the plume and only a poor (or no) estimate of the deposition velocity. This was because the near-surface concentration field of the depositing tracer was not adequately resolved. However, Doran and Horst (1985) applied the surface depletion concept used by Horst (1977) in his numerical plume depletion model to design a dual tracer experiment from which deposition velocities, averaged over the path of the plume, could be determined.

Table 2 summarizes the results of a joint Environmental Protection Agency (EPA) and DOE field study on the Hanford diffusion grid using SF_6 as the nondepositing tracer and ZnS, uranine, and lithium carbonate as depositing particulate tracers. Figure 6 shows the crosswind distribution of the tracers at various distances. A comparison of the observed deposition velocities to those predicted by the empirical model of Sehmel and Hodgson (1980) was made by integrating the model-predicted deposition velocity over three expected size distributions for particulate tracers. Figure 7 shows that observed and predicted results agree quite well for deposition velocities less than 2 cm/s. The higher deposition velocities were associated with higher wind speeds that may have accentuated the filtration effect of the sagebrush canopy. As discussed before, the empirical model parameters do not include characteristics of the canopy responsible for filtration. Hence, underprediction at higher deposition velocities is expected.

Conclusions

The Dry Deposition and Resuspension research program has, over 15 years, produced a significant data base on wind tunnel deposition velocities that can be used to formulate and test empirical and theoretical models of particle dry deposition. Field studies in this program and others have demonstrated the utility of the dual-tracer approach for

TABLE 2. Deposition Velocities for the ZnS and Uranine Aerosols in the Joint EPA[(a)]/DOE[(b)] Hanford Diffusion Grid Study

Date, YY/MM/DD	u_*, cm/s	L, m	Arc, m	Deposition Velocity ZnS, cm/s	Deposition Velocity Uranine, cm/s
83/5/18	40	166	800	4.21	0.74
			1600	4.05	4.27
			3200	3.65	NA
83/5/26	26	44	800	1.93	0.16 - 0.52 S/N
			1600	1.80	1.69 - 2.08 S/N
			3200	1.74	S/N
83/6/5	27	77	800	3.14	2.29 - 2.66
			1600	3.02	-0.6 - 0.11 S/N
			3200	2.84	NA
83/6/12	20	34	800	1.75	1.18 - 1.30
			1600	1.62	1.00 - 1.26
			3200	1.31	2.21 - 2.45 S/N
83/6/24	26	59	800	1.56	0.95 - 1.36
			1600	1.47	0.58 - 1.68
			3200	1.14	S/N
83/6/27	30	71	800	1.17	0.39 - 1.12
			1600	1.15	S/N
			3200	1.10	S/N

(a) Data for ZnS, u_*, and L from Doran and Horst (1985).
(b) Data for uranine from Sehmel (personal communication to Ballantine, 1985).
NA = No uranine analysis available.
S/N = Small uranine signal above background concentration on filters.

estimating deposition velocities in the field. Empirical and theoretical modeling studies have shown that canopy characteristics must be included in the models to yield reasonable predictions. However, our inability to characterize the canopy limits the usefulness of these models.

References

Doran, J. C., and T. W. Horst. 1985. "An Evaluation of Gaussian Plume-Depletion Models with Dual-Tracer Field Measurements." Atmos. Environ. 19(6):939-951.

Horst, T. W. 1977. "A Surface Depletion Model for Deposition from a Gaussian Plume." Atmos. Environ. 11:41-46.

Nickola, P. W., and G. H. Clark. 1974. "Measurement of Particulate Plume Depletion by Comparison with Inert Gas Plumes." In Pacific Northwest Laboratory Annual Report for 1973 to the USAEC Division of Biology and Medicine: Part 3 - Atmospheric Sciences. BNWL-1850 PT3, pp. 49-60, Pacific Northwest Laboratory, Richland, Washington.

Nickola, P. W., and G. H. Clark. 1975. "Prospects for Tracer Mass Balance Computations on a Dense Three-Dimensional Sampling Grid." In Pacific Northwest Laboratory Annual Report for 1974 to the USAEC Division of Biology and Medicine: Part 3 - Atmospheric Sciences. BNWL-1950 PT3, pp. 189-192, Pacific Northwest Laboratory, Richland, Washington.

Sehmel, G. A. 1967. "The Density of Uranine Particles Produced by a Spinning Disc Aerosol Generator." Amer. Ind. Hyg. Assoc. J. 28:491-492.

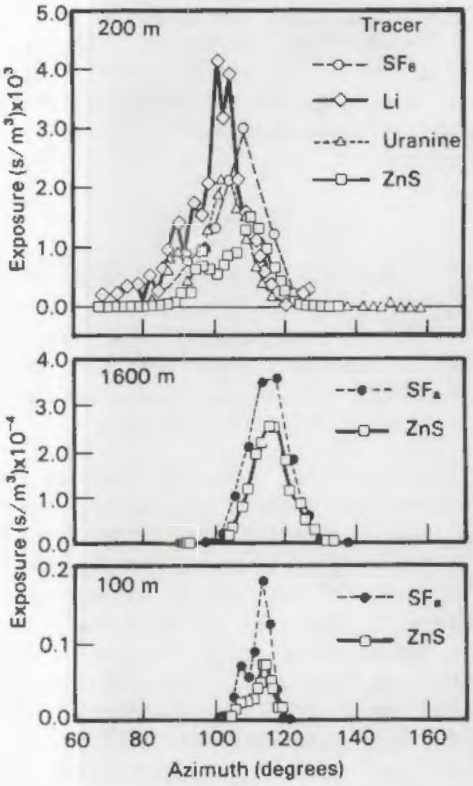

FIGURE 6. Crosswind Distributions of the Airborne Concentration of SF_6 and Three Depositing Tracers at Various Distances (Arcs) from the Release site. The 100-m arc data are from Sehmel (1985); data for the 200- and 1600-m arcs are from Doran and Horst (1985).

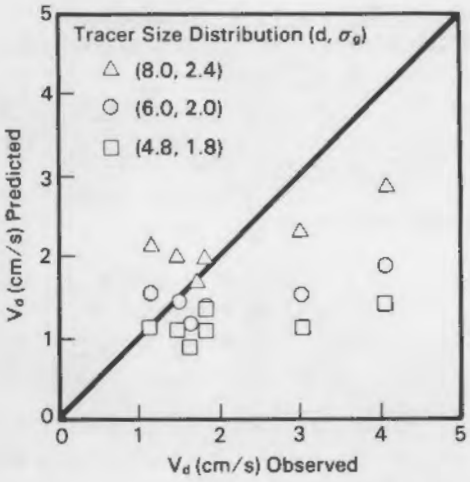

FIGURE 7. Effective Deposition Velocities for Three Possible Size Distributions of ZnS Aerosols Observed at the 1600-m Arc Compared to the Deposition Predicted from Sehmel and Hodgson's (1980) Empirical Model Adjusted to a 1.5-m Sampling Height (Doran and Horst 1985).

Sehmel, G. A. 1976. "Comparison of Deposition Velocities Predicted from Dimensionless Analysis Correlations." In Pacific Northwest Laboratory Annual Report for 1975 to the USERDA Division of Biomedical and Environmental Research: Part 3 - Atmospheric Sciences. BNWL-2000 PT3, pp. 83-85, Pacific Northwest Laboratory, Richland, Washington.

Sehmel, G. A. 1984. "Improved Predictions of Dry-Deposition Velocity of Particles." In Pacific Northwest Laboratory Annual Report for 1983 to the DOE Office of Energy Research: Part 3 - Atmospheric Sciences. PNL-5000 PT3, pp. 37-39, Pacific Northwest Laboratory, Richland, Washington.

Sehmel, G. A., and W. H. Hodgson. 1975. "Particle Dry Deposition Velocities." In Pacific Northwest Laboratory Annual Report for 1974 to the USAEC Division of Biology and Medicine: Part 3 - Atmospheric Sciences. BNWL-1950 PT3, pp. 175-180, Pacific Northwest Laboratory, Richland, Washington.

Sehmel, G. A., and W. H. Hodgson. 1977. "Improved Particle Deposition Model." In Pacific Northwest Laboratory Annual Report for 1976 to the USERDA Assistant Administrator for Environment and Safety: Part 3 - Atmospheric Sciences. BNWL-2100 PT3, pp. 61-65, Pacific Northwest Laboratory, Richland, Washington.

Sehmel, G. A., and W. H. Hodgson. 1980. "A Model for Predicting Dry Deposition of Particles and Gases to Environmental Surfaces." In Implications of the Clean Air Act Amendments of 1977 and Energy Considerations for Air Pollution Control. Amer. Inst. Chem. Eng. Symposium series no. 196, 76:218-230.

Sehmel, G. A., W. H. Hodgson and S. L. Sutter. 1974. "Dry Deposition of Particles." In Pacific Northwest Laboratory Annual Report for 1973 to the USAEC Division of Biomedical and Environmental Research, Volume II: Part 3 - Atmospheric Sciences. BNWL-1850 PT3, pp. 157-162, Pacific Northwest Laboratory, Richland, Washington.

Sehmel, G. A., and L. C. Schwendiman. 1970. "Wind Tunnel for Particle Deposition Measurements." In Pacific Northwest Laboratory Annual Report for 1969 to the USAEC Division of Biology and Medicine, Volume II: Part 1 - Atmospheric Sciences. BNWL-1307 PT1, pp. 122-125, Pacific Northwest Laboratory, Richland, Washington.

Sehmel, G. A., S. L. Sutter and M. T. Dana. 1973. "Dry Deposition Processes." In Pacific Northwest Laboratory Annual Report for 1972 to the USAEC Division of Biomedical and Environmental Research, Volume II: Part 1 - Atmospheric Sciences. BNWL-1751 PT1, pp. 43-49, Pacific Northwest Laboratory, Richland, Washington.

Slinn, W. G. N. 1976. "Modeling Preliminaries for Dry Deposition to a Canopy." In Pacific Northwest Laboratory Annual Report for 1975 to the USERDA Assistant Administrator for Environment and Safety: Part 3 - Atmospheric Sciences. BNWL-2000 PT3, pp. 65-68, Pacific Northwest Laboratory, Richland, Washington.

Slinn, W. G. N. 1982. "Predictions for Particle Deposition to Vegetative Canopies." Atmos. Environ. 16(7):1785-1794.

RESUSPENSION RESEARCH WITH TRACERS AT PNL

G. A. Sehmel

Resuspension occurs when wind blowing over a surface moves particles from that surface up into the air and transports them downwind. Resuspension is a concern in environmental assessments because it causes movement of previously deposited pollutants. This article summarizes tracer resuspension research conducted at PNL between 1971 and 1985. It identifies the factors involved in calculating resuspension, describes field experiments and their results, and recommends areas for further research and assumptions that should be implemented in environmental assessments.

Two factors that are of concern in estimating the impact of resuspension are the resuspension rate and the decrease of airborne contaminant concentration with time. Resuspension rates (fraction resuspended/unit time) are sources for atmospheric transport and diffusion models that describe the vertical flux of resuspended contaminant (amount/unit area/unit time). The resuspension rate, RR, is a ratio of the vertical resuspension flux to local surface-contamination source-strength:

$$RR = F/G$$

where F is vertical flux (in units of M^{-2}/time) and G is surface concentration (in units of M^{-2}). Resuspension rates have units of fraction resuspended per unit time (s^{-1}) and are dimensionally consistent with particle diffusion-deposition models.

Airborne contaminant concentrations may decrease with time above a resuspension source. This change in airborne concentration with time is reported in terms of the apparent time required for the average airborne concentration to reduce to one-half the original value: the airborne concentration half-life, or weathering half-life. The half-life may be one of the controlling parameters in environmental assessment evaluations. At the start of this research, the weathering half-life was considered to be approximately 35 days for the decrease of airborne radionuclide concentration after the Plumbbob test. In the Plumbbob study starting in May 1957, the 35-day half-life was determined for an air sampling time period of less than 5 months. However, more recent results near the Plumbbob location indicate a great uncertainty about these short half-lives. Starting in the summer of 1958, airborne concentrations were measured intermittently for durations of up to 15 months. In comparing results from these two Plumbbob site studies, no appreciable change was reported in airborne concentrations within the data scatter at a site 230 m from the original test location.

At the start of this research in 1971 there was only one data set for resuspension rates. Healy and Fuquay (1959) reported resuspension rates from 10^{-8} to 3.5×10^{-6} s^{-1} for time-integrated resuspension of ZnS particles from test surfaces at Hanford described as furrowed, snow fence, grass and rock. The surface was the only variable controlled. Resuspension rates were calculated using meteorological models and samples collected at one height.

To expand the science describing resuspension of surface contaminants, research was directed toward evaluating resuspension rates, wind speed dependencies, and weathering half-lives. Resuspension rates caused by winds, vehicles, and pedestrians were investigated in field experiments so that average resuspension rates could be determined over source and surface nonuniformities. The objectives of these tracer experiments were to determine:

1. wind-caused resuspension rates for respirable- and nonrespirable-sized particles

2. variation of resuspension rates between sites

3. tracer attachment as a function of aerodynamic particle diameter of the airborne host-soil particles upon which tracer is transported

4. weathering half-life changes with time over several years.

Wind Resuspension

Tracer sources were deposited on the ground at two study sites from a water suspension of calcium molybdate ($CaMoO_4$). Tracer sources were uniform in a circular area around a centrally located air sampling tower. Tracer areas were large: radii of each circular area were 22.9 m and 29.9 m. Airborne tracer was collected as a function of height on the towers. Samples were collected as a function of wind speed in cascade particle-impactor cowl systems.

Resuspension rates were measured with control of source strength. However, the source strength could not, and still cannot, be determined as a function of particle size after the surface was contaminated or treated. The source strengths and hence resuspension rates were assumed independent of tracer particle size.

Wind-caused resuspension rates for particles range from a lower limit of about 10^{-13} to an upper limit of about 10^{-6} fraction resuspended per second. The magnitude of these resuspension rates implies that contamination source-strengths on the ground do not change rapidly. Since there are 3.15×10^7 s/yr, only 3×10^{-4}% of the source would resuspend during an entire year at the lower resuspension rate limit. In contrast, the source would be depleted during a year for the upper resuspension rate limit. However, resuspension rates on the order of 10^{-6} fraction resuspended per second correspond only to high wind speeds; yearly average wind speeds and resuspension rates are much lower.

Resuspension Rates as a Function of Wind Speed

Experiments investigated resuspension rate dependencies for wind speed ranges and resuspension rate changes as a function of time. In general for the range of wind speeds investigated, resuspension rates increase as a power function of wind speed, $x(U - U_T)^n$, where the exponent n is greater than 3. However, the threshold wind speed (UT) was not identified. The coefficient x and exponent n are dependent on particle size, and confidence limits for both are needed.

At the first study site, resuspension rates were determined for a 4-year time period. Resuspension rates ranged from about 10^{-13} to 10^{-6} fraction resuspended per second. In general, resuspension rates increase with increasing wind speed.

Resuspension rates appear higher during the autumn than in the spring and summer. In general, resuspension rates for each wind speed range remained constant over a 3-year time period except for seasonal variations. However, the seasonal variation was not explicitly investigated since experimental time periods were determined in part by the frequency of high wind speeds without precipitation.

Surface contamination resuspends while attached to all airborne host-particle sizes. Dependencies of resuspension rates on particle size were investigated for 4 years. Tracer particles continued to resuspend as functions of particle size throughout the duration of the experiments.

For the second test site, resuspension rates ranged from about 10^{-12} to 10^{-7} fraction resuspended per second. For all airborne particle diameters, resuspension rates increased as power functions of wind speed, U^n, where the exponent n was greater than 3. Also, resuspension rates decreased with

time during 2 years. However, this time duration may have been too limited to show any seasonal variation as was shown for the first test site.

Different exponents can be obtained when examining resuspension rates as a function of either large or small wind speed increments. Resuspension rates increased with the 1.0 to 4.8 power of wind speed. Most of the data were obtained using the smaller wind speed increments. In this case, wind-caused resuspension rates increased with wind speed to about the 5th power.

Resuspension rates for nonrespirable particles are less than resuspension rates for respirable-size particles. Nonrespirable particle resuspension rates were nearly independent of time and were of the order of 10^{-11} fraction resuspended per second.

Conclusions for Wind-Caused Resuspension Rates

Resuspension rates were comparable for the sites investigated. Wind-caused resuspension rates increase, in general, with increasing wind speed. If a power function dependency is assumed (xU^n), resuspension rates increase with greater than the third power of wind speed. The exponent is greater than for soil erosion, an exponent of 3. This increase in the exponent above 3 reflects that respirable size particles resuspend more readily than larger soil particles. For respirable size particles an average exponent is about 5.

Seasonal variations in resuspension rates might have been caused in part by resuspension mechanisms which might include precipitation effects. Resuspension rates were maximum during the fall. This is the time period during which most rain occurs. Rain impact could loosen contaminant from the soil and splash contaminant onto vegetation. This process could cause the contaminant to be more available for resuspension during winds after vegetation surfaces have dried.

An important result from these experiments with controlled-source characteristics is that resuspension rates might not decrease with time. At the first study site, resuspension rates were nearly constant (except for seasonal variations) for over 3 years. These results stand in contrast to the often-reported results that airborne concentrations, after the Plumbbob nuclear test, decreased with a weathering half-life of 35 to 40 days. Further evidence that resuspension rates are nearly independent of time is the fact that airborne plutonium concentrations currently at nuclear locations are usually near fallout concentrations. If the 35- to 40-day half-life were valid, back calculation from current concentrations would predict relatively high airborne plutonium concentrations in earlier years. At least to the author's knowledge, such high concentrations were not measured in earlier years.

Although resuspension rates were expected to decrease in time, decreases were not consistently measured during the time scale of these tracer experiments. Since these are the only long-term controlled resuspension-source experiments, the author concludes from the existing data base that there is no experimental foundation for assuming a decreasing availability of surface contamination for resuspension.

Mechanical Resuspension

Mechanical resuspension was examined in a field study for vehicular traffic and for a walking pedestrian. Resuspension rates are reported as the fraction of particles resuspended each time a vehicle is driven along, or a pedestrian walks along, a contaminated lane (fraction resuspended per pass).

Vehicular Resuspension

Resuspension caused by traffic on one lane of an asphalt road can be significant. When a car is driven along a contaminated (tracer) lane at speeds up to 30 mph, resuspension rates increased from about 10^{-4} to 10^{-2} fraction resuspended per pass. The dependency of the square of car speed means that resuspension is proportional to car-generated turbulence. When the car is driven on the adjacent lane, resuspension rates were lower for each vehicle speed, and increased with vehicle speed from about 10^{-5} to 10^{-3} fraction resuspended per pass.

When a 3/4-ton truck was driven along the contaminated (tracer) lane at speeds up to 30 mph, resuspension rates increased from about 10^{-3} to 10^{-2} fraction resuspended per pass. Since resuspension rates were greater

than for car traffic, truck-generated turbulence appears to have been much greater than car-generated turbulence. For vehicle speeds above 20 mph, resuspension rates for car and truck passage are comparable. This similarity might be caused by tire surface-stress turbulence rather than by air turbulence.

Vehicle-caused resuspension from an asphalt road decreased with time. In this case, the contaminant (tracer) had been on the road for four days. Vehicle-generated resuspension rates increased from about 10^{-5} to about 10^{-3} fraction resuspended per pass as vehicle speed increased from 5 to 50 mph. Resuspension was greater when the vehicle was driven through the contaminated lane than when driven on the lane adjacent to the contaminated lane.

Resuspension by vehicular traffic from a vegetated area was also investigated. The fraction of particles resuspended from a road per vehicle pass ranged from 10^{-6} to 10^{-2}. Resuspension from the vegetated surface was less than from the asphalt road. The decreased resuspension from the cheat grass road is attributed to the protective action of cheat grass in hindering vehicle-generated turbulence from reaching the ground and resuspending contaminant.

Pedestrian-Caused Resuspension

Resuspension occurs when a person walks in a contaminated area. A 3-m-wide contaminated lane of an asphalt road was used. With wind speeds of 3 to 4 m/s, pedestrian-caused resuspension rates were from 1×10^{-5} to 7×10^{-4} fraction resuspended per pass along the contaminated lane. During these experiments wind resuspension was low, being only 5×10^{-9} to 6×10^{-8}/s for average wind speeds from 2 to 9 mph.

Time Dependency of Source Strengths

Water solubility of contaminants is an important parameter affecting resuspension source-concentration changes with time. Source-strength changes for a contaminant of low water solubility were investigated using $CaMoO_4$ as a tracer.

Resuspension rates calculated from low-solubility contaminant source-strength changes in 5-1/4 years show agreement with resuspension rates calculated from samples of airborne contaminant. The total source had depleted 39% in 5-1/4 years. This 39% depletion corresponds to an average resuspension rate of 3.7×10^{-9} fraction resuspended per second. This average resuspension rate is within the range of resuspension rates from about 10^{-13} to 10^{-6} fraction resuspended per second calculated from air samples.

Resuspension Research Needs

Resuspension experiments should include four scales: the laboratory bench, wind tunnels in a laboratory, wind tunnels in the field, and field experiments. Emphasis should be on experimental evaluation of parameters known or suspected of controlling resuspension and on gathering basic data to develop sub-models and to guide theoretical modeling. Although continued field research is important to develop models for aged sources and area sources, a balance is needed between field, wind tunnel, and laboratory experiments.

Field experiments should continue to use the experimental techniques developed in this program. Resuspension rates are evaluated using a sampling tower centrally located in a circular contamination-source of tracer. Airborne concentrations of contaminants and tracers should be investigated as a function of wind speed and aerodynamic particle diameter.

References

Healy, J. W., and J. J. Fuquay. 1959. "Wind Pickup of Radioactive Particles from the Ground." In Progress in Nuclear Energy. Health Physics Series XII, Vol. 1, pp. 427-436, Pergamon Press, New York.

Sehmel, G. A. 1986. "Transuranic Resuspension." In Proceedings of the DOE Symposium on Environmental Research for Actinide Research for Actinide Elements. In press.

Sehmel, G. A. 1984. "Deposition and Resuspension Processes." In Atmospheric Sciences and Power Production, ed. D. Randerson, pp. 533-583. DOE/TIC-27601, National Technical Information Service, Springfield, Virginia.

Sehmel, G. A. 1983. "Resuspension Rates from Aged Inert-Tracer Sources." In Precipitation Scavenging, Dry Deposition, and Resuspension (1982), eds. H. R. Pruppacher, R. G. Semonin, and W. G. N. Slinn, pp. 1073-1086. Elsevier Science Publishing Co., New York.

Sehmel, G. A. 1980. "Transuranic and Tracer Simulant Resuspension." In Transuranic Elements in the Environment, ed. W. C. Hanson, pp. 236-287. DOE/TIC-24800, National Technical Information Service, Springfield, Virginia.

Sehmel, G. A. 1980. "Particle Resuspension: A Review." Environment International 4:107-127.

Sehmel, G. A., and F. D. Lloyd. 1976. "Particle Resuspension Rates." In Proceedings of the Atmosphere-Surface Exchange of Particulate and Gaseous Pollutants-1974 Symposium, pp. 846-858, ERDA Symposium Series, CONF-740921, National Technical Information Service, Springfield, Virginia.

Processing of Emissions by Clouds and Precipitation (PRECP)

PROCESSING OF EMISSIONS BY CLOUDS AND PRECIPITATION (PRECP)

- **PRECP/Nonlinearity/Scavenging Studies**

The objectives of the PRECP program are to define and reduce current inaccuracies in the mathematical modeling of the processing of emissions by clouds and precipitation. PRECP is a multilaboratory effort, organized by the National Laboratory Consortium (NLC) and DOE, and is coordinated with other projects in the National Acid Precipitation Assessment Program (NAPAP) by the Interagency Task Force on Acid Precipitation, through Task Group C, Atmospheric Processes.

The prime contributors to PRECP are scientists at three national laboratories: Argonne National Laboratory (ANL), Brookhaven National Laboratory (BNL) and Pacific Northwest Laboratory (PNL). Important contributions have also been made in 1985 by scientists at Colorado State University, the University of Denver, the University of Maryland, the State University of New York at Albany (SUNYA), the National Center for Atmospheric Research (NCAR) and the National Oceanic and Atmospheric Administration (NOAA) through subcontracts with PNL.

Scientists at PNL are primarily responsible for field studies of precipitation scavenging. In 1985, the principal focus of activity was conducting and participating in two field experiments: PRECP-I (APRIL) and PRECP-II (PRECP in PRESTORM). Theoretical and numerical studies were also conducted. Articles in this section describe the scientific goals of the PRECP studies and document the field experiments and analyses conducted in 1985.

- **PRECP/Nonlinearity/Scavenging Studies**

Objectives of this study are:

To define and reduce current inaccuracies in the mathematical modeling of the processing of emissions by clouds and precipitation through field, laboratory, theoretical, and statistical investigations.

To contribute, through observations, to understanding the processing of pollutants by clouds and precipitation.

To re-examine a significant portion of the substantial environmental data bases that related to acidic deposition for indications of nonlinearities.

To perform laboratory studies that measure rates and extents of dissolution/attachment of gaseous reactants and oxidants into/on aqueous droplets and ice particles and of acid production in laboratory-simulated clouds and precipitation.

To test hypotheses and identify "signatures" that should be sought after in field studies.

THE PRECP PROGRAM--Pacific Northwest Laboratory's Contribution to the Department of Energy's Multilaboratory Study of the Processing of Emissions by Clouds and Precipitation

W. G. N. Slinn, K. M. Busness, D. S. Daly, M. T. Dana, W. E. Davis, R. C. Easter, R. K. Hadlock, R. N. Lee, D. J. Luecken, A. C. D. Leslie, C. G. Lindsey, D. C. Powell, and J. M. Thorp

- If sulfur dioxide (SO_2) emissions in the northeastern United States were reduced by 50% during the next decade, what would be the resulting change in deposition of sulfate ($SO_4^=$) to surfaces in the same area? How would the change be monitored? What would be the resulting change in the pH of rain (i.e., in the hydrogen ion concentration $[H^+]$ in precipitation)?

- Instead, for the more targeted goal of decreasing H^+ deposition in selected watersheds (e.g., so that rain in the Adirondacks would only rarely have a pH less than 4.5), what would be the least expensive policy of emission controls? For example, should nearby sources be controlled more than distant sources? What mix of controls is appropriate? Is the reliability of estimates good enough to support a specific proposal?

- What controls should be imposed on local versus distant sources of nitrogen oxides (NO and NO_2 = NO_x), in part because of their influence on precipitation's acidity, but especially if nitrogen compounds (e.g., nitric acid, HNO_3) and ozone (O_3) are found to contribute directly to significant forest damage?

- If NO_x and reactive-hydrocarbon emissions are reduced, would the $SO_4^=$ deposition-pattern change? Then there would be less competition for hydroxyl radicals, which contribute to the gas-phase oxidation of SO_2, and less production of O_3, which is important in the aqueous-phase oxidation of SO_2.

These questions are just some of those that NAPAP must address and expects PRECP to help answer. Table 1 identifies NAPAP goals and indicates those for which PRECP is involved.

The PRECP program is conducted by approximately 40 scientists, technicians, and support staff; a substantial portion of the funding (approximately 10%) is used for needed services, especially research-aircraft flight time. This report will give an overview of results from a research effort of approximately 12 person-years at PNL, plus contributions from PNL subcontractors, covering work done by universities and research flight time on NCAR and NOAA aircraft. However, it is emphasized that FY-85 was only the first year of the approved 5-year program; much effort during FY-85 was expended in defining the full 5-year program, and many

TABLE 1. Goals of NAPAP in Which PRECP is Involved

The NAPAP Goal

"To develop...an objective and comprehensive information base on the causes and effects of acid deposition and its effective management"

Major NAPAP Research Questions

- ▱ • What are the potential consequences of acid deposition?
- • What is the extent and location of the resources at risk?
- • How much damage has occurred and at what rate?
- • What is the dose-response function for sensitive resources?
- ▱ • What are the temporal and spatial patterns of acid deposition?
- • What are the sources of chemical species and amounts?
- ▱ • How must emissions be changed to obtain a specific change in deposition at sensitive receptors?
- ▱ • What are the emission control options?
- • What are the receptor mitigation options?
- ▱ • What are the costs, benefits, and impacts of acid deposition management strategies?

▱ Logo identifies NAPAP goal in which PRECP is involved.

of the results from this year's studies will not be available until later in the program.

Figure 1 shows the organizational structure of PRECP. As can be seen in Figure 1, there are three major components of PRECP:

1. Precipitation Scavenging Studies
2. Wet Chemical Processes
3. Synthesis of Results for Applications.

At PNL, PRECP personnel are primarily responsible for progress in precipitation scavenging studies.

During FY-85, by far the largest effort of the Precipitation Scavenging Studies component of PRECP has been in field experiments (approximately a 9 person-year effort at PNL). There has also been approximately a 1 person-year effort in theoretical and numerical studies, a 1 person-year effort in analysis of previous data, and a relatively large effort in administration (approximately 1 person-year), in part to administer the subcontracts. The purpose of this introductory article is to give an overview of FY-85 goals and progress in PRECP at PNL; following articles present more details about field experiments and analyses.

Precipitation Scavenging Parameters

For applications, knowledge about precipitation scavenging is coded in terms of three interrelated quantities: rates, ratios, and efficiencies.

Rates

Rates are the most fundamental of the three quantities, though they in turn can depend on such variables as collection efficiencies, hydrometer size-distributions, and concentrations of catalysts. The number of rates potentially important in precipitation scavenging calculations is surprisingly large, as can be appreciated by starting the count with hundreds of chemical reaction rates.

Ratios

There are also a great number of ratios of interest: the ratio of the concentration of a pollutant in precipitation to its concentration in air entering a storm, the ratio of a pollutant's concentrations in cloud-water to cloud-interstitial air, concentrations in the outflow air to the inflow air, and so on. Ratios are attractive, both theoretically and experimentally, for a number of reasons. Two examples are illustrative.

1. If one rate is known (such as the precipitation rate), other rates can be inferred from appropriate ratios (e.g., using the ratio of the concentrations of NO_3^- in the inflow air and in the precipitation).

2. Some rates (e.g., the condensational growth-rate of particles within clouds) are so rapid that other rates are rate limiting, and therefore, it is only the ratios that are needed in modeling applications.

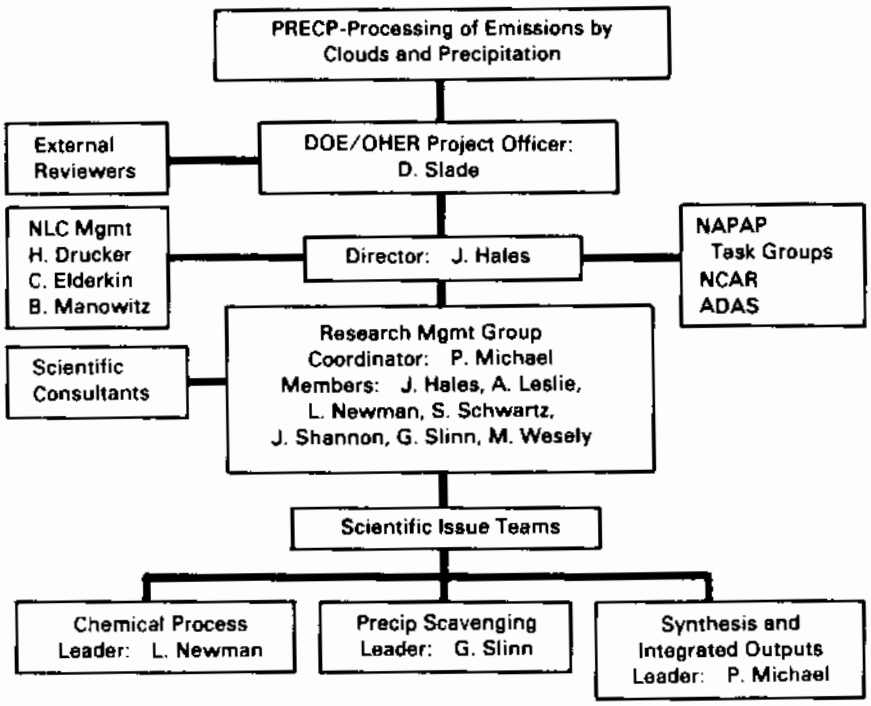

FIGURE 1. Organizational Structure of PRECP.

Efficiencies

Finally, in some cases, efficiencies are the most desired and most interesting quantities. Relevant questions include:

1. What mass fraction of the inflow aerosol is incorporated into cloud water during nucleation of the cloud droplets?

2. What fraction of the $SO_4^=$ and NO^- entering a storm is deposited with the precipitation?

3. What fraction of the SO_2 and NO_x is simply transported through a storm; i.e., what is the precipitation inefficiency of a storm?

Theoretically, scavenging rates, ratios, and efficiencies can be interrelated by taking progressively more spatial and temporal averages of scavenging rates. This theoretical result is presumed to be clear qualitatively. However, obtaining the relationships quantitatively is rather difficult (e.g., Slinn 1983).

Experimentally, in a meteorological setting, it is generally easier to obtain ratios than rates or efficiencies. In PRECP, chemical-reaction rates are generally sought only in laboratory studies; in field studies, the "noise" in measurements of rates of meteorological processes is generally larger than the "signal" from rates of chemical reactions. It might seem that the measurement of some efficiencies would be relatively easy (e.g., the efficiency of nucleation scavenging), but many storms cannot be safely penetrated with the research aircraft available to PRECP, and some efficiencies (e.g., the fraction of the total inflow pollution that is scavenged by a storm) require a range of temporal and spatial sampling that exceeds PRECP's capabilities to cover. Ratios (and relative rates), on the other hand, can be pursued experimentally with a minimum of meteorological support, and both point and large-scale and long-time average values are generally meaningful and therefore useful.

PRECP Field Studies

Consistent with the differences in meteorological information needed to extract ratios, on the one hand, and rates and efficiencies, on the other, PRECP field studies can be

placed in two categories. In the first category, illustrated by PRECP-I (APRIL) and PRECP-III (Snow Studies), ratios are emphasized. In the second category, illustrated by PRECP-II (PRESTORM) and PRECP-IV (GALE), state-of-the-technology meteorological support is available and attempts are made to measure not only ratios, but some rates and efficiencies as well.

For the first half of PRECP, four major field studies were planned. During FY-1985, two of these field studies were conducted, and by the time this report is published, the second two will be under way. A comprehensive list of scientific questions to be addressed by these field studies is given in PRECP's Summary Operational Plan (Michael 1984). In a very much abbreviated form, the first four PRECP field studies are described in the following paragraphs.

PRECP-I

Acidic Precipitation Ratios with Inflow Located (APRIL). The first PRECP field study was conducted during April 1985, with base of operations at Columbus, Ohio. As indicated by its acronym, one of the prime goals of the APRIL field studies was to obtain "improved" scavenging ratios: the improvement over available scavenging ratios was to base them on concentrations of pollutants not in surface-level (and usually pre-frontal) air, but on concentrations, measured by aircraft, in the air flowing into storms. To accomplish this objective, a number of other objectives had to be met, including the ability to sample precipitation from aircraft and to travel to storm locations (which we dubbed the MASS = Mobile Airborne and Surface Sampling approach). As is described in the article by Busness et al., the approach and its execution were successful. In summary, the number of "improved" scavenging ratios, available for use in regional-scale acidic deposition models, will have been increased substantially.

PRECP-II

PRECP in PRESTORM. It is expensive to conduct field studies that emphasize even just the chemical component of the acid rain phenomenon, but to define, also, the meteorological aspects of acid rain requires more resources than PRECP alone can provide. PRECP has therefore actively sought to join forces with scientists involved in field studies of meteorological phenomena, and so for PRECP-II, we joined with NOAA's PRESTORM (Preliminary Regional Experiment of STorm-scale Operational and Research Meteorology). PRESTORM's goal was to define and understand large-scale convective storms (the so-called Mesoscale Convective Complexes or MCC's); PRECP's goal in PRESTORM was to use its state-of-the-technology definition of these storms to help us understand the PRECP-measured chemical budgets of the storms. For PRECP, a disadvantage of PRESTORM was its location (in Kansas and Oklahoma, where there are reported cases of basic rather than acidic rain), but there were more-than-compensating advantages, as described in the article by Daly et al. Although it will require at least a year to use the PRESTORM-defined meteorology in PRECP's models of scavenging, we can already see that PRECP-II has provided us with important results about scavenging in relatively unpolluted environments. These results include likely the best-available definition of lightning-produced NO_x in storms, and (to our knowledge) the first-ever definition of the flow of surface-level air out through the top of deep convective storms.

PRECP-III

PRECP Adirondack Mountains Snow Scavenging Studies (PAM3S). From the start of planning for PRECP, the dearth of snow-scavenging data was apparent. Meteorologists have been criticized for performing field studies so frequently in clear weather; scavenging field studies have, at least, been conducted during stormy weather, but almost always just for rainstorms. In PRECP-III, the emphasis will be on scavenging by cold-frontal, orographic, and lake-effect snowstorms. PRECP-III will be conducted from January 7 to February 7, 1986, with base of aircraft operations at Syracuse, New York (where, with a wind-chill factor, temperatures of -25°F are not unexpected). Surface sampling of snow will be performed by personnel from ANL, BNL, PNL, and NOAA (and possibly from the Atmospheric Environment Service, Canada, and the Warren Springs Laboratory, United Kingdom); airborne sampling will be performed by three comparably equipped aircraft: BNL's Queen Air,

PNL's DC-3, and NOAA's King Air (subcontracted by PRECP, and with subcontracted contributions from York University, Ontario).

Six major goals of PRECP-III are:

1. To obtain "improved" scavenging ratios for snowstorms,

2. To measure pollutant concentrations in the outflow from winter storms,

3. To obtain relative scavenging rates of different chemical species as a function of ice-crystal structure,

4. To define the particle/ice-crystal collection efficiency as a function of ice-crystal properties (habit and degree of riming),

5. To examine relations between precipitation and scavenging efficiencies for orographic storms, and

6. To define reagents and products for chemical reactions in snowstorms.

Attaining these scientific objectives will require the accomplishment of several operational objectives, including satisfactory intercomparisons of newly designed systems for airborne and surface sampling of snow, the latter including the capture of individual ice crystals for analysis by scanning electron microscopy. Figure 2 shows one of two new ice-crystal collectors to be tested onboard PNL's DC-3.

PRECP-IV

GALE Acidic Precipitation Studies (GAPS). During a part of the snow scavenging studies in the Adirondacks, and later for the 2-week period February 20 through March 7, 1985, PRECP will join forces with another large meteorological field study, this one conducted on the East Coast and dubbed GALE (Genesis of Atlantic Lows Experiment). GALE is funded by the National Science Foundation, Office of Naval Research, and other organizations, and there is a cooperative, simultaneous experiment off the east coast of Canada, the Canadian Atlantic Storms Program (CASP).

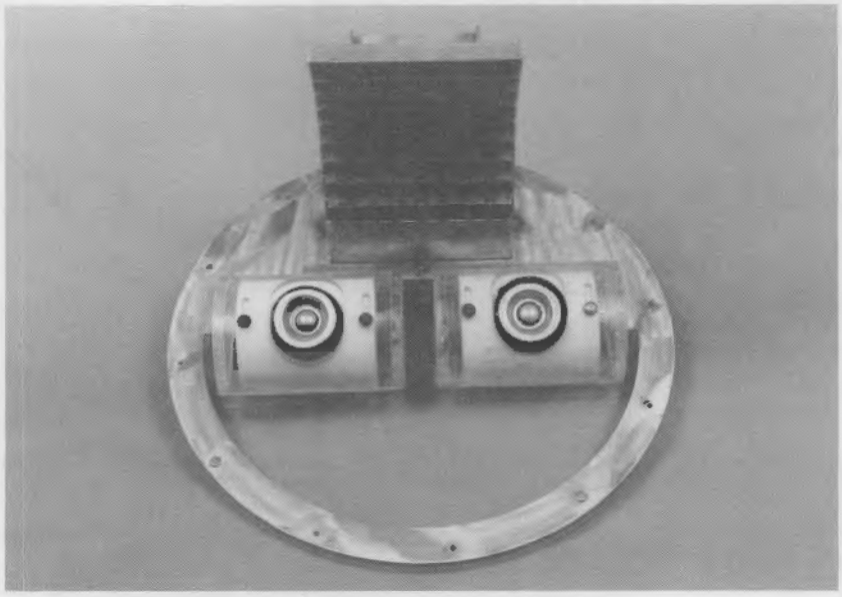

FIGURE 2. Prototype of PNL's Airborne Snow Collector for Chemical Analysis (ASCCA) to be used in PRECP-III.

PRECP studies in GALE will be conducted on three spatial scales. At the meso-gamma scale (2 to 20 km), the rainband studies will seek to obtain a data base for the description of pollution budgets for individual rainbands within frontal storms; the studies will be conducted in cooperation with the University of Washington (UW) and will primarily use UW's Convair C-131A research aircraft, NCAR's Electra, the NCAR dual-Doppler radars, and PRECP's collection of sequential precipitation samples. At the meso-beta scale (20 to 200 km), the frontal-storm studies will seek improved scavenging ratios, relative scavenging rates, and storm outflow/inflow ratios; to conduct these studies, PRECP will subcontract sequential precipitation sampling and has arranged for chemical sampling onboard the NCAR Electra and Sabreliner, and on NOAA's P-3 aircraft. In addition, the three PRECP aircraft will join in the frontal-storm studies during the time period February 21 through March 7. Finally, at the meso-alpha scale (200 to 2000 km), the regional-scale studies will seek to define scavenging ratios and sub-cloud scavenging for storms that move north along the East Coast. For these studies, PRECP aircraft will travel with the storm either from Syracuse or Raleigh, joined by NCAR's Electra, NOAA's P-3, and the CASP DC-3. Thus PRECP is in the process of augmenting precipitation and air sampling along the entire East Coast, from South Carolina to Newfoundland.

Storm-Scale Modeling Activities

In conjunction with the field studies described above, PRECP is developing and applying numerical models to describe acid production in and deposition from a variety of storm types. Highlights of progress during FY-1985 are briefly listed below.

1. During the year, PLUVIUS-II (a comprehensive numerical code to describe three-dimensional, time-dependent chemical processing and scavenging) has been made operational.

2. A Request for Proposals soliciting output windfields and microphysics from dynamic cloud-models was distributed, and the resulting contract was awarded to Dr. William Cotton, Colorado State University. Model history tapes for two-dimensional convective-cloud case-studies were obtained, and at the end of FY-1985, work has begun on driving PLUVIUS-II from the data on these tapes.

3. Flow fields from a warm-frontal rainband were obtained from Dr. Stephen Rutledge (Oregon State University) and Dr. Dean Hegg (UW) and used for simulations of scavenging. The PLUVIUS-II simulations agreed closely with those of Hegg et al. (1984), as is illustrated in Figure 3.

4. Simulations were made to study the linearity of scavenging, for several different assumptions about SO_2 aqueous-phase oxidation mechanisms. Simulations were made in pairs, first using initial SO_2 and sulfate fields as per the "nonproportional polluted" case used by Hegg et al., and then reducing initial SO_2 and sulfate concentrations by one-half. From each

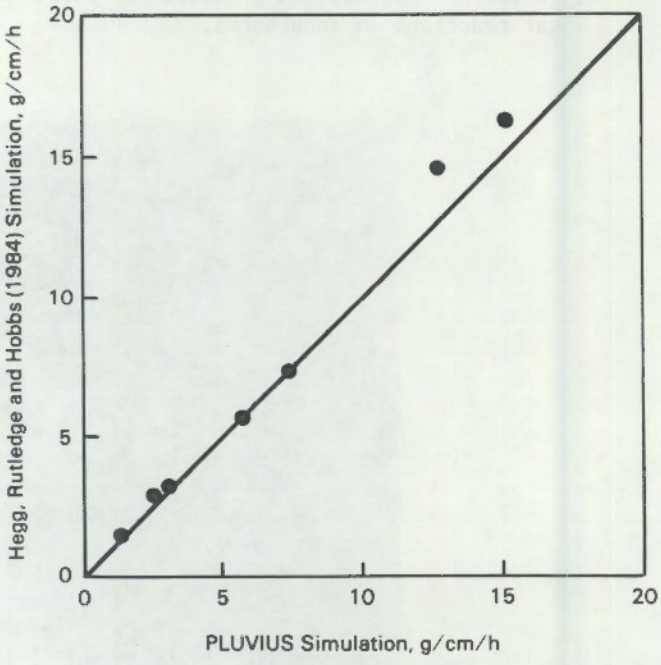

FIGURE 3. Comparisons of Total Sulfate Deposition Rates from Seven Parallel Simulations by the PLUVIUS and the Hegg, Rutledge and Hobbs (1984) model. Hegg et al. describe nine different simulations with the Type-II warm-frontal rainband in their paper; seven of these were performed with PLUVIUS-II; the two simulations without nucleation scavenging were omitted.

pair, a linearity factor, defined as the relative reduction in sulfate deposition divided by the relative reduction in initial sulfur concentrations, was calculated. If the system is truly linear, a value of 1.0 results. The simulations were made with five different mechanisms for aqueous SO_2 oxidation, and the results are shown in Table 2. As can be seen, the linearity factor is quite sensitive to the assumed SO_2 oxidation mechanism.

During FY-1986, it is expected that PLUVIUS-II will be used, driven by simulations of some of the PRESTORM case studies, to interpret PRECP-II field data.

Larger-Scale Modeling Activities

For larger than storm scales, PRECP modeling activities are progressing to assist the interpretation of some of the PRECP-I (APRIL) and PRECP-IV (GAPS) field-study results. We plan to use PLUVIUS Applied at Larger Scales (PALS) and the available Sulfur Transport Eulerian Model (STEM), developed by Dr. Greg Carmichael (University of Iowa), and Dr. Len Peters (University of Kentucky), and to drive these codes with acquired output from the Limited Fine Mesh and Boundary Layer models for the days of the field studies. In addition, we will use National Weather Service-reported precipitation. Most of these data and codes are now available for applications during FY-1986.

Analytical models are also under development, as is illustrated in a report by Slinn (see list of publications), as are studies of available precipitation chemistry network data, illustrated in the article by Dana and Easter in this volume.

Workshops and Reviews

This first year for PRECP has been very active. In addition to the activities sketched above, the following calendar is illuminating:

October:	PRECP Workshop at ANL
November:	PRECP Workshop at BNL, with approximately 20 consultants
December:	DOE-sponsored Review of PRECP Plans
January:	PRECP Workshop at Battelle, Washington, D.C.
March:	NAPAP-sponsored Review of PRECP
April:	PRECP-I Field Study
June:	PRECP-II Field Study
August:	PRECP Modelers Workshop at Battelle, Denver
September:	PRECP Field Studies Workshop at Seattle
September:	NAPAP-sponsored Review of PRECP

TABLE 2. Results of Linearity Runs with Warm-Frontal Rainband Case

Mechanism	Linearity Factor
1. Empirical rate (based on field measurements) used by Hegg et al. (1984)	0.98
2. Same as case 1, but initial cloud-water pH determined by sulfate-aerosol scavenging (rather then assumed initial value of pH of 4.0, as used in case 1)	0.78
3. Oxidation by H_2O_2, assuming fixed aqueous H_2O_2 concentration of 400 ppb, as used by Hegg et al.	0.97
4. Oxidation by H_2O_2, assuming initial gas phase concentration of 1 ppb	0.64
5. Oxidation by O_3, assuming initial gas phase concentration of 50 ppb	0.73

Acknowledgments

Substantial contributions to the program were made by G. W. Dennis, D. W. Glover, J. L. Gregory, R. V. Hannigan, L. C. Harrison, G. L. Laws, and D. S. Sharp.

References

Hegg, D. A., S. A. Rutledge and P. V. Hobbs. 1984. "A Numeric Model for Sulfur Chemistry in Warm-frontal Rainbands." J. Geophys. Res. 89:7133-7147.

Michael, P., ed. 1985. PRECP Summary Operation Plan. Available from Brookhaven National Laboratory, Attn. P. Michael, Meteorology Department, Upton, Long Island, New York.

Slinn, W. G. N. 1983. "Air-to-Sea Transfer of Particles." In Air-Sea Exchange of Gases and Particles, eds. P. S. Liss and W. G. N. Slinn, Chapt. 6, pp. 299-396. Reidel, Boston, Massachusetts.

PNL'S CONTRIBUTIONS TO THE PRECP-I (APRIL) FIELD STUDIES

K. M. Busness, M. T. Dana, W. E. Davis, W. G. N. Slinn, and J. M. Thorp

The PRECP-I (APRIL) field study was a cooperative venture between the Wet Chemistry and Precipitation Scavenging Components of PRECP. There was cooperation, also, with independent, simultaneous field studies that were being conducted by NCAR in the Midwest and by a number of contractors for EPA at Philadelphia. R. Tanner of BNL was the coordinator of APRIL; D. Sisterson of ANL, P. Daum and T. Kelly of BNL, and W. Davis and G. Slinn of PNL led the respective DOE laboratory teams. This article describes the goals of the Precipitation Scavenging Component of PRECP-I and indicates how completely these goals were achieved.

Scientific Goals

As described in the preceding article by Slinn et al., the APRIL field studies emphasized ratios and relative rates. The prime goal of the Precipitation Scavenging Component of PRECP-I was to obtain data from which improved scavenging ratios could be calculated. Scavenging ratios reported in the literature (e.g., Junge 1963, Engelmann 1970, Slinn 1984) almost invariably are derived from taking the ratio of a trace substance's concentration in surface-level precipitation to its concentration in surface-level air. These classical scavenging ratios have been useful, especially for bomb-debris radionuclides for which the variability has not been excessive. For air pollutants, however, these classical scavenging ratios have been found to vary by at least an order of magnitude, and effort has therefore been expended to try to understand and eliminate the variations, especially since scavenging ratios are frequently used in regional-scale models of acidic deposition.

One of the prime suspects for variations in classical scavenging ratios (e.g., Barrie 1985) is that they are based on surface-level air concentrations. Are these surface-level air concentrations representative of the pollution entering the storm? In particular:

- At what times are the surface air-concentrations measured relative to the time of frontal passage?
- What is the vertical distribution of the pollution entering the storm?
- What is the flow of pollution through the storm; i.e., if the inflow pollution is sampled, where is it deposited?

Other suspected causes of variations in classical scavenging ratios, leading to additional lists of questions, deal with storm type, pollution speciation and other characteristics, and in-cloud chemical reactions.

With such questions, we set our prime scientific goal to be the determination of improved scavenging ratios, improved in the sense that if, for each storm, the inflow air-concentrations were measured by aircraft and the sampled precipitation contained pollution from the sampled air, then the resulting scavenging ratios would be expected to be more understandable, have less variability, and therefore be more valuable for use in acidic deposition models.

There were other scientific goals of the Precipitation Scavenging Component of PRECP-I, some related to the goal of obtaining improved scavenging ratios, all listed in the APRIL Operational Plan, and all supported by two review committees. The other goals will not be described in detail, but are listed in Table 1.

In pursuit of the scientific goals, two major operational aims for PRECP-I were taken. First was to test the feasibility of the Mobile Airborne and Surface Sampling (MASS) approach. Simply stated, the aim was to attempt to increase the rate of data collection by travelling to storms, rather than waiting for storms to come to a fixed surface network. In our planning for the field studies we evaluated many of the advantages (and disadvantages) of the MASS approach, but only through testing could we examine its feasibility. One aspect of the MASS approach was to arrange for the weather forecasting

TABLE 1. Summary of Precipitation Scavenging Objectives for APRIL

1. Test the MASS approach
2. Test the Airborne Precipitation Collector (APC)
3. Obtain "improved" scavenging ratios
4. Define precipitation chemistry spatial variability
5. Relative scavenging via surface sequential samples
6. Relative scavenging via airborne precipitation sampling
7. Define "noise" from subcloud scavenging
8. Scavenging at warm versus cold fronts
9. Assist PRECP/WCP in documentary studies
10. Drizzle from cumulus clouds
11. Scavenging ratios from warm-sector rain
12. Scavenging ratios for cumulonimbus clouds
13. Precipitation chemistry for an occlusion
14. Precipitation chemistry around a low
15. Orographic inflow/outflow

for the field study to be performed not in the field, but from the base laboratories (at BNL and PNL). The second operational aim, crucial for the first and for most of the scientific goals, was to test the feasibility, reliability, and representativeness of obtaining precipitation samples from an aircraft.

Status Report

Table 1 listed the main goals of the Precipitation Scavenging Component of PRECP-I. The current status and progress toward achieving these goals are described below. The numbers of the goals correspond to those given in Table 1.

1. Test the MASS Approach

April 1985 turned out to be a good month for testing the MASS approach: Columbus, Ohio (the chosen base of operations), had the second driest April on record. With a fixed field operation near Columbus, we would have sampled only four storms, and these would not have been the most interesting. In contrast, with the MASS approach, 18 systems were sampled; these included long-range (ca. 1000 km) transport and then scavenging of pollution, two orographic precipitation events, and two case studies of large-scale precipitation-chemistry spatial variations within a single storm. Table 2 identifies the studies conducted during APRIL based on the MASS approach; Figure 1 gives an overview of the flights taken by PNL's DC-3 during APRIL.

The MASS approach is feasible and, as expected, provides a great number and variety of sampling opportunities. However, it was found to be overly demanding to seek surface sampling via automobile travel to distant sites and sometimes to transport surface-sampling crew members in the research aircraft. In the execution of the MASS approach, a number of other principles were learned (such as get the water first; rely most on surface reports of rain; and phase the aircraft in time), but details will be omitted here. In addition, if the forecasters have access to adequate meteorological products, it is preferable that they be with the crew in the field.

Given the demonstrated feasibility of the MASS approach and the success of sampling precipitation by aircraft, we recommend that future studies choose one of the following options: (i) sample precipitation only by aircraft, (ii) sample precipitation by aircraft and, for surface sampling, sample only at some of the many network stations (MAP3S, UAPS, NADP, CAPMON, etc.), preferably with arrangements for sequential sampling by station operators, or (iii) significantly increase the number of surface-sampling crew members. For PRECP-IV (especially for the GALE frontal-storm and regional-scale studies), we plan a combination of options (i) and (ii).

In summary, the test of the MASS approach was educational, and we strongly recommend that the procedure (with suggested modifications) be applied in future PRECP field studies.

2. Test of the Airborne Precipitation Collector (APC)

During APRIL, 58 precipitation samples were collected with new, PNL-designed Airborne Precipitation Collectors (APC), shown in Figure 2a. Thirty-five cloud-water samples were also collected, but with the SUNYA sampler (shown in Figure 2b). Figure 3 shows a comparison of sequential precipitation samples taken from the aircraft and at the surface; both sampling activities started at the onset of precipitation. That the aircraft commenced sampling approximately one hour before the surface station reflects that the aircraft was located approximately 30 km upwind of the surface station; however, since

TABLE 2. Precipitation Events Sampled During PRECP-I

Date	Meteorological Conditions	Area	Prime Goals (numbers refer to list in Table 1)
4/4	Pre warm front	Indiana, Kentucky	3
4/5	Pre cold front	Ohio, Indiana, Kentucky	3
4/7	Showers	Ohio, Kentucky	1, 2, 3
4/9	Scattered clouds	Ohio	Intercomp. Flight with BNL
4/11	Pre cold front	Ohio, West Virginia	2, 3
4/12	Inflow warm sector	Indiana, Illinois, Ohio	3
4/13	Shower activity, weak warm front	Ohio, Illinois, Michigan	1, 3
4/19	Inflow weak stationary front	Ohio	1, 3
4/20	Inflow to stationary front	Pennsylvania, Ontario	3
4/23	Shower activity warm sector	Ohio, Kentucky	1, 3
4/24	Inflow cold front	Ohio, West Virginia, Maryland	1, 2, 3, 4
4/25	Post cold front	New Jersey, Pennsylvania	2, 3, 4
4/27	Warm sector showers	Kentucky	1, 2, 3, 11
4/28	Pre cold front	West Virginia, Virginia, North Carolina	2, 3, 15
4/30	Pre cold front	Kentucky, Tennessee	3, 4
5/1	Pre and post cold front	Tennessee, Kentucky, Indiana, Ohio	1, 2, 3, 4

there were no major sources of pollution between the aircraft and the surface sight (at the airport at Frankfort, Kentucky), it is doubtful that the differences in concentrations seen in Figure 3 were caused by this spatial separation. Moreover, if there were additional pollution sources between the two locations, the surface concentrations would have been higher, given the rainfall rates, than the airborne concentrations; yet the data show the opposite trend.

A likely cause of the differences seen in Figure 3 is that they reflect real differences in chemical composition of precipitation aloft and at the surface at the onset of precipitation. Thus, there are likely larger (and less polluted) drops reaching the surface first, and some of the smaller drops (with larger pollution concentrations) evaporate at the onset of rain before they reach the ground. If this interpretation is correct, then the differences in concentrations should decrease with increasing time (e.g., as the subcloud air becomes saturated), and this trend is reflected in the data. This interpretation is also supported by the results shown in Table 3, which lists compositions measured in airborne versus surface samples taken within about 50 km and one hour of one another, and for a case of fairly steady precipitation (i.e., not at the onset of rain). For the first two cases listed, the differences in the chemical

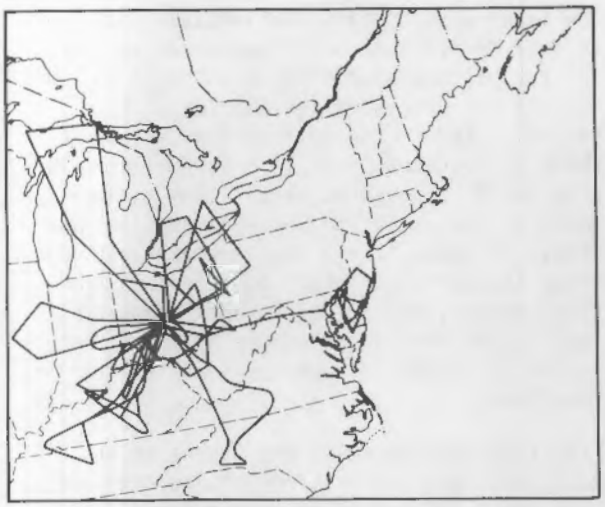

FIGURE 1. Mosaic of Flights Conducted During APRIL by PNL's DC-3.

compositions between airborne and surface sampling is no larger than would be expected for two surface stations.

For the third case listed in Table 3, however, differences between airborne and surface precipitation chemistry are substantial, but not among the three aircraft samples that were taken in the neighborhood of the surface station. Notes from the surface sampling station mention suspected contamination of the funnel. The fourth entry in this case shows composition of the 18-h event sample at the surface (2.5 cm of rain), and it is seen to yield compositions closer to the three 10-min airborne samples.

Also during the May 1 storm, two comparisons were made between the chemical compositions of precipitation and cloud water, both sampled aboard PNL's DC-3. One pair of samples

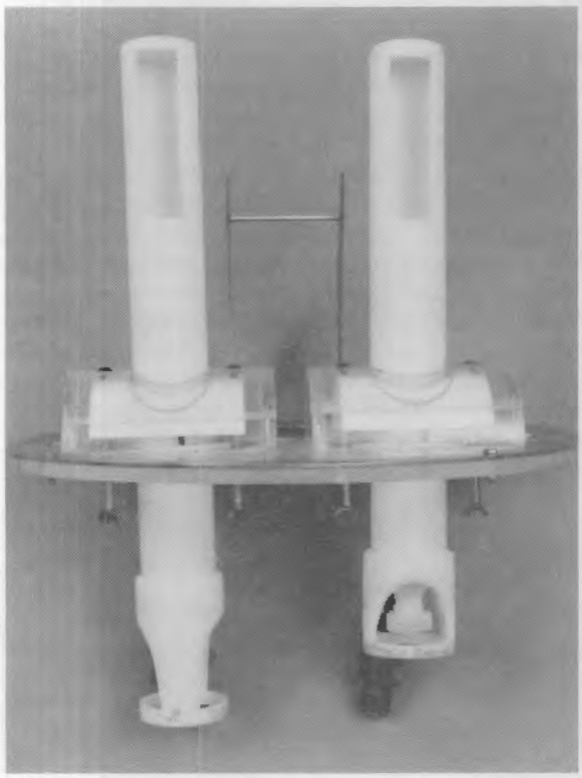

(a)

(b)

FIGURE 2. Airborne Water Collectors: a) PNL's APC and b) SUNYA's cloud water collector.

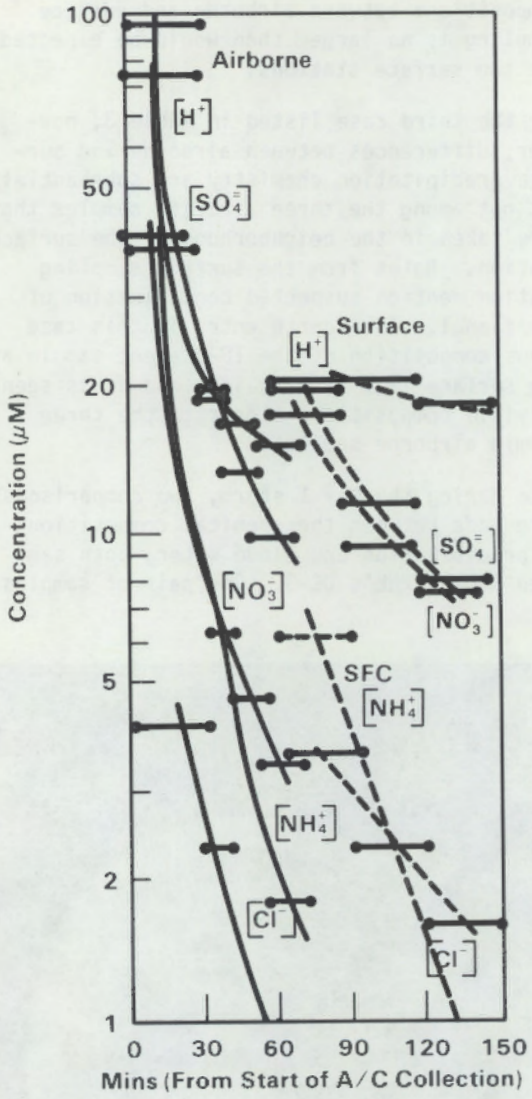

FIGURE 3. Surface Versus Airborne Precipitation Collected Near Frankfurt (μM). Dashed lines show surface collection, solid lines airborne collection.

was taken at 3,000 ft over Indianapolis, and as seen in Table 4, the cloud water sample (only 3 ml) had almost twice as much $SO_4^=$ and NO_3^- as the precipitation sample (a 10 ml sample). The second pair of samples, taken about ten minutes later in the same storm but at 3,500 ft, showed no significant differences in concentrations between the two samples. It seems likely that the aircraft was in an industrial or urban plume during the first sample, but the difference measured could have been caused simply by variations in the cloud liquid water contents at the two locations.

From these measurements and others to be described later in this report, we conclude that PNL's APC can provide consistent and meaningful samples of precipitation chemistry. From its design and performance, we have no hesitancy in claiming that the APC gives an unbiased collection of all droplets larger than about 10 μm. However, the results may differ from surface sampling data (which may have a bias toward large drops, especially at the start of precipitation, and may easily suffer from contamination by large aerosol particles), and may differ from data for cloud-water collectors of the SUNYA design (which almost certainly shatter and do not collect large drops, for which, of course, the SUNYA sampler was not designed). As an additional practical matter, the APC was found to collect precipitation samples at a rate approximately three times the rate of the SUNYA sampler, probably in large measure not because of drop shattering in the SUNYA sampler, but because of the larger collecting area of the APC.

TABLE 3. Comparisons of Surface and Airborne Precipitation Chemistry Samples (μM)

Date	Type	pH	$[SO_4]^=$	$[NO_3]^-$	$[NH4]^+$	$[Cl]^-$
5/1	sfc	4.07	73	55	48	13.0
	a/c	4.07	58	44	41	6.0
5/1	sfc	4.02	53	58	42	9.0
	a/c	4.14	76	46	55	10.0
5/1	sfc	5.44	36	32	21	6.0
	a/c	4.63	18	11	23	1.3

TABLE 4. Concentrations in Cloud Water Versus Precipitation (μM)

Date, Time	Type	pH	$[SO_4]^=$	$[NO3]^-$	$[NH4]^+$	$[Cl]^-$
5/1/85	Precip.	4.38	46.0	27.9	43.1	3.6
1817-1824	Cld. Wtr.	--	87.7	52.9	--	3.6
5/1/85	Precip.	4.50	18.1	11.0	8.8	3.1
1827-1838	Cld. Wtr.	4.63	19.0	13.1	10.1	2.8

3. Obtain "Improved" Scavenging Ratios

The success of obtaining improved (i.e., more understandable) scavenging ratios cannot be evaluated quantitatively at this time because the chemical analyses for aerosol ions and for trace metals in air and precipitation are not yet complete. However, if these analyses proceed as expected, then at least qualitatively it is clear that this goal was achieved with substantial success. An indication of this success can be obtained simply from counting samples:

- If account is taken only of event samples taken by PNL PRECP personnel and for cases when preliminary meteorological analysis demonstrate that inflow air samples were obtained, and further, if credit is taken only for the ions for which precipitation analysis is already completed plus detection of 10 trace metals, then approximately 200 scavenging ratios will result.

- If, in addition, account is taken of all precipitation samples collected by air and if analyses are performed, as expected, for at least 20 species, then at least 1000 scavenging ratios will result.

4-7. Gridded Precipitation Chemistry

In the APRIL Operational Plan, objectives 4 through 7 were included as a group; all dealt with measuring spatial or temporal variations of precipitation chemistry. Objective 7, to examine contributions to precipitation chemistry from subcloud scavenging of cool-sector air (beneath a warm front), especially for NO_3^- and $SO_4^=$, was not achieved: no stable warm front occurred in the Northeast during April 1985. Objective 5, to compare relative scavenging rates via surface-level sequential sampling, was achieved (an example was shown in Figure 3), but because the surface sampling crew members were moved so frequently this goal was not pursued with the thoroughness desired. Objectives 4 and 6, dealing with precipitation chemistry spatial variability and relative scavenging rates measured via airborne sampling were achieved: on April 24, precipitation samples were collected from near Dayton, Ohio, to Baltimore, Maryland, and on May 1, samples were obtained for a 500-km north-south extent from near Nashville, Tennessee, to Columbus, Ohio, and for 800 km from Indianapolis, Indiana, to Philadelphia, Pennsylvania.

To our knowledge, spatial variations in precipitation chemistry such as shown in Figures 4, 5, and 6 for the May 1 storm have never been seen before. Results for temporal variations from a single surface-station are available, but their interpretation is complicated by many factors, especially by changing wind patterns at the surface during the many hours of a typical storm passage and by changes in relative contributions from incloud and subcloud scavenging. In contrast, Figures 4, 5, and 6 give, in essence, a snapshot of the precipitation chemistry, essentially at a single time and for an entire storm. It is true that the interpretation of the results shown in Figures 4, 5, and 6 will be complicated by the spatial distribution of emissions, uncertainties in rainfall rates, and the existence of embedded convection, but work is in progress to use available emission inventories (and definitions of the meteorological fields) to interpret the results. In the meantime, a number of obvious features of the data are noted below.

Figure 7a shows the radar echo for 1900 Z on May 1, with superimposed frontal position and flight path. By comparing Figures 4, 5, and 6 with 7b near 1740 Z, it is seen that NH_4^+, $SO_4^=$, and NO_3^- concentrations dropped dramatically, by a factor of about 5, as the DC-3 crossed from pre-frontal showers into

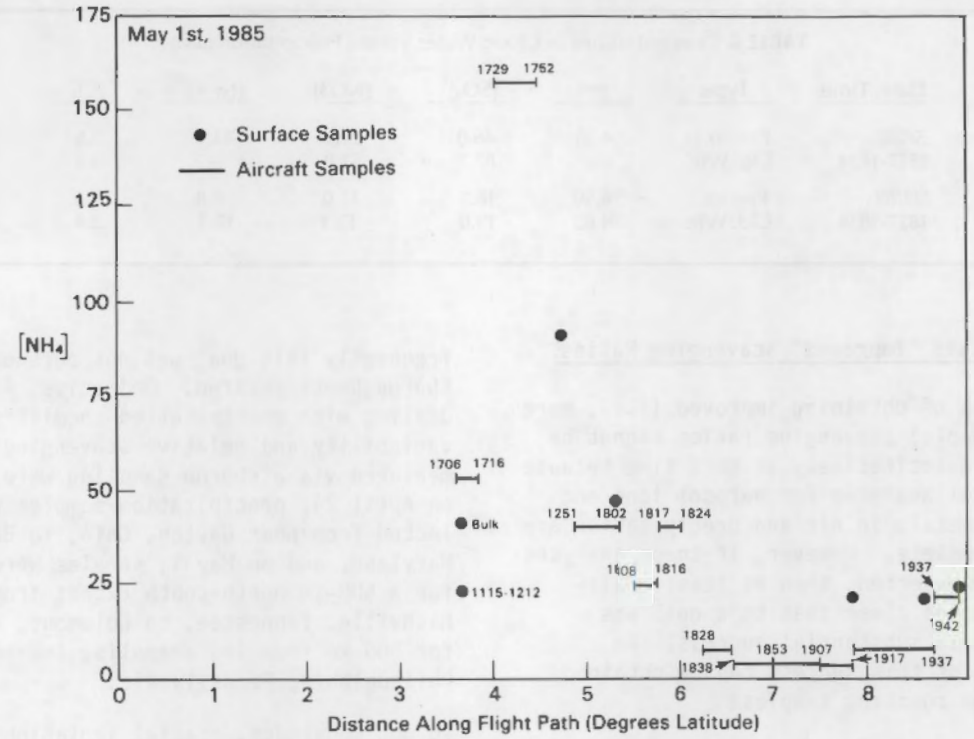

FIGURE 4. Spatial Variations in Precipitation Chemistry for NH_4^+ (μM).

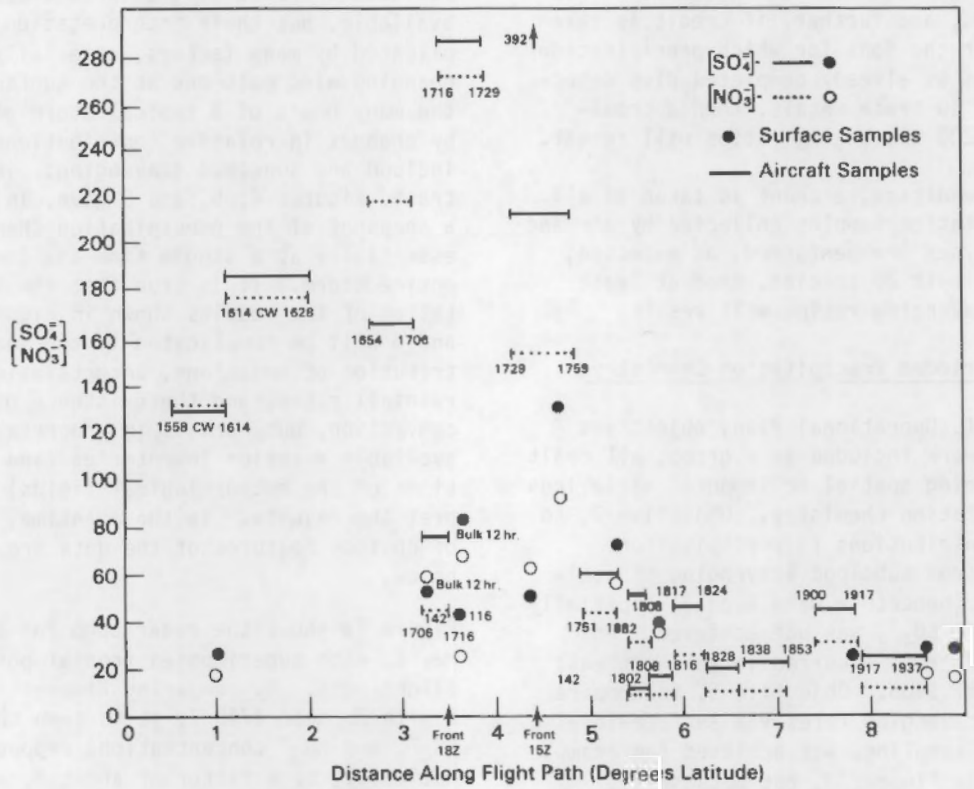

FIGURE 5. Spatial Variations in Precipitation Chemistry for $SO_4^=$ and NO_3^- (μM).

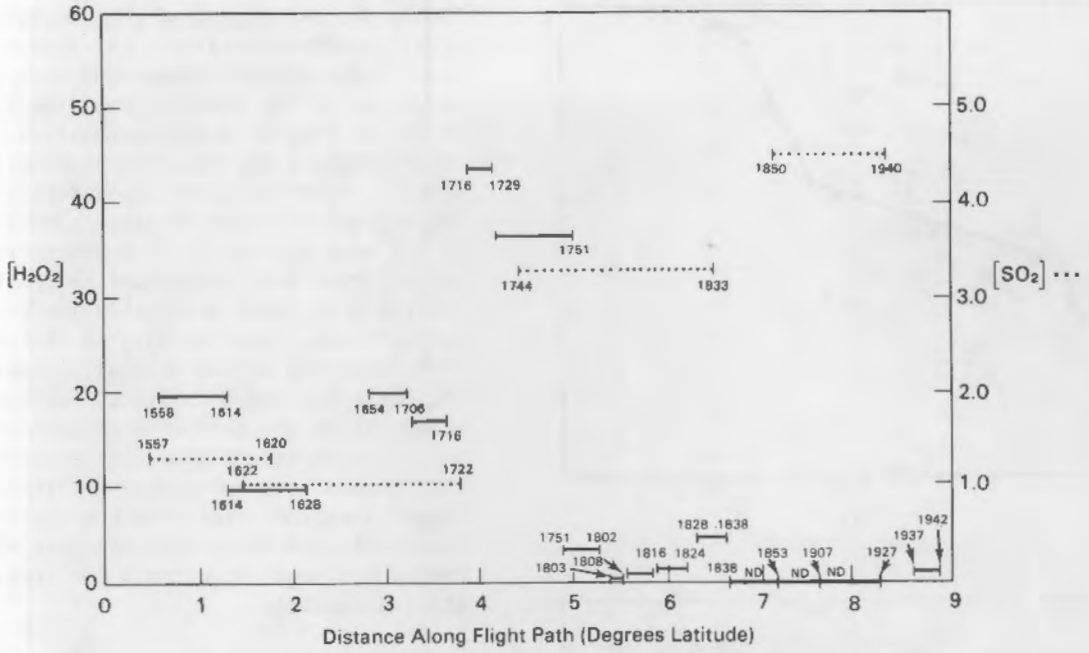

FIGURE 6. Spatial Variations in Precipitation Chemistry for H_2O_2 (μM).

heavy postfrontal rain; this occurred in spite of the expected increase in $SO_4^=$ from additional emissions along the Ohio River.

Figure 8 gives another indication that the local contribution to precipitation chemistry from local pollution sources can be less than expected. Thus, there is little doubt that the NO and NO_2 "plumes" sampled from 1746 Z to 1804 Z were caused by sources near Cincinnati. Yet the precipitation samples obtained simultaneously in the Cincinnati plume (see Figure 5) show at most only a small increase in NO_3^- (and $SO_4^=$), presumably because there was insufficient time for oxidation of the emitted NO_2 and SO_2.

The rate of oxidation of SO_2 is expected to depend to a significant degree on the H_2O_2 concentration, and in this regard, Figure 6 is illuminating. It shows that the aqueous-phase H_2O_2 concentration drops more rapidly within the storm than do either $SO_4^=$ or NO_3^- (see Figure 5). This may be caused by the increase in $SO_4^=$ and NO_3^- from SO_2 and NO_x emissions, but tentatively we suggest that the results reflect the following: whereas $SO_4^=$ and NO_3^- are both scavenged and produced within the storm, H_2O_2 decreases both by scavenging and by chemical consumption; therefore, the H_2O_2 should decrease relatively rapidly as the air progresses through a storm. However, as the analysis of the data proceeds, this simple picture may need to be revised: when the aircraft climbed from 3000 ft to 3500 ft, a higher concentration of H_2O_2 was found aloft.

8-15. Other Goals

Other goals were listed for the Precipitation Scavenging Component of APRIL, but these were not described in detail in the Operational Plan either because they were relatively obvious (e.g., assisting other groups and obtaining scavenging ratios for warm-sector showers) or because of low probability of appropriate weather conditions. Brief comments are made about each of these goals:

8. Compare scavenging from the same air mass at both the warm and cold fronts:

   The necessary meteorological condition did not occur during April 1985 in the northeastern United States.

9. Assist the Wet Chemistry Component of PRECP in the pursuit of their goals:

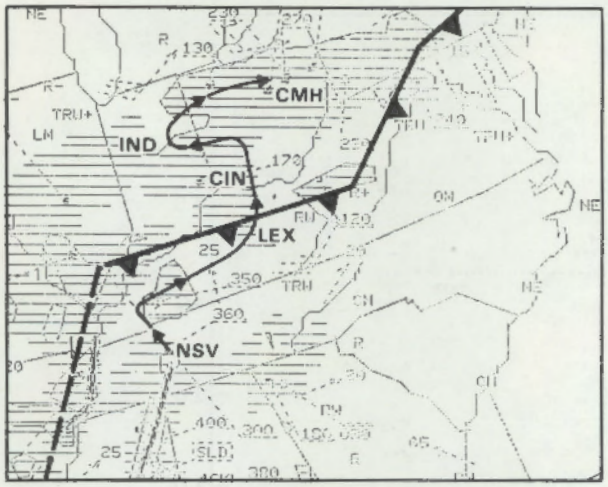

(a)

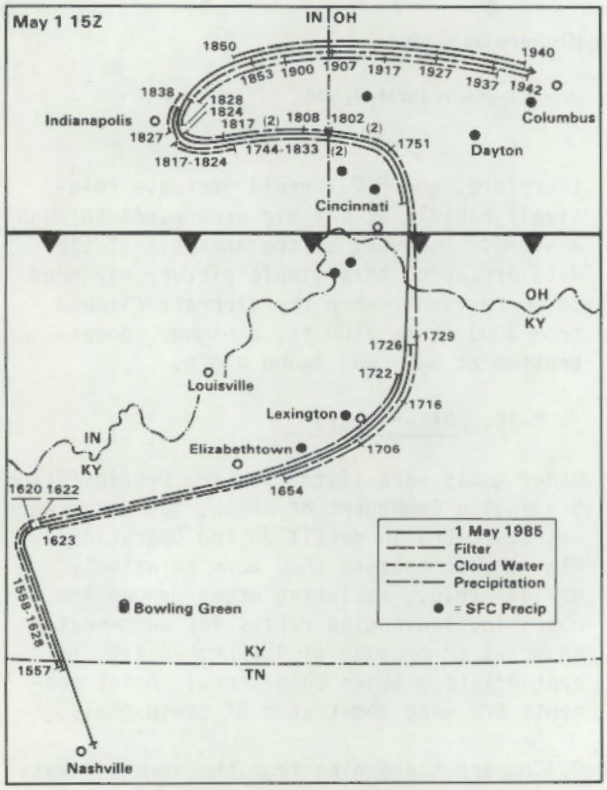

(b)

FIGURE 7. Sampling Flight Path for May 1: a) Radar Echo with Superimposed Frontal Position and Flight Path; b) Schematic of Flight Position and Samples Obtained.

Figure 9 shows a plot of SO_2 in precloud or cloud-interstitial air vs. aqueous-phase H_2O_2 concentrations, and suggests an extension of the results, found by Daum et al. of BNL, of a strong negative correlation between SO_2 and H_2O_2 concentrations. The results are consistent with the concept of rapid in-cloud oxidation of SO_2 by H_2O_2, but it is noted that the present results (in contrast to those communicated by Daum) are mostly for precipitating clouds, and the H_2O_2 in the precipitation may not be in equilibrium with the local SO_2 concentration. Further screening of the data will be performed, but it is of interest to note already that the range of the H_2O_2 concentrations in Figure 9 extends over more than three orders of magnitude, and over this wider range, the negative correlation trend is still suggested.

10. Chemical-conversion signals from fair-weather cumulus clouds (Cu):

Although a number of incidents of fair-weather Cu's occurred, in no cases was the cloud deck judged to be sufficiently uniform to permit the planned study.

11 - 12. Scavenging ratios for warm-sector showers and isolated cumulonimbus clouds (Cb):

Measurements for a number of events of this type were conducted and will be reported when the chemical analyses are complete. However, one of the results that is already apparent might usefully be mentioned at this time. For the six cases (of the approximately 20 cases, total) when only a small amount of water (typically less than 10 ml) could be collected (during the half-hour circling in the rain shaft), the ratio of precipitation-borne NO_3^- to HNO_3 in nearby air was typically a factor of about five higher than for the cases with substantial rain. When the NO_3^- aerosol analysis is complete, an explanation of this result might be apparent.

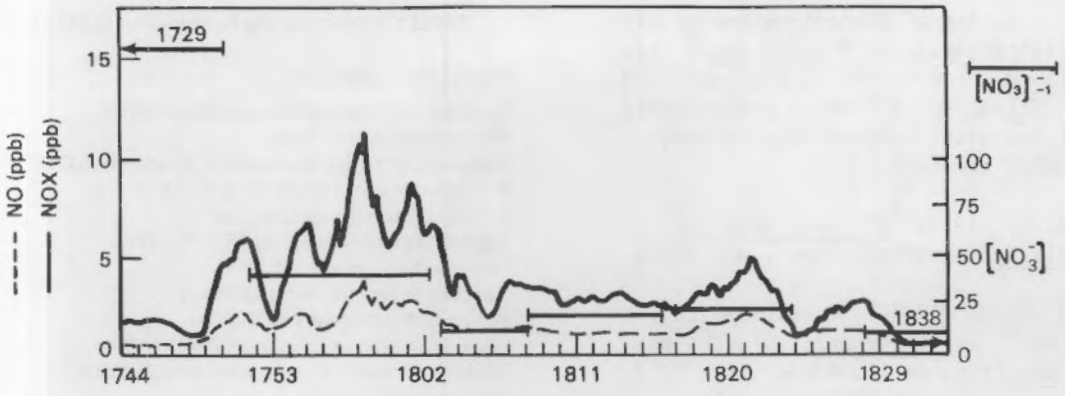

FIGURE 8. Concentration of NO and NO_x (ppb), and NO_3^- (μM) Near Cincinnati.

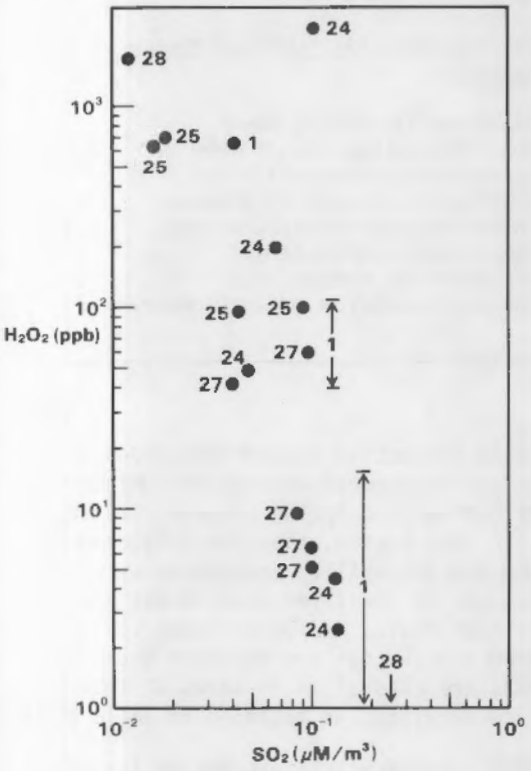

FIGURE 9. SO_2 Versus H_2O_2 Concentrations.

13 - 14. Precipitation chemistry for an occluded front and around a low:

One event of the second type did occur during April (over Wisconsin), but the crew was exhausted after a long flight to the upper peninsula of Michigan, and attempts to pursue this objective were abandoned.

15. For orographic clouds, compare inflow and outflow concentrations:

Two cases of this type were accomplished (one with the DC-3 on April 11, and the second with the Queen Air and the DC-3 on April 28). The results of these studies will be reported when the chemical analyses are completed.

Summary

Success of PRECP-I will be judged by data quality, applicability, and what is learned from the data analysis. Since even the preliminary analysis of the data is not yet complete, an assessment of achievements of APRIL cannot yet be made. However, the analysis to date is encouraging.

Acknowledgments

Substantial technical and logistical contributions were made by G. W. Dennis, D. W. Glover, J. L. Gregory, R. V. Hannigan, and R. N. Lee.

References

Barrie, L. A. 1985. "Scavenging Ratios, Wet Deposition, and In-Cloud Oxidation: An Application to the Oxides of Sulphur and Nitrogen." J. Geophysical Research 90(D3):5789-5800.

Engelmann, R. J. 1970. "Scavenging Prediction Using Ratios of Concentrations in Air and Precipitation." In Precipitation Scavenging (1970), coords. R. J. Engelmann and W. G. N. Slinn, pp. 475-486. CONF-700601, National Technical Information Service, Springfield, Virginia.

Junge, C. E. 1963. Air Chemistry and Radioactivity. Academic Press, New York.

Slinn, W. G. N. 1984. "Precipitation Scavenging." In Atmospheric Sciences and Power Production, ed. D. Randerson, pp. 466-532. DOE/TIC-27601, National Technical Information Service, Springfield, Virginia.

PNL'S CONTRIBUTIONS TO PRECP-II (PRESTORM)

D. S. Daly, M. T. Dana, A. C. D. Leslie, C. G. Lindsey, and W. G. N. Slinn

This article summarizes PNL's contributions to PRECP-II. In large measure, these contributions were to coordinate the many PRECP contributors to PRECP-II and to coordinate interactions with the PRESTORM community: Leslie led the first of these coordinations; Lindsey, the second. Table 1 lists the organizations participating in PRESTORM and in PRECP-II; Figure 1 gives an indication of the components of PRECP in PRESTORM. In this article, first, will be a brief description of PRESTORM, then an overview of PRECP's role in PRESTORM, and finally, mission summaries and indications of the next steps in this research.

The PRESTORM Program

PRESTORM, as its acronym implies, was a first step in NOAA's STORM program, which seeks to improve the ability to forecast middle-scale (or mesoscale) storms. PRESTORM was directed by the Environmental Research Laboratory's Weather Research Program (NOAA/ERL/WRP) and was designed by individuals from a host of organizations (see Table 1) both to test state-of-the-technology measurement systems, in preparation for the STORM-Central field studies scheduled for 1990, and to initiate studies of storms described as Mesoscale Convective Systems (MCSs).

TABLE 1. Organizations Participating in PRESTORM

PRESTORM Operations

Hurricane Research Division (NOAA/HRD)
Illinois State Water Survey
National Center for Atmospheric Research (NCAR)
- Convective Storms Division (CSD)
- Field Observing Facility (FOF)

National Environmental and Satellite Data Information Service (NESDIS)
National Severe Storms Laboratory (NSSL)
National Weather Service (NWS)
Wave Propogation Laboratory (NOAA/WPL)
Weather Research Program (NOAA/ERL/WRP)
Universities:
- Colorado State University
- Oregon State University
- South Dakota School of Mines and Technology
- University of Washington
- University of Wyoming

PRECP Contributors to PRESTORM (and Principal Investigators)

Pacific Northwest Laboatory (G. Slinn)
Brookhaven National Laboratory (T. Kelly)
Argonne National Laboratory (R. Coulter)
NOAA Air Resources Laboratory (J. Boatman)
NCAR Research Aviation Facility (A. Schanot)
University of Maryland (R. Dickerson)
Denver University (D. Stedman)
State University of New York - Albany (V. Mohnen)

Mesoscale Convective Systems are especially common in the central and eastern United States during late spring through late summer. In this region, they are triggered by atmospheric instability associated with the convergence of low-level warm, moist air from the Gulf of Mexico and upper-level cold, dry air from the central and northern Rockies. The MCSs are classified in terms of their size and duration, as outlined in Table 2.

PRESTORM's primary interest was to investigate the meso-beta and meso-alpha-scale MCSs. Meso-gamma storms were studied as precursors to the larger storms. Typically, the meso-gamma storms begin forming during late afternoon hours. If the atmospheric environment favors their continued development and organization into the larger systems, the meso-beta and meso-alpha storms become most active during the night. The

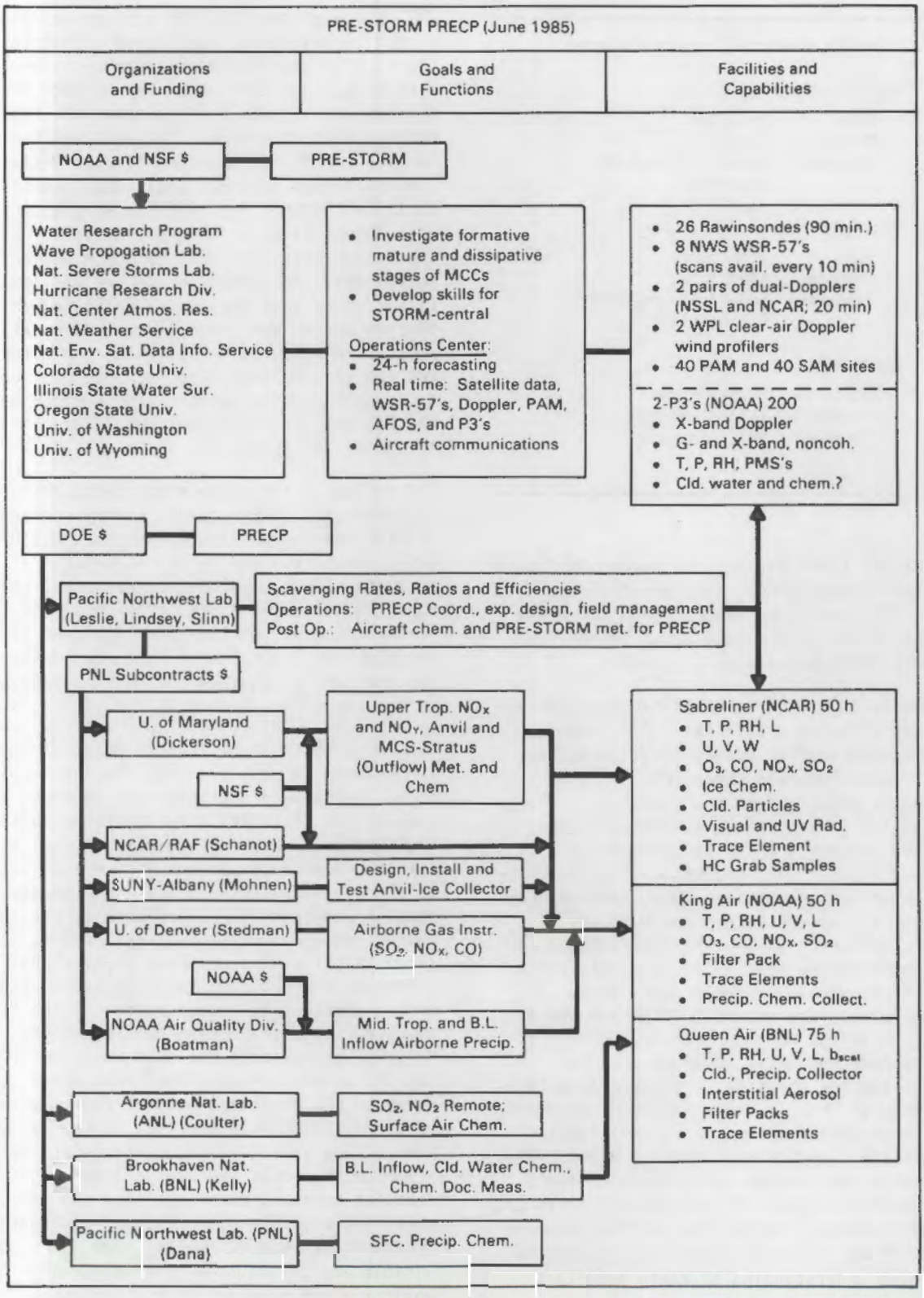

FIGURE 1. Organizational Structure of PRECP-II.

TABLE 2. Mesoscale Convective Systems

Gamma-scale	
Size:	2 to 20 km
Duration:	1 to 6 h
Examples:	Isolated Cb, Multicell, Supercell
Beta-scale	
Size:	20 to 200 km
Duration:	6 to 12 h
Examples:	Squall Line, Convective Cloud Cluster
Alpha-scale	
Size:	200 to 2000 km
Duration:	12 h to a few days
Examples:	MCC, Hurricane

largest of these storms, the Mesoscale Convective Complex (MCC), can last for several days; MCCs have been tracked from the Great Plains states to the East Coast and beyond (Maddox 1980, Bartels et al. 1984).

Mesoscale convective systems can have serious impacts on human activities. For example, many severe weather events (e.g. tornadoes, hail, downbursts/windshear, etc.) are observed to occur before the formation of large MCSs. The links between smaller, intense weather systems and the larger mesoscale systems are not well understood, but evidence indicates that conditions favorable for MCSs need to be present before the outbreak of severe weather. During the later stages of MCS development, especially at night, large stratiform precipitation regions form. Although stratiform rainfall rates are not so great as in the more convective portions of the storms, the areas affected are much larger and the duration of the precipitation is longer. Thus, a large amount of rainfall can occur over a wide area, significantly increasing flooding potentials. Given these circumstances, better understanding of MCS evolution is needed if forecasting skills are to be improved. Hence, the basic mission of PRESTORM was to begin the effort leading to improved understanding of these important weather events.

The design of the PRESTORM program was based on monitoring convective storms with both a fixed, high density observing network and with long-range aircraft. The surface-based instrumentation was deployed over the entire Kansas-Oklahoma region. National Weather Service rawinsonde stations over an 8-state area performed numerous additional soundings during PRESTORM. The aircraft were based at Will Rogers Airport, Oklahoma City, which was the headquarters for most of the experiment's activities. An Operations Center was established there that included a dedicated forecasting center and numerous real-time data acquisition systems for planning and directing the various components of each mission. Additional mission support was provided by the National Severe Storms Laboratory (NSSL) in Norman, Oklahoma.

The design of the surface observing network is summarized in Figure 2. Eighty surface stations were established over the PRESTORM area. Each recorded basic meteorological parameters such as winds, temperature, moisture, radiation, and precipitation. The northernmost 40 stations were equipped with the NCAR PAM II (Portable Automated Mesonet) systems, which provided the data in real-time to the Operations Center.

For PRESTORM, a significantly enhanced upper air network was established. Twelve supplemental rawinsonde stations were deployed to augment the 14 existing NWS stations in the PRESTORM area. During experiments, all the stations routinely performed soundings at up to 90-min intervals. In addition, three Doppler wind profilers were used to provide hourly soundings of tropospheric winds. The supplemental rawinsondes and Doppler profilers were positioned to support operation of two dual-Doppler radar systems. The NSSL operated its dual-Doppler network in the Oklahoma area, while the NCAR CP-3 and CP-4 Doppler radars were deployed near Wichita, Kansas. NWS digitized weather radars were monitored from the Operations Center and were used extensively during the course of the experiments. NSSL operated a lightning detector network, which recorded the time, position, and intensity of cloud-to-ground lightning flashes. Finally, satellite-visible and IR images were continuously monitored and recorded at the Operations

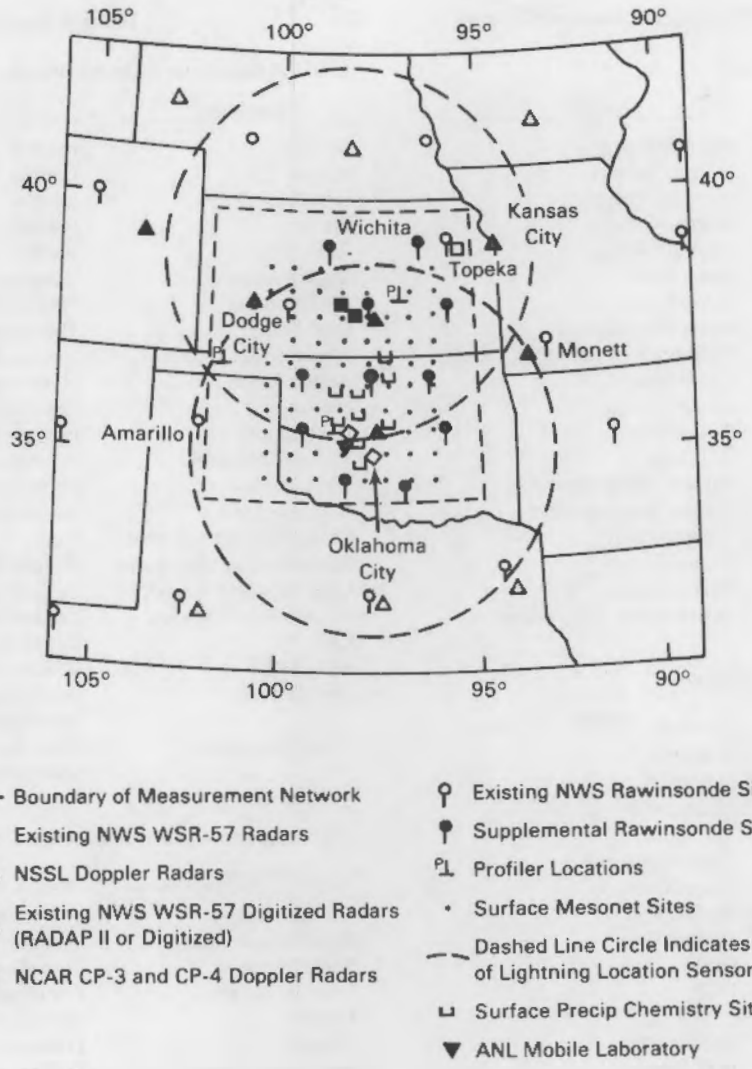

FIGURE 2. PRESTORM Surface Measurement Network.

Center. Likewise, all NWS products (surface and upper-level charts, satellite data, forecast products, station observations, etc.) were archived during the course of PRESTORM.

PRESTORM aircraft operations used two Lockheed P-3 research aircraft. These four-engine, turhoprop airplanes are capable of carrying large payloads for missions lasting up to 10 hours. The P-3s are operated by NOAA's Hurricane Research Division and are regularly used for storm penetrations during the hurricane season. Some of the aircraft observing capabilities are summarized in Table 3a. Both aircraft are equipped with extensive radar capabilities, including an airborne Doppler radar on the NOAA-43 aircraft. During PRESTORM, the basic mission for the NOAA-43 aircraft was to fly at constant altitudes and to provide Doppler radar coverage of the storm environment. The NOAA-42 aircraft was used primarily as a microphysics platform and performed numerous soundings within the storms themselves. In addition to the radar reflectivity data, these aircraft provided high resolution coverage of three-dimensional winds, temperatures, moisture, and radiation.

PRESTORM missions were conducted throughout May and June 1985. A number of successful missions were completed and a large data set

TABLE 3. PRECP/PRESTORM Aircraft Instrumentation

a) NOAA P-3 Instrumentation

Parameter	Sensor
Position	Inertial/Omega
u, v, w	Inertial/Omega
Heading	Inertial/Omega
Pitch	Inertial/Omega
Roll	Inertial/Omega
Ambient Pressure	Transducer
Dynamic Pressure	Transducer
True Altitude	Radar Altimeter
Air Temperature	Platinum Resistance Radiometer
Dew Point	Cooled Mirror
Surface Temperature	Radiometer
Cloud Liquid Water	Hot Wire
Cloud Particle Images	Optical Spectrometer
Precip Particle Images	Optical Spectrometer
PPI Reflectivity	C-band Radar
RHI Reflectivity	X-band Radar
RHI Doppler (43 only)	X-band radar
Photography	16 mm Color Time Lapse

b) NOAA King Air Instrumentation

Parameter	Sensor
Position	LORAN-C
u, v	LORAN-C
Air Temperature	Platinum Wire
IR Radiometer	
Dew Point	Cooled Mirror
Pressure	Transducer
Cloud Water	Slotted Rod
Liquid Water Content	Heated Wire FSSP
Drop Concentration and Distribution	FSSP
Aerosol Size Distrib.	ASASP-100x
Aerosol Size/Compos.	PIXE Filters
SO_4, NO_3, SO_2	Filters
CO	U. Denver, Modified
NO_x, NO_y	U. Maryland, Modified
SO_2	Flame Photometric, Modified

TABLE 3. (contd)

c) NCAR Sabreliner Instrumentation

Parameter	Sensor
Position	Inertial
u, v, w	Inertial
Heading	Inertial
Pitch	Inertial
Roll	Inertial
Static Pressure	Variable Capacitance
Air Temperature	Platinum Resistance
Dew Point	Thermoelectric
Absolute Humidity	Lyman-alpha Hygrometer
Attack Angle	Flow Angle Sensor
Sideslip	Flow Angle Sensor
IR Radiation	Pyrgeometer
Visible Radiation	Pyranometer
UV Radiation	Photometer
Ice Detector	Accretion of Droplets
Cloud Droplet Spectrum	FSSP
Hydrometeor Spectrum	Optical Spectrometer
Cloud Particle Images	Optical Spectrometer
Hydrometeor Images	Optical Spectrometer
CO	U. Maryland, Modified
NO_x, NO_y	U. Maryland, Modified
Ice Collector	Inertial Rod, SUNY-Albany, Specially Made Prototype
Trace Elements	RAM Air Filter, Custom Built by PNL

d) BNL Queen Air Instrumentation

Parameter	Sensor
Temperature	Thermistor, Reverse Flow
Relative Humidity	Weather Measure
Static Pressure	Transducer
True Air Speed	Pitot/transducer
Heading	Humphry Gyro
Position	LORAN-C
Horizontal Winds	LORAN-C
Scattering Coefficient	Nephelometer
Turbulence Intensity	Turbulence Meter
Cloud Liquid Water	Hot Wire
NO_x, HNO_3, NO, NO_2	BNL Modified Monitor Labs 8840
Ozone	AID 560
SO_x, SO_2, Sulphate	BNL Modified Melloy
Cloud Water Collection	Warm: Standard SUNY CW Collectors Supercooled: AES Modified SUNY Collectors, with Extractable Meshes
Rainwater Collection	Standard SUNY Collectors
Filter Pack and Flow Monitoring System, for Aerosol Chemical Composition, HNO_3, SO_2	BNL Design with CERL Separator for Water Extraction

is being prepared from which researchers can select specific cases of interest. These missions will not be discussed here, but WRP is preparing a mission summary document, which will be available in late 1985. Actual data management for PRESTORM rests with the WRP staff, who are responsible for preparing and maintaining an archive of nearly all observations acquired during the course of the experiments. At present, the scheduled

date for availability of PRESTORM data is January 1986. Requests for these observations from PRECP researchers will be coordinated through the PNL data manger, Don Daly, who in turn will work with his counterpart at WRP.

PRECP'S Role in PRESTORM

An important goal of the PRECP program is the collection of data for the interpretation of wet scavenging processes associated with a variety of storm types (e.g., stable frontal, unstable frontal, convective, orographic, etc.). PRECP's overall goal during PRESTORM was to collect data that could be used to evaluate the role of deep MCSs as pollutant-scavenging mechanisms. Such systems represent a potentially significant scavenging mechanism throughout the eastern United States. Recent evidence suggests that a mature MCS may process as much as 10^6 km^3 of boundary-layer air during its lifetime. This volume can be represented reasonably by a box of air 1000 km x 1000 km x 1 km. As mentioned earlier, precipitation amounts from such storms are usually quite large and in fact may account for up to one-half the annual precipitation over a large area of the United States. Also, the highly convective nature of these storms produces strong vertical circulations through much of the troposphere. Hence, such storms may be able to redistribute unreacted pollution to the upper troposphere, where it can be subject to long-range transport by upper-level winds. Finally, during May and June these storms tend to occur regularly with a period of only a few days between events. These considerations suggest that the MCS-type storm can digest a significant fraction of the air pollution found in the central and east-central United States. To learn how they do so, and how well they do it, was the primary objective of PRECP's efforts during PRESTORM.

From PRECP's viewpoint, a drawback to PRESTORM was its location: concentrations of anthropogenic pollutants in the Oklahoma-Kansas region were expected to be lower than in the more industrialized northeastern United States. This assumption was subsequently verified by observations. However, it was anticipated (and also confirmed by observations) that pollutant concentrations would be more homogeneous spatially, simplifying extrapolations from a necessarily limited number of observations to a large spatial scale. Thus the smaller gradients of pollutant concentrations will better serve to isolate the meteorological variability of scavenging processes from variations caused, for example, by changing rates of pollutant emissions, common in the Northeast. Moreover, since a goal of PRECP is to define any nonlinearities in precipitation scavenging, the PRESTORM location can be expected to provide PRECP with benchmark data at low pollutant concentrations to contrast with results from the Northeast.

Table 4 lists the specific objectives of PRECP in PRESTORM. In pursuit of these objectives, PRECP adopted the basic mission concept sketched in Figure 3. Three research aircraft were used to monitor pollutant concentrations in the inflow and outflow regions of the convective storms. The BNL Queen Air operated in the low-level inflow zone, generally at the "front" of the storm. The Queen Air also was used to collect airborne precipitation as flying conditions permitted. The NOAA King Air was used to monitor concentrations in mid-tropospheric regions (where secondary inflow regions often form at the "back" of the convective storms) and in the low-level inflow zone. Finally, the NCAR Sabreliner jet was used to measure pollutant concentrations in the upper-level outflow and anvil regions of these large storms. The Sabreliner also performed profiles between these high altitudes and the boundary layer.

The PRECP aircraft were instrumented to measure standard meteorological parameters and a number of chemical species (see Figure 1 and Tables 3b, c, and d for a listing of the basic variables measured). The species sampled included SO_2, SO_4, NO_x, NO_y, CO, O_3, and a host of trace metals. The surface precipitation samples are being analyzed for major ions, H_2O_2, and trace metals. State-of-the-art gas-phase NO_x/NO_y instruments were used by the University of Maryland onboard the Sabreliner and were provided for use on the King Air. Denver University deployed SO_2, CO, and O_3 instruments for some of the aircraft. The Sabreliner was equipped to collect ice samples from the anvil regions of the storms; a prototype ice collector was designed for PRESTORM by researchers at SUNY-Albany.

TABLE 4. Scientific Objectives of PRECP in PRESTORM

1) To determine the mass of boundary layer air transported by convection into the free troposphere on various convective scales, using CO and other relatively inert tracers of boundary layer air and using PRESTORM definition of winds for the estimation of fluxes.

2) Using data from 1) and measured concentrations of SO_2, SO_4, NO_x, NO_y, and trace metals in inflows and outflows, to define the relative efficiency of pollutant transport from the planetary boundary layer.

3) Using data from 1), 2), and both surface and airborne measurements of chemical composition of precipitation, to determine scavenging ratios and efficiencies and relative scavenging rates for the chemical species already listed plus all other major anions and cations.

4) Using data from 1) and 3) plus cloud microphysics and dynamics information from other PRESTORM participants, to obtain a data set for testing precipitation scavenging models such as PLUVIUS.

5) To document pollutant concentrations via clear air profiles, cloud water samples, and interstitial air measurements, for comparison with similar measurements from the northeastern United States.

6) To determine evidence for in-cloud pollutant processing in nonconvective or slightly convective situations, using measurements from clear air, interstitial air, cloud water, and stratiform precipitation for species such as SO_2 and H_2O_2.

7) To determine differences in chemical composition between cloud and rain water, especially to define subcloud NO_3-scavenging.

8) To examine aerosol production/enhancement by evaporation of clouds in the free troposphere.

9) To determine the chemical composition of ice and interstitial particles and gases in the outflow of deep storms.

10) To verify the existence of strata of photochemically produced 03 by the observation of bands of O_3, CO, and NO_x.

11) To examine cloud entrainment from top and sides using O_3 and CO as tracers of opportunity.

12) To verify and quantify production of NO_x in clouds without lightning, e.g., in fair weather Cu, stratus clouds etc.

13) To test the photostationary state as a function of altitude.

14) To determine the mean profile of NO_x in the troposphere, (e.g. to determine the relative contribution of stratospheric or PBL sources).

15) To examine if the resultant influence of storm processing on vertical profiles of pollutants is detectable and interpretable.

While the aircraft measured pollutants flowing into and out of the storms, PNL and ANL staff collected precipitation at the surface for chemical analyses. PNL maintained a fixed precipitation-chemistry network where automatic samplers were used. The locations of these stations are shown in Figure 2. During missions, the PNL and ANL staff collected sequential precipitation samples after travelling to areas where rainfall was occurring or was expected to occur. ANL also provided its mobile laboratory, where continuous measurements were made of integrated SO_2 (later NO_2) profiles and where air samples were taken with filter packs (for aerosol ions, SO_2, and HNO_3) and a "streaker" sampler (for 4-h concentrations of trace elements in "coarse" and "fine" size-classified aerosols).

The final component of the basic mission concept was of course the acquisition of data by the PRESTORM network and aircraft. By combining these observations with the chemistry measurements, budget studies can be undertaken to investigate the various scavenging mechanisms active in the MCS-type storm. For example, CO and several of the trace metals can be used as tracers for monitoring the fate of boundary layer air in the storm circulations and for deducing the effectiveness of the storms at incorporating sulfate, nitrate, and other pollutants into cloud water and subsequently depositing these materials in precipitation at the surface. The next section briefly summarizes some of the missions, expected analyses, and preliminary findings from PRECP-II.

Mission Summaries and Future Research Efforts

Because of the limited range of the PRECP aircraft, most research missions were restricted to the Oklahoma portion of the

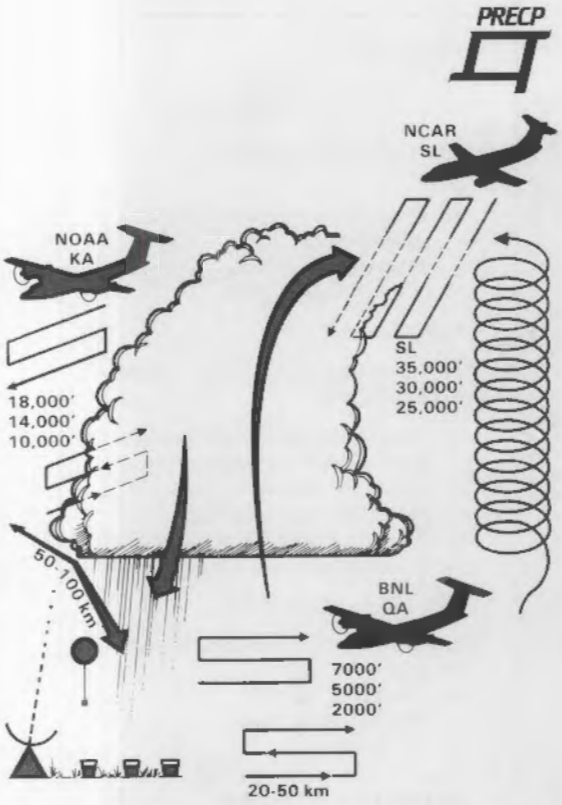

FIGURE 3. Basic Mission Concept for PRECP Operations During PRESTORM.

PRESTORM network. However, this did not hinder operations significantly owing to the frequency and size of the storms that occurred during June. Nighttime operations posed more of a hazard to the small research aircraft. During the first half of June, all missions were restricted to daylight, Visual Flight Rules (VFR) flying. The flight crews and mission coordinators acquainted themselves with PRESTORM operations and the type of flying conditions to be encountered in the presence of large, convective storms. During the second half of June, several successful missions were undertaken in conjunction with the P-3 aircraft during nighttime hours.

Summaries of the PRECP missions are given in Table 5. Listed are the dates, the prevailing weather conditions studied, the aircraft used for each mission, the supporting meteorological and precipitation chemistry data available, and remarks on the nature of each mission. At present, several missions have been identified as particularly successful. These missions will be the subject of the first set of studies from the PRESTORM program. In order of priority, the data sets to be analyzed are: June 15, June 26/27, June 21/22, and June 10. These missions were chosen because they include some or all of the elements of the basic mission concept outlined above. Other missions are more suitable for evaluating aspects of clear air and cloud water chemistry. These will not be elaborated on further here. A brief summary of each mission and some of the proposed studies using these data are given below.

For the June 15 case, the three PRECP aircraft sampled in the vicinity of an isolated cumulonimbus convective storm. The Queen Air and King Air flew in the inflow zone, sampling at various altitudes from the boundary layer to mid-tropospheric levels. The Sabreliner sampled in the upper-level outflow region at 35,000 ft and performed several profiles between high altitudes and the boundary layer. From preliminary results, this mission provided the first clear evidence of transport of boundary-layer air to the upper troposphere by convective storms. Using CO as an inert tracer, boundary-layer concentrations were on the order of 250 ppb, while in the anvil, CO concentrations were on the order of 200 ppb. Sensitive NO_x measurements indicated the possible production of NO_x, as upper-level concentrations were of the order of 7 ppb while boundary layer concentrations were from 2 to 3 ppb. While it is not yet clear what may have caused this apparent increase in NO_x, one possibility being investigated is lightning. The June 15 case is well suited for a first set of analyses because the storm was small and short-lived, yet well documented by the aircraft measurements. Both observations and numerical simulations will be used to examine the transport and scavenging of pollutants by this storm.

The most complex mission took place on June 26/27. A cold front moved through the PRESTORM network from northwest to southeast, triggering a linear MCS. During daylight hours on the 26th, intense convection dominated all along the frontal boundary. During the evening of the 26th and progressing through the early hours of the 27th, a large stratiform precipitation region formed behind the front. This pattern is fairly typical of the temporal evolution of MCSs. PRECP aircraft conducted two separate missions, one

TABLE 5. PRECIP Mission Summaries for PRESTON Operations

DATE	WX	Aircraft	Surface	Remarks
6/4	Upper level⩀; strat. precip. (8inch at OKC)	QA	• ⊔ ⚲ ⚳	Shakedown; H20 collection
6/5	1) AM: same as 6/4	QA, KA	• ⊔ ⚲ ⚳	• Same as 6/4; document air mass concentration
	2) PM: clean air	SBRL	•	• Shakedown; document mid and upper trop.✕'s over KS, OK
6/6	Light rain	QA	• ⊔ ⚲ ⚳	H_20 collection
6/8	Clear	QA, KA, SBRL	⊥ o	PRECP a/c intercomparison; clear air documentation
6/10	Small⌈⥹; otherwise clear (precip. in SFC net. in evening)	QA, KA, SBRL	• ⊥ ⚲ ⚲ ⚳ ⏶ ⊔ ⥹ ⊥	• Coordinated inflow/outflow mission on Cb; mature, dissipative stage; ice sample in anvil; no precip; passes beneath cell (Virga). • Document air mass✕'s prior to nocturnal precip.
6/12	Clear	SBRL	⊥ o	Clear air documentation
6/15	⌈⥹ Dissipative B-scale	QA, KA, SBRL	• ⚲ ⚳ ⥹	Inflow/outflow on early/nocturnal dissipative stages of Cb: • 300 ppb CO @ 3500′ 200 ppb CO @ 35,000′ • PBL 2 ppb NO_x Upper trop., anvil 7 ppb NO_x • QA: 3500′, 5500′, 8500′ KA: 10,000′, 14,000′ SBRL: 18,000′, 25,000′, 35,000′
6/16	Clear w/developing ⌈⥹ in KS; developing B-scale MCS along cold front	QA, KA, SBRL (N43, N42)	• ⊥ ⚲ ⚲ ⚳ ⥹ ⊥	• QA, KA: clear air docum.; inflow concentrations • SBRL: profiles near large Cb • Page (ANL) overflight
6/17	I) AM: cold front w/⌈⥹	QA, SBRL	• ⊥ o ⊔ ⚲ ⥹ ⊥	• QA: inflow✕'s and H_20 collect. • SBRL: upper level outflow
	2) PM: cold front w/⌈⥹	KA, SBRL	• ⊥ o ⚲ ⚳ ⏶ ⥹ ⊥	• inflow/outflow • No precip. collected
6/18	Weak cold front with showers over Northern TX	KA, SBRL		Scrubbed - AP
6/20	Clear	SBRL, N43		SBRL - P3 intercomparison
6/21-22	1) Cold front; conv. line ⌈⥹; heavy precip. (late evening)	KA	• ⊥ o ⚲ ⚲ ⚳ ⏶	• KA: inflow along line 3500′, 5000′, 7000′
		N43, N42	⊔ ⥹ ⊥	• N42, N43: flow fields, microphysics • SFC precip: auto and sequential ✕'s behind line
	2) Weak cold front; (early AM)	QA	• ⊥ o ⚲ ⚳ ⥹ ⊥	
	3) Clear (afternoon)	SBRL		• Storm chase - monitor outflow • Doc. pollut. redistribution post storm
6/25	Clear;⌈⥹over TX pan.	QA, KA, SBRL	• ⊥ o ⚲ ⚳ ⥹	• QA, KA intercomparison; clear air docum. • SBRL: outflow from TX storm

TABLE 5. (Continued)

6/26-27	1) Cold front; advancing convective line; heavy precip. (afternoon); ⌈≀	QA, KA, SBRL	•⊥○⊔	• QA, KA: inflow to line; H_20 cell. • SBRL: outflow, ice • SFC: event and sequential precip.
	2) Cold front; conv. and strat. regions; ⌈≀ (late even., early morning)	QA, KA, SBRL N42, N43	•⊥○⊔	• KA: inflow • QA: inflow (aborted after. apprx. 2 hrs) • SBRL: outflow, inflow to back of storm; profiles • N43, N42: full dynamics and microphys. mission
	3) Clear (afternoon)	SBRL		• SFC: event and sequen. precip.; pollutant distribution documentation

Symbols

QA	Queen Air	•	Surface Mesonet Station
KA	King Air	⊥	SO_2/NO_2 COSPEC
SBRL	Sabreliner	○	Sfc Air Chemistry
N43	NOAA-43 Doppler P-3	⊔	Sfc Precip. Chemistry
N42	NOAA-42 Cloud Physics P-3		NWS RAOB
CTG	Cloud-to-ground		Supplemental RAOB
✕	Air Concentration		NWS Digitized Radar
Cb	Cumulonimbus		Doppler Radar
	Doppler Profiler	⊥	CTG Lightning Indicator
⌈≀	Alto-stratus	≀	Thunderstorm
SFC	Surface		

during the afternoon and the other later at night. All PRESTORM resources were available for these missions, except that the P-3 aircraft did not fly during the afternoon mission. All five aircraft were used for the nighttime mission. The King Air and Queen Air operated in the low-level inflow zone ahead of the line of convection, while the Sabreliner made passes through the upper-level outflow zone. The P-3s operated parallel to both sides of the line of storms and made several transects through the storm as conditions permitted. Full rawinsonde and Doppler radar coverage of this storm is available. Precipitation chemistry samples were collected at all of the fixed network stations. Sequential samples were taken at three sites.

The June 26/27 storm likely will be the most intensely studied of all the PRECP-II case studies. The nature of the storm will be amenable to two-dimensional studies, initially, greatly simplifying analysis procedures. The dual missions also will provide an opportunity to investigate differences in scavenging mechanisms between hard convective situations and more benign stratiform processes. In addition, the dual missions will support investigations of the diurnal evolution of precipitation scavenging. Possible decoupling of the nocturnal inflow zone from the boundary layer may prove responsible for any differences observed between daytime and nighttime scavenging processes. Also, this storm was highly electrified. Some initial investigations of NO_x production by lightning are under way at ANL, BNL, and PNL.

The June 21/22 storm was similar in nature to the June 26/27 event. A line of hard convection formed late in the evening of June 21 along the Kansas-Oklahoma border. All PRESTORM resources, including both P-3 aircraft, were used to study this event. The King Air sampled extensively in the low-level inflow, ahead of the line. Both fixed and sequential precipitation samples were collected at the surface. However, the Sabreliner was unable to join in the mission, so that no measurements are available of upper-level outflow concentrations. Nevertheless,

this case will be useful for studying precipitation scavenging and evaluating scavenging efficiencies. Again, because of the linear nature of this storm, two-dimensional analyses (including numerical simulations) can be used during the initial investigations of this event.

The June 10 case is expected to be the focus of several PRESTORM research efforts. PRECP did not fly during the actual storm event, but documented the clear air concentrations in the inflow air feeding the storm and in the residual air mass following storm dissipation. Several precipitation samples were collected in the fixed network. This case can be used as a verification data set to test the conclusions drawn from analysis of the preceding cases.

Summary

PRESTORM provided PRECP researchers with an important opportunity to study, in great detail, dynamical and microphysical processes involved in precipitation-scavenging by convective storms. The PRESTORM experience was both beneficial and successful in terms of the goals established by PRECP before the field program. It is likely that the data acquired will be the subject of in-depth investigations over the next several years.

At present, both PRECP and PRESTORM are involved in preparation of final, archived data sets from the numerous platforms used during the experiments. The PRESTORM data will be available for general dissemination by January 1986. The PRECP data are nearly complete as of this writing, with the exception of analyses of the filters and precipitation samples for trace elements. These should be completed by early 1986. PNL is responsible for archiving the complete PRECP/PRESTORM data set. Activities are under way to produce a standardized data base that will be compatible with other experiment data sets produced during the course of the PRECP program.

Acknowledgments

Substantial technical and logistical contributions were made by D. W. Glover. All of the PRECP staff involved in PRESTORM express their gratitude to the PRESTORM community for their cooperation and assistance during preparation and execution of the PRECP experiments. Special thanks go to John Cunning and his staff at NOAA/ERL/WRP. Without their help, PRECP's participation and successes would not have been possible.

References

Bartels, D. L., J. M. Skradski, and R. M. Menard. 1984. "Mesoscale Convective Systems: A Satellite Data Based Climatology." NOAA Technical Memorandum, ERL ESG-8, Environmental Research Laboratory, Boulder, Colorado.

Maddox, Robert A. 1980. "Mesoscale Convective Complexes." Bull. Amer. Meteor. Soc. 61(11):1374-1387.

ANALYSES OF PRECIPITATION CHEMISTRY DATA FROM THE MAP3S AND APN NETWORKS

M. T. Dana and R. C. Easter

Statistical analyses of precipitation chemistry data from monitoring networks were performed for the "event" or daily sampling networks MAP3S and APN.[a] (APN is now incorporated in CAPMON, the Canadian Precipitation Monitoring Network.) The third national network with sampling frequency less than weekly, the Utility Acid Precipitation Sampling Program (UAPSP), should be the subject of future investigations. The Precipitation Chemistry Laboratory (PCL) data base for MAP3S (operated by PNL for EPA under interagency agreement) was used to update an earlier comprehensive statistical study (MAP3S 1982) to include data through 1983. Most of the same analyses for the previous paper were performed: ionic species concentration distributions, time trends (linear and periodic), monthly and annual precipitation-weighted averages, and species-pair and multiple-species regressions. Complete results and descriptions of techniques are in an article submitted for publication (Dana and Easter 1985); this article is a summary of highlights of that work and of a related

(a) Multi-State Air Pollution Power Production Study (MAP3S); Atmospheric Precipitation Network (APN).

study of deposition-episode statistics, which also includes some APN data.

Precipitation Chemistry from MAP3S, 1977 Through 1983

Table 1 is a summary of basic statistics for the four major ionic species: sulfur (sulfate plus oxidized sulfur-IV), NO_3^-, free H^+ (from pH), and NH_4^+. With the exception of the two coastal sites, Brookhaven, New York, and Lewes, Delaware (where Na^+ and Cl^- are important), these four species make up almost 90% of the total ionic equivalents in an average event sample. The concentration distributions are better approximated by log-normal than normal distributions, as suggested by the closer agreement between the medians and the geometric means than between the medians and the arithmetic means.

Linear and periodic (period fixed at 1 year) time-trend analyses were performed for the major species; a typical example of an event data-scatter plot, with regression curves applied for sulfur at the Penn State site, is shown in Figure 1. None of the linear time regressions is significant at $P < 0.05$ (student-t test), although the slopes of the trends are mostly negative. The lack of trends is not surprising, since the data set is still time-limited and since emissions of SO_x and NO_x have leveled off and/or decreased slightly during the period of MAP3S operation (EPA 1984).

Seasonal variations in event ionic concentrations are also illuminated by consideration of monthly precipitation-weighted concentrations (MPWC) and ratios of these for important species-pairs. Since the PCL data base includes results for at least 5 years for 8 sites, year-to-year variations in chemistry can be smoothed by consideration of "accumulated" MPWC, where each month's average is derived from data for the month collected in all 5 years:

$$MPWC = \frac{\Sigma\, c_i\, p_i}{\Sigma\, p_i}\,, \qquad (1)$$

where c_i and p_i are event concentration and precipitation, respectively, and the summations are over all events of the month during 5 years.

Figures 2 through 5 show these MPWC values for sulfur, and the ratio of sulfur to nitrate (molar), with the 8 sites divided into two groups representing the inland Northeast sites (INE), and the Midwest and coastal sites (MC). The coastal sites have a weak seasonal trend in nitrate, and the Midwest sites show higher sulfur values for the winter months. Thus, the seasonal trend in the ratio is less prominent for the MC sites than the INE sites. Potential reasons for this difference include:

- the tendency toward drier winters in the Midwest
- different storms or types of storms (e.g., frontal versus air-mass convective) that may be responsible for major depositions in the various parts of the MAP3S region
- oxidants for sulfur oxide conversion that may be more prevalent in the Midwest during the winter because of the greater influence of maritime tropical air from the Gulf of Mexico.

Deposition Episodes for MAP3S and APN

The product of concentration and precipitation amount, deposition, is of particular concern for acidic deposition effects research, and examinations of the distributions of deposition can help to assess the impact of particular high deposition events ("episodes") and identify the meteorological or geographical factors potentially responsible. The distribution of the product of concentration and precipitation is better described by the log-normal than the normal form, as are, separately, the concentration or the precipitation. Though these two factors are weakly negatively correlated, the deposition distribution is still quite broad, allowing for a considerable fraction of the total deposition to be accounted for by relatively few events.

Figure 6 illustrates the typical deposition-distribution pattern. On the abscissa is centile of deposition (i.e., event numbers, normalized highest to lowest from left to right), and the ordinate is fraction of the total deposition for the year. The range of these curves for the 9 sites in 1982 is quite narrow, indicating small spatial variation

TABLE 1. Unweighted Concentration (μmol/) and Precipitation Statistics for Whole-Year Records (1977 through 1983)

Site	NTOT[a]	NEDT[b]	YRS[c]	MIN[d]	MAX	A-MEAN[e]	A-SD[f]	G-MEAN[g]	G-SD[h]	Centile Values[d] MED[i]	05	25	75	95
SPECIES SULFUR														
WH	613	529	7	1.7	190.0	27.7	23.5	20.1	2.3	22.0	4.7	11.0	35.0	77.0
IT	496	449	7	0.7	240.0	39.9	35.4	28.6	2.3	30.0	6.8	17.0	49.0	100.0
PS	620	535	7	1.9	340.0	44.9	39.7	31.7	2.4	35.0	6.5	18.0	60.0	110.0
VA	440	351	7	2.9	250.0	38.4	32.6	28.2	2.2	29.0	6.8	16.0	50.0	100.0
IL	499	303	6	2.5	280.0	39.6	28.5	32.6	1.9	32.0	13.0	21.0	50.0	85.0
BR	379	296	5	0.5	170.0	33.7	30.3	23.5	2.4	24.0	5.5	13.0	43.0	100.0
LE	354	291	5	1.9	130.0	29.3	23.2	22.2	2.2	21.0	6.1	13.0	40.0	67.0
OX	434	313	5	1.7	180.0	39.0	27.0	31.5	2.0	31.0	12.0	21.0	48.0	92.0
OR	189	183	3	4.3	250.0	36.0	30.5	28.5	2.0	29.0	7.8	19.0	43.0	84.0
SPECIES NO_3^-														
WH	613	530	7	*	260.0	30.5	27.7	22.1	2.3	23.0	5.7	12.0	38.0	82.0
IT	496	450	7	2.5	280.0	42.2	32.1	33.3	2.0	34.0	10.0	21.0	53.0	100.0
PS	620	535	7	2.0	280.0	50.5	40.6	38.0	2.2	40.0	9.7	23.0	64.0	140.0
VA	440	351	7	3.2	530.0	37.1	39.0	27.2	2.2	28.0	7.5	16.0	44.0	92.0
IL	499	302	6	6.5	150.0	37.7	25.6	30.8	1.9	31.0	11.0	18.0	48.0	88.0
BR	379	297	5	*	280.0	37.4	42.4	21.1	3.2	23.0	2.7	9.7	49.0	110.0
LE	354	291	5	*	320.0	29.7	32.3	18.4	2.9	20.0	2.9	8.7	40.0	82.0
OX	434	312	5	3.0	140.0	34.5	24.0	27.9	1.9	27.0	9.0	19.0	45.0	80.0
OR	189	183	3	1.8	130.0	26.6	21.5	20.2	2.1	21.0	5.8	12.0	32.0	71.0
SPECIES H^+														
WH	613	520	7	0.5	295.0	57.9	40.7	44.9	2.2	49.0	13.2	28.2	79.0	130.0
IT	496	438	7	2.4	479.0	87.0	62.0	70.3	2.0	71.5	21.4	47.9	109.6	200.0
PS	620	493	7	0.2	479.0	93.2	68.5	69.2	2.5	77.6	16.6	45.0	120.0	234.4
VA	440	341	7	6.8	850.0	81.7	73.0	62.5	2.1	63.0	20.0	38.9	100.0	204.2
IL	499	320	6	0.3	380.0	63.3	50.6	41.9	3.3	51.3	2.2	33.1	79.4	158.5
BR	379	313	5	0.4	370.0	72.5	68.0	45.0	3.0	50.0	6.8	20.9	100.0	218.8
LE	354	293	5	2.2	331.0	57.7	51.8	39.3	2.5	42.0	7.2	20.4	79.4	147.9
OX	434	322	5	0.1	309.0	68.3	47.3	52.6	2.4	57.5	12.6	38.0	83.2	162.2
OR	189	183	3	1.6	398.0	63.5	50.0	50.2	2.0	51.3	17.0	31.6	77.6	151.4
SPECIES NH_4^+														
WH	613	519	7	*	160.0	17.4	19.8	9.2	3.6	11.0	0.7	4.1	23.0	54.0
IT	496	449	7	*	120.0	22.3	21.8	13.6	3.1	16.0	1.8	6.9	36.0	62.0
PS	620	522	7	*	250.0	24.1	26.3	14.5	3.0	17.0	2.1	7.3	31.0	66.0
VA	440	348	7	*	200.0	20.6	22.3	11.9	3.3	15.0	1.3	5.7	28.0	57.0
IL	499	302	6	0.7	210.0	28.4	24.9	20.6	2.3	22.0	4.8	12.0	34.0	74.0
BR	379	299	5	*	160.0	19.4	25.1	9.4	3.7	10.0	0.9	3.9	25.0	66.0
LE	354	291	5	*	79.0	16.5	15.7	9.3	3.4	10.0	1.0	4.3	26.0	50.0
OX	434	312	5	*	200.0	24.4	22.8	16.3	2.8	18.0	2.6	9.7	32.0	63.0
OR	189	183	3	*	100.0	15.2	15.6	8.6	3.4	11.0	0.7	3.9	22.0	38.0

(a) Total number of events.
(b) Number of events after edit.
(c) Years of record.
(d) Asterisk indicates at or below minimum detection limit.
(e) Arithmetic mean.
(f) Arithmetic standard deviation.
(g) Geometric mean.
(h) Geometric standard deviation.
(i) Median.

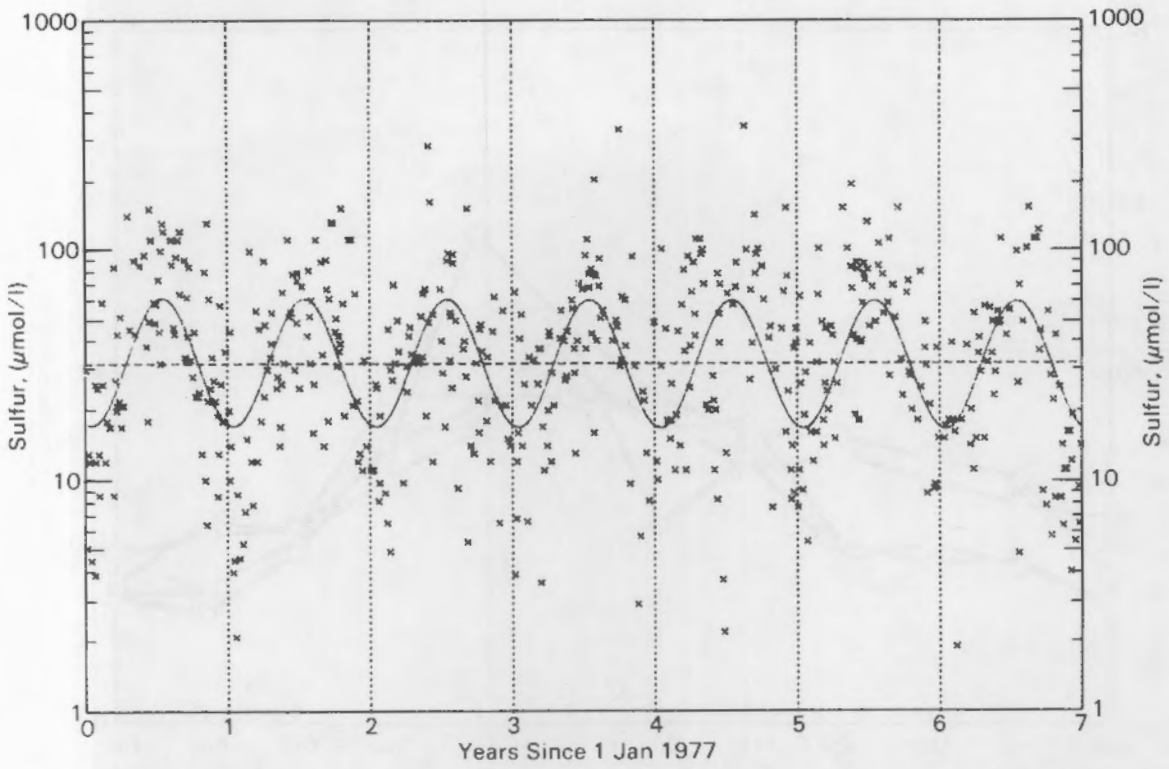

FIGURE 1. Event Sulfur Concentrations Scatter Plot, With Linear and Periodic Time Trend Regressions: The Penn State MAP3S Network Site.

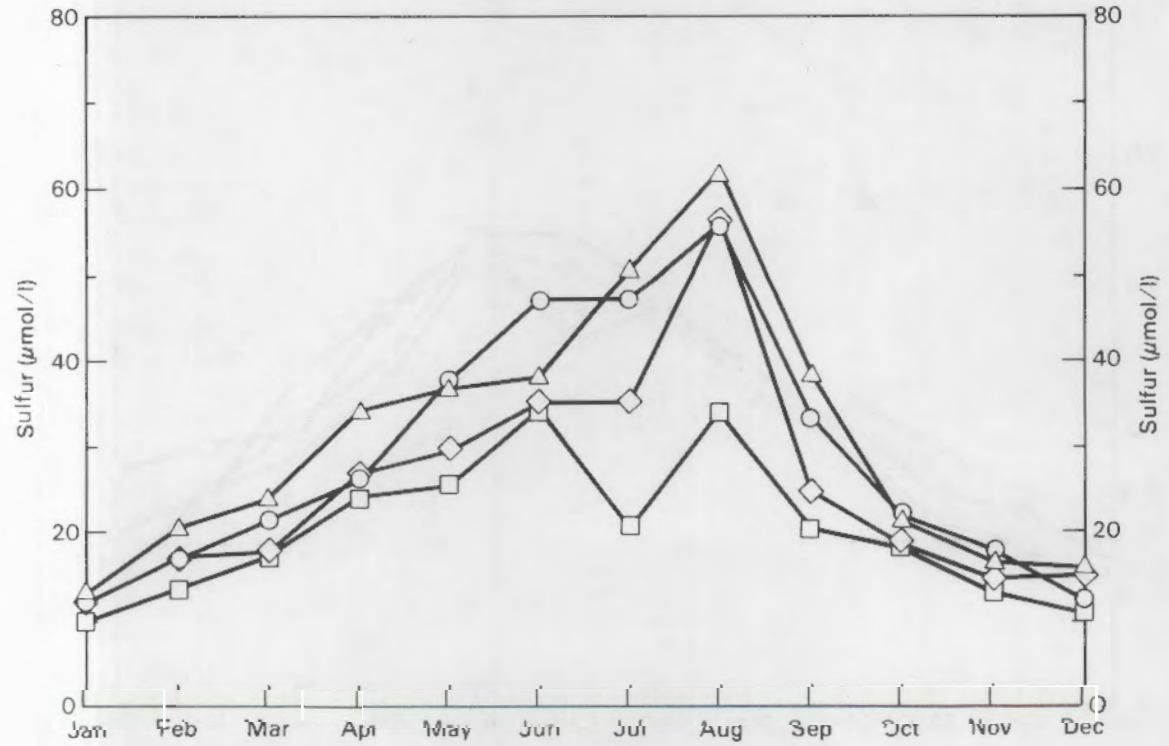

FIGURE 2. Cumulative Precipitation-Weighted Monthly Average Concentrations (MPWC) for Sulfur (1979-1983): Inland Northeast Sites (Whiteface □, Ithaca O, Penn State Δ, and Virginia ◊).

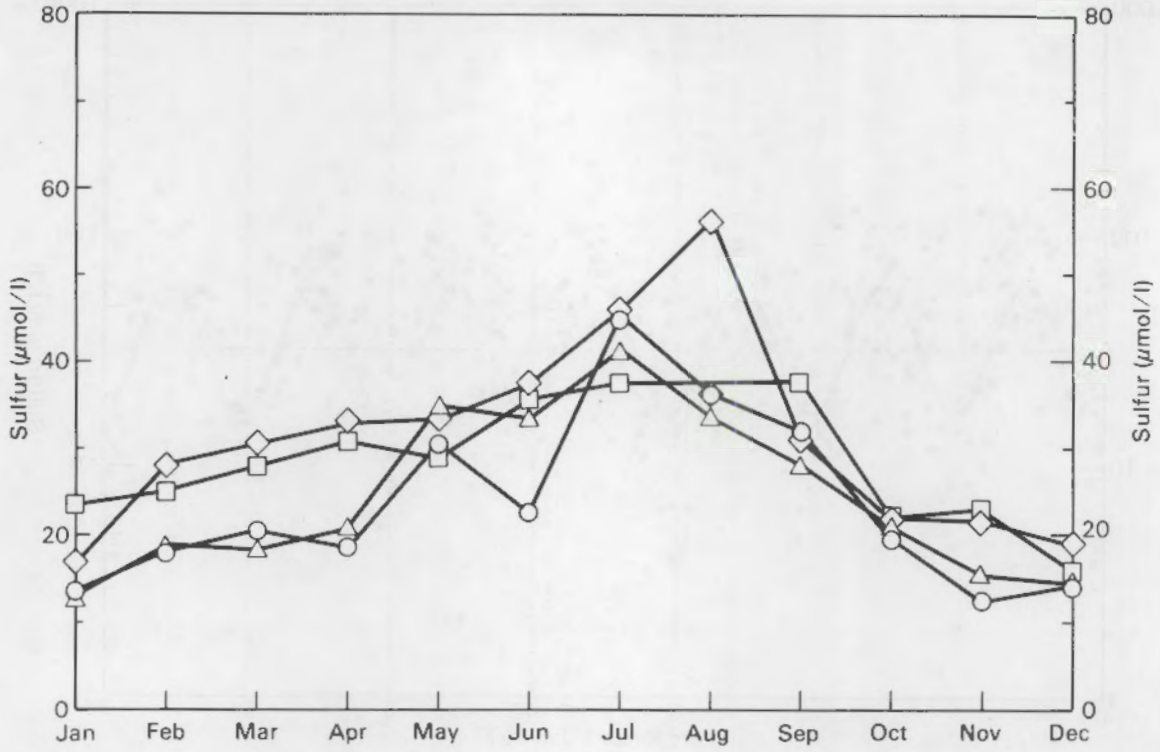

FIGURE 3. Cumulative MPWC for Sulfur (1979-1983): Coastal and Midwest Sites (Illinois □, Brookhaven O, Lewes Δ, and Oxford ◊).

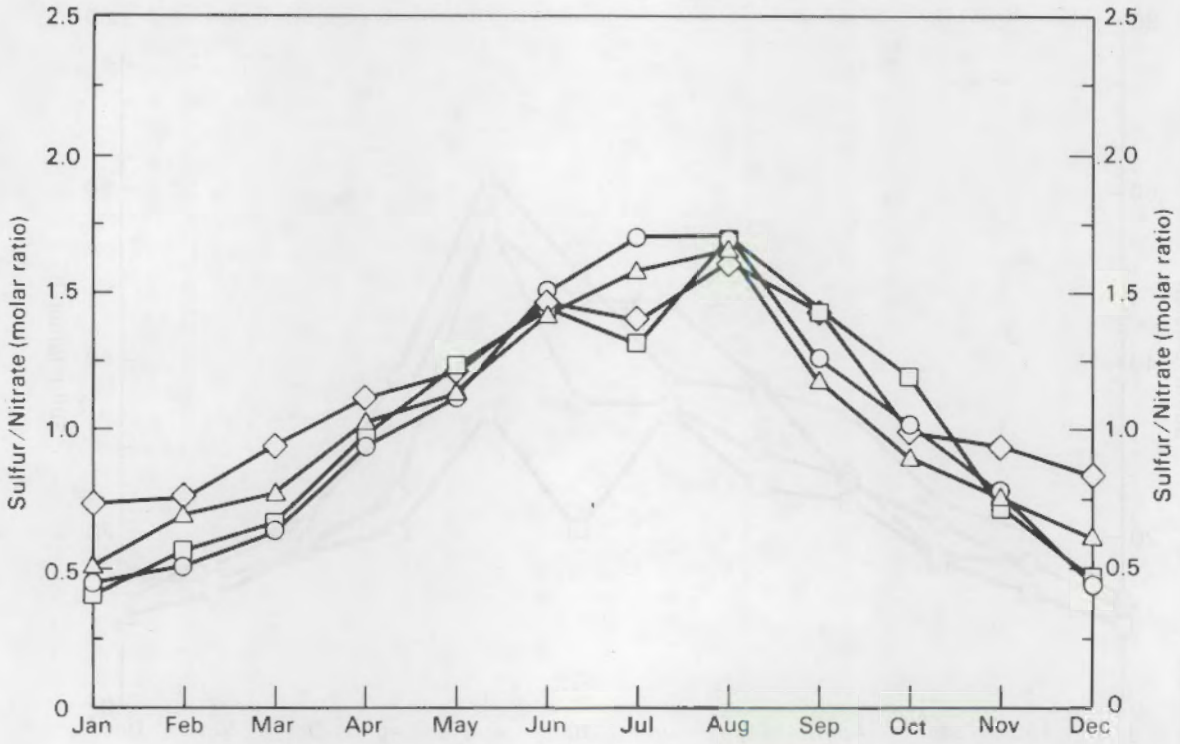

FIGURE 4. Ratios of Sulfur/Nitrate Cumulative MPWC. Site Designations as in Figure 2.

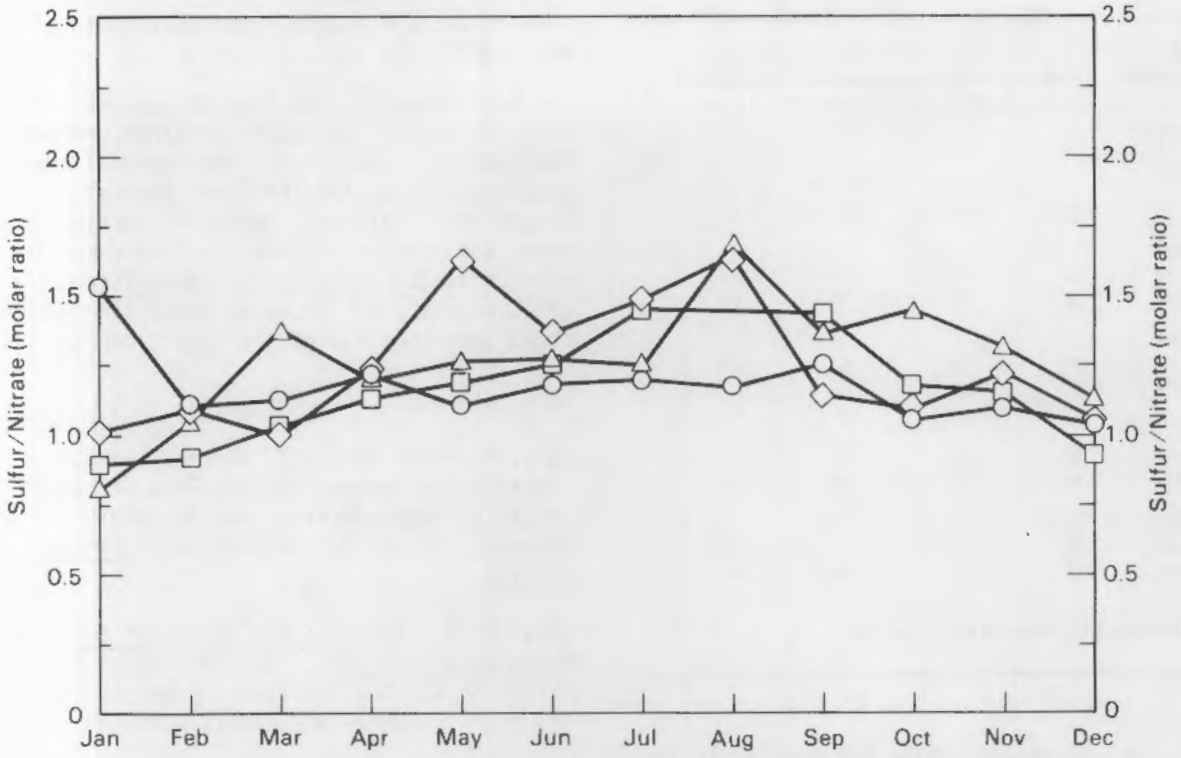

FIGURE 5. Ratios of Sulfur/Nitrate Cumulative MPWC. Site Designations as in Figure 3.

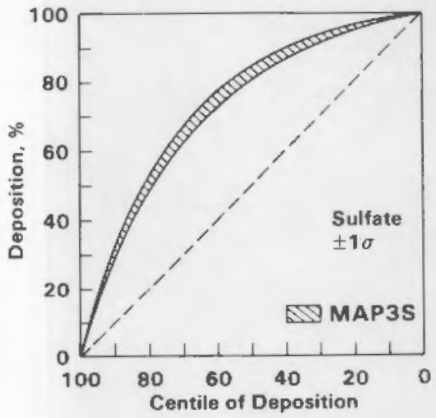

FIGURE 6. Cumulative Deposition for Sulfate as a Function of Fraction of Events, Ordered by Deposition. See Text for Explanation.

over the MAP3S region. Furthermore, the variance from year to year at any site is even less than the spatial variance for a given year.

The APN data for 1982 (when 7 sites were active for the entire year) were subjected to the same analyses for the major species. The APN sites appear to be more episodic (that is, divergence of curves as in Figure 6 from the linear trend is greater than for MAP3S), and the influence of concentration rather than precipitation amount on deposition is greater. This latter is illustrated by Table 2, where the fractions of event and year depositions are listed for the accumulation of events whose depositions are greater than the mean deposition. The fourth column, which is the ratio of the second and third columns, represents the mean concentration of the events whose deposition is above the mean, divided by the mean concentration for all events, and is a measure of the relative importance of concentration over precipitation.

The APN may be more episodic because several of the sites (in midwestern Canada, and in the far Northeast) are farther removed from major pollution sources, and less likely to be uniformly affected by acidic deposition as the direction of air motion during storms varies. However, the differences between the networks may be to some degree artifactual, since the MAP3S sampling protocol allows more

TABLE 2. Network Averages for Percentages of Events, Deposition, and Precipitation, Represented by the Events Whose Depositions were Greater Than the Mean Deposition: 1982

	Events	Deposition	Precipitation	$\bar{C}_m/\bar{C}$[(a)]
Sulfate				
MAP3S	36	71	62	1.1
APN	32	72	56	1.3
Nitrate				
MAP3S	39	69	64	1.1
APN	36	73	54	1.4
Hydrogen				
MAP3S	37	71	65	1.1
APN	30	75	52	1.4
Ammonium				
MAP3S	36	75	56	1.3
APN	32	77	48	1.6

(a) The ratio of columns 2 and 3–see text.

than one-day events, while APN uses strictly daily sampling. During 1982, the event-average precipitation amount for MAP3S was almost double that of the APN, while the network-average yearly precipitation totals were nearly the same.

For both networks, the time of year when the greatest deposition events occurred generally followed the usually observed seasonal trends in concentration for the major species. Although some individual events at particular sites and particular years could account for as much as 20% of the year's deposition, the great majority of the major deposition events shows less than 10% of the year's deposition.

References

Dana, M. Terry and R. C. Easter. 1986. "Statistical Summary and Analyses of Event Precipitation Chemistry from the MAP3S Network, 1976-1983." Submitted to Atmos. Environ.

EPA. 1984. National Air Pollution Emission Estimates, 1940-1983. EPA 450/4-84-028, Office of Air Quality Planning and Standards, Research Triangle Park, North Carolina.

MAP3S. 1982. "The MAP3S/RAINE Precipitation Chemistry Network: Statistical Overview for the Period, 1976-1980." Atmos. Environ. 16:1603-1631.

Publications and Presentations

PUBLICATIONS

Dana, M. T., and R. C. Easter. 1986. "Statistical Summary and Analyses of Event Precipitation Chemistry from the MAP3S Network, 1976-1983." Submitted to Atmospheric Environment.

Fritschen, L. J., J. R. Simpson, C. D. Whitman, and M. M. Orgill. 1985. "Energy Balance Stations in a Deep Colorado Valley: ASCOT 84." In Proceedings, 17th Conference on Agriculture and Forest Meteorology, pp. 1-3. American Meteorological Society, Boston, Massachusetts.

Horst, T. W. 1984. "The Modification of Plume Models to Account for Dry Deposition." Boundary Layer Meteorology 30:413-430.

Horst, T. W. 1985. "Nocturnal Drainage Flow on Simple Slopes." Boundary Layer Meteorology, in press.

Orgill, M. M., and R. I. Schreck. 1984. "Dissipation of Temperature Inversions and Drainage Conditions on a Mountain Slope." In Proceedings of the Third Conference on Mountain Meteorology, pp. 54-57. American Meteorological Society, Boston, Massachusetts.

Orgill, M. M., and R. I. Schreck. 1985. "An Overview of the ASCOT Multilaboratory Field Experiments in Relation to Drainage Winds and Ambient Flow." Bull. Am. Met. Soc. 66(10):1263-1277.

Orgill, M. M., R. N. Lee, R. I. Schreck, K. J. Allwine, and C. E. Whiteman. 1984. "Early Morning Ventilation of an SF_6 Tracer from a Mountain Valley." In Proceedings of the Joint Session of the Fourth Joint Conference on Applications of Air Pollution Meteorology and the Third Conference on Mountain Meteorology, pp. J36-J39. American Meteorological Society, Boston, Massachusetts.

Orgill, M. M., J. M. Thorp, and R. Coulter. 1985. "Interaction of Submesoscale Flows in Complex Terrain during Nocturnal Drainage Conditions." In Proceedings of Seventh Conference on Turbulence and Diffusion, pp. 244-247. American Meteorological Society, Boston, Massachusetts.

Simpson, J. R., L. J. Fritschen, C. D. Whiteman, and M. M. Orgill. 1985. "Surface Energy Balance in a Deep Colorado Valley: ASCOT 84." In Proceedings, 17th Conference on Agriculture and Forest Meteorology, pp. 8-11. American Meteorological Society, Boston, Massachusetts.

Slinn, W. G. N. 1985. "Concentration Statistics for Dispersive Media." Tellus-B, in press.

Whiteman, C. D., and K. J. Allwine. 1985. VALMET: A Valley Air Pollution Model. PNL-4728, Pacific Northwest Laboratory, Richland, Washington.

Whiteman, C. D., and S. Barr. 1984. "Atmospheric Mass Budget for a Deep, Narrow Valley in Colorado." In Preprints, Third Conference on Mountain Meteorology, pp. 61-64. American Meteorological Society, Boston, Massachusetts.

Whiteman, C. D., and S. Barr. 1985. "Atmospheric Transport by Along-Valley Wind Systems in a Deep Colorado Valley." Accepted for publication by J. Climate and Appl. Meteor.

Whiteman, C. D., L. J. Fritschen, J. R. Simpson, and M. M. Orgill. 1985. "Radiation Balance in a Deep Colorado Valley: ASCOT 84." In Proceedings, 17th Conference on Agriculture and Forest Meteorology, pp. 4-7. American Meteorological Society, Boston, Massachusetts.

PRESENTATIONS

Fritschen, L. J., J. R. Simpson, C. D. Whiteman, and M. M. Orgill. 1985. "Energy Balance Stations in a Deep Colorado Valley: ASCOT 84." Paper presented at the 17th Conference on Agricultural and Forest Meteorology, May 21-24, 1985, Scottsdale, Arizona.

Lee, R. N., K. J. Allwine, and M. M. Orgill. 1985. "Experimental Studies Using a Portable Gas Chromatograph for Real-Time Analysis of Perfluorocarbon Tracers in Atmospheric Samples." Paper presented at the American Chemical Society's 40th Northwest Regional Meeting, June 19-21, 1985, Sun Valley, Idaho.

Orgill, M. M., and R. I. Schreck. 1984. "Dissipation of Temperature Inversions and Drainage Conditions on a Mountain Slope." Paper presented at the Third Conference on Mountain Meteorology, October 16-19, 1984, Portland, Oregon.

Orgill, M. M., R. N. Lee, R. I. Schreck, K. J. Allwine, and C. E. Whiteman. 1984. "Early Morning Ventilation of an SF6 Tracer from a Mountain Valley." Paper presented at the Joint Session of the Fourth Joint Conference on Applications of Air Pollution Meteorology and the Third Conference on Mountain Meteorology, October 16-19, 1984, Portland, Oregon.

Orgill, M. M., C. D. Whiteman, L. J. Fritschen, and J. R. Simpson. 1985. "Surface Energy Budget in a Valley." Paper presented at the Annual Meeting of the American Association for the Advancement of Science, Pacific Division, June 9-14, 1985, Missoula, Montana.

Orgill, M. M., C. D. Whiteman, K. J. Allwine, R. N. Lee, J. M. Thorp, and R. I. Schreck. 1986. "The Role of Local Winds and Thermal Stability in Transport and Diffusion Within a Narrow Valley." Accepted for presentation at Clean Air Society of Australia and New Zealand's 7th World Clean Air Congress, August 25-29, 1986, Sydney, Australia.

Simpson, J. R., L. J. Fritschen, C. D. Whiteman, and M. M. Orgill. 1985. "Energy Balance in a Deep Colorado Valley: ASCOT 84." Paper presented at the 17th Conference on Agriculture and Forest Meteorology, May 21-24, 1985, Scottsdale, Arizona.

Slinn, W. G. N., and M. T. Dana. 1985. "Statistical Analyses of Seven Years of MAP3S Network Data: Spatial Variability of Species Ratios and Deposition Episodes." Paper presented at the International Conference on Acidic Precipitation, September 15-20, 1985, Muskoka, Ontario, Canada.

Thorp, J. M., and M. M. Orgill. 1985. "Cascading Airflow in a Canyon." Paper presented at the Annual Meeting of the American Association for the Advancement of Science, Pacific Division, June 9-14, 1985, Missoula, Montana.

Whiteman, C. D. 1985. "Mountain Meteorolgy Studies in a Deep Colorado Valley - The U.S. ASCOT Program 1982 and 1984." Paper presented at the Zurich ETH Seminar, April 22, 1985, Zurich, Switzerland.

Whiteman, C. D. 1985. "Mountain Meteorology Studies in a Deep Colorado Valley - The U.S. ASCOT Program 1982 and 1984." Paper presented at a University of Munich Seminar, June 13, 1985, University of Munich, Munich, West Germany.

Whiteman, C. D. 1985. "Tracer Experiments and Atmospheric Mass Budget Calculations in a Deep Colorado Valley." Paper presented at the Darmstadt/Frankfurt A. M./Mainz Colloquium, June 20, 1985, University of Darmstadt, Darmstadt, West Germany.

Whiteman, C. D. 1985. "Studies of the Meteorology of a Deep Colorado Valley - The U.S. ASCOT Experiments of 1982 and 1984." Paper presented at a seminar at the Zurich ETH Meteorological Institute, July 4, 1985, Zurich, Switzerland.

Whiteman, C. D., L. J. Fritschen, J. R. Simpson, and M. M. Orgill. 1985. "Radiation Balance in a Deep Colorado Valley: ASCOT 84." Paper presented at the 17th Conference on Agricultural and Forest Meteorology, May 21-24, 1985, Scottsdale, Arizona.

Author Index

AUTHOR INDEX

Allwine, K. J.; 7

Barchet, W. R ; 24
Busness, K. M.; 37, 44

Daly, D. S.; 37, 54
Dana, M. T.; 37, 44, 54, 64
Davis, W.E.; 37, 44
Doran, J. C.; 13, 15

Easter, R. C. ; 37, 64

Hadlock, R. W.; 37
Horst, T. W.; 11, 13

Lee, R. N.; 37
Leslie, A.C.D.; 37, 54
Luecken, D. J.; 37
Lindsey, C. G.; 37, 54

Orgill, M. M.; 3, 7

Powell, D. C.; 37

Schreck, R. I.; 7
Sehmel, G. A.; 19, 30
Slinn, W. G. N.; 37, 44, 54

Thorp, J. M.; 3, 37, 44

Whiteman, C. D.; 7, 9

Organization Chart Distribution

Environment, Health and Safety Research

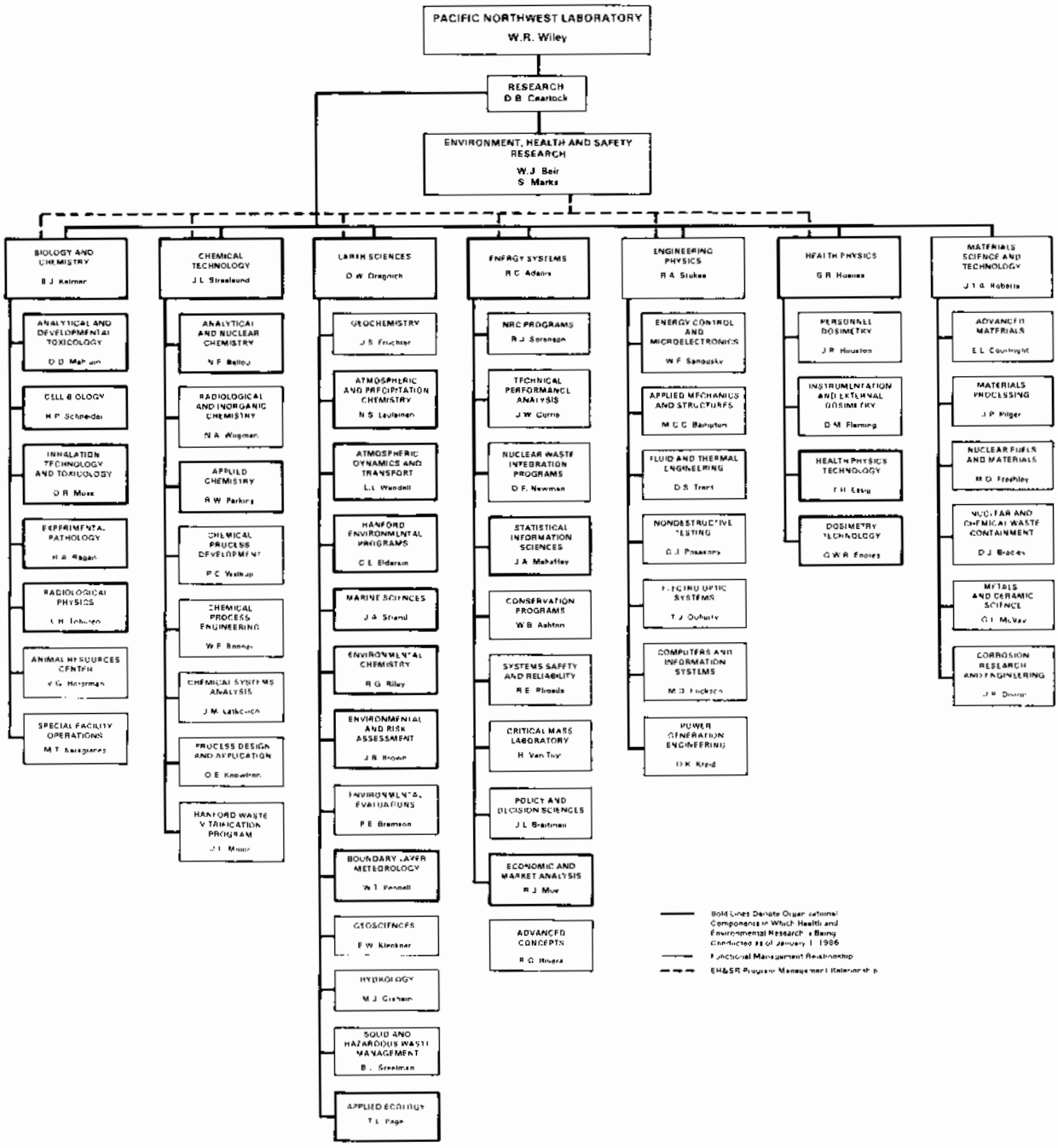

DISTRIBUTION

PNL-5750 PT3
UC-11

No. of Copies

OFFSITE

30 DOE Technical Information Center

G. E. Adams
Director
Medical Research Council
Radiobiology Unit
Harwell, Didcot
Oxon OX11 ORD
ENGLAND

W. R. Albers
EH-12, GTN
Department of Energy
Washington, DC 20545

R. Alexander
ORPBR, NL
Nuclear Regulatory Commission
Washington, DC 20545

E. L. Alpen
Donner Laboratory
University of California
Berkeley, CA 94720

T. W. Ambrose, Vice President
Multicomponent Operations
Battelle Memorial Institute
505 King Avenue
Columbus, OH 43201

M. Anderson
Library
Department of National Health & Welfare
Ottawa, Ontario
CANADA

J. A. Auxier
Applied Science Laboratory
1550 Bear Creek Road
Box 549
Oak Ridge, TN 37831

No. of Copies

R. E. Baker
Directorate of Regulatory Standards
Nuclear Regulatory Commission
Washington, DC 20555

D. S. Ballantine
ER-74, GTN
Department of Energy
Washington, DC 20545

R. W. Barber
EH-131, GTN
Department of Energy
Washington, DC 20545

A. D. Barker
Battelle, Columbus Laboratories
505 King Avenue
Columbus, OH 43201

J. R. Barker
Office of Environmental Audit and Compliance
Department of Energy
Washington, DC 20545

N. F. Barr
ER-73, GTN
Department of Energy
Washington, DC 20545

S. Barr
Environmental Studies Group
MS-D466
Los Alamos National Laboratory
P.O. Box 1663
Los Alamos, NM 87544

J. K. Basson
Raad Op Atomic
Atoomkrag Energy Board
Privaatsk X 256
Pretoria 0001
REPUBLIC OF SOUTH AFRICA

No. of Copies

E. W. Bean
Rocky Flats Area Office
Albuquerque Operations Office
Department of Energy
P.O. Box 928
Golden, CO 80401

Mrs. A. M. Beau, Librarian
Commissariat à l'Energie Atomique
Departement de Protection Sanitaire
BP 6, F-92260
Fonteney Aux Roses
FRANCE

D. Beirman
Document Service Branch
Central Intelligence Agency
Attn: CRS/DPSD/DSB/IAS/409779/DB
Washington, DC 20505

D. J. Beninson
Gerencia de Proteccion Radiologica y Seguridad
Comision Nacional de Energia Atomica
Avenida del Libertador 8250
1429 Buenos Aires
ARGENTINA

J. A. Bibb
DOE - Oak Ridge Operations Office
P.O. Box E
Oak Ridge, TN 38730

L. C. Brazley, Jr.
NE-22, GTN
Department of Energy
Washington, DC 20545

No. of Copies

A. Brink
SASOL-One Limited
P.O. Box 1
Sasolburg 9570
REPUBLIC OF SOUTH AFRICA

P. Buhl
FE-34, GTN
Department of Energy
Washington, DC 20545

G. Burley
Environmental Protection Agency
Washington, DC 20460

W. W. Burr
Oak Ridge Associated Universities
P.O. Box E
Oak Ridge, TN 37830

N. Busch
Risø National Laboratory
DK-4000 Roskilde
DENMARK

L. Bustad
College of Veterinary Medicine
Washington State University
Pullman, WA 99163

G. H. Clark
Australian Atomic Energy Commission
Private Mail Bag
Sutherland NSW 2232
AUSTRALIA

J. A. Coleman
NE-24, GTN
Department of Energy
Washington, DC 20545

Council on Environmental Quality
72 Jackson Place, NW
Washington, DC 20006

No. of Copies

H. T. Daw, Director
International Atomic Energy Agency
Kaerntner ring 11
A1010 Vienna 1
AUSTRIA

Wu De-Chang
Institute of Radiation Medicine
11# Tai Ping Rd.
Beijing CHINA

C. P. DeLisi
Department of Energy
ER-70, GTN
Germantown, MD 20545

Li De-ping
Professor and Director of North China Institute of Radiation Protection, NMI
Tai-yuan, Shan-xi
THE PEOPLE'S REPUBLIC OF CHINA

Director
Commissariat à l'Energie Atomique
Centre d'Études Nucléaires
Fontenay-aux-Roses (Seine)
FRANCE

Director
Commonwealth Scientific and Industrial Research Organization
Aspendal, Victoria
AUSTRALIA

Director
Laboratorio di Radiobiologia Animale
Centro di Studi Nucleari Della Casaccia
Comitate Nazionale per l'Energia Nucleare
Casella Postale 2400
00100 Roma
ITALY

No. of Copies

D. Djuric
Institute of Occupational and Radiological Health
11000 Beograd
Deligradoka 29
YUGOSLAVIA

H. Drucker
Argonne National Laboratory
9700 South Cass Avenue
Argonne, IL 60439

A. P. Duhamel
ER-74, GTN
Department of Energy
Washington, DC 20545

H. J. Dunster
National Radiological Protection Board
Harwell, Didcot
Oxon OX11 ORQ
ENGLAND

J. L. Durham
Environmental Protection Agency
Atmospheric Sciences Research Laboratory (MD-80)
Research Triangle Park, NC 27711

W. H. Ellett
Project Director
National Academy of Sciences, JH-554
2101 Constitution Avenue, NW
Washington, DC 20418

B. M. Erickson
DOE - Schenectady Naval Reactors Office
P.O. Box 1069
Schenectady, NY 12301

S. J. Farmer
Battelle - Seattle
4000 NE 41st Street
Seattle, WA 98105

No. of Copies

L. Feinendegen, Director
Institut für Medezin
Kernsforschungsanlage
Jülich
Postfach 1913
D-5170 Jülich
FEDERAL REPUBLIC
OF GERMANY

G. J. Foley
Environmental Protection
Agency
401 M St., S.W. (RD-676)
Washington, DC 20460

P. Frenzen
Argonne National
Laboratory
Building 203
Argonne, IL 60439

G. B. Gerber
Radiobiology Department
Commission of European
Communities
Rue de la Loi
Brussels, BELGIUM

A. R. Gopal-Ayengar
c/o P. K. Dayanidhi
15-D Gulmarg,
Anushaktinagar
Bombay 400094
INDIA

G. H. Gronhovd
Grand Forks Energy
Research Center
Department of Energy
Box 8213, University
Station
Grand Forks, ND 58202

J. W. Healy
Los Alamos National
Laboratory
P.O. Box 1663
Los Alamos, NM 87545

No. of Copies

Wang Hengde
North China Institute of
Radiation Protection
P.O. Box 120
Taiyuan, Shanxi
THE PEOPLE'S REPUBLIC
OF CHINA

B. Hicks
National Oceanic
and Atmospheric
Administration
Atmospheric Turbulence
and Diffusion Division
P.O. Box E
Oak Ridge, TN 37830

International Atomic
Energy Agency
Documents Library
Attn: Mrs. Javor
Vienna 1, Kaerntnerring 11
AUSTRIA

D. Irwin
Librarian
Supervising Scientist for
the Alligator Rivers
Region
P.O. Box 387
Bondi Junction 2022
AUSTRALIA

H. Ishikawa
General Manager
Nuclear Safety Research
Association
P.O. Box 1307
Falls Church, VA 22041

K. E. Lennart Johansson
National Defense Research
Institute
FOA 45 1
S-901-82, Umea
SWEDEN

L. J. Johnson
EG&G Idaho
P.O. Box 1625
Idaho Falls, ID 83415

No. of Copies

G. Y. Jordy, Director
ER-30, GTN
Department of Energy
Washington, DC 20545

V. A. Kamath
Scientific Information
Officer
Library & Information
Service
Atomic Energy
Establishment Trombay
Apollo Pier Road
Bombay-1
INDIA

Dr. rer. nat. Hans-Joachim
Klimisch
BASF Aktiengesellschaft
Abteilung Toxikologie
D-6700 Ludwigshafen
FEDERAL REPUBLIC
OF GERMANY

F. Koomonoff
ER-12, GTN
Department of Energy
Washington, DC 20545

R. T. Kratzke
EH-131, GTN
Department of Energy
Germantown, MD 20545

L. Kristensen
Physics and Meteorology
Risø National Laboratory
DK-4000 Roskilde
DENMARK

L. Kulp
National Acid
Precipitation
Assessment Program
722 Jackson St.
Washington, DC 20006

T. Kumatori, Director
National Institute of
Radiological Sciences
9-1, 4-Chome, Anagawa
Chiba-shi, Chiba 260
JAPAN

No. of Copies

Professor D. Lal
Physical Research Laboratory
Ahmedabad 380 009
INDIA

W. Lauder
Office of Health and Environmental Research
Office of Energy Research
Department of Energy
Germantown, MD 20545

Librarian
Atomic Energy of Canada Ltd.
Whiteshell Nuclear Research Establishment
Pinawa, Manitoba ROE 1LO
CANADA

Librarian
Atomic Energy Research Establishment
Building 465
Harwell, Didcot
Oxon OX11 ORD
ENGLAND

Librarian
Australian Atomic Energy Commission
Riverina Laboratory
P.O. Box 226
Deniliquin, New South Wales
AUSTRALIA 2710

Librarian
Brookhaven National Laboratory
Research Library, Reference
Upton, Long Island, NY 11973

Librarian
Centre d'Etudes Nucléaires de Saclay
P.O. Box 2, Saclay
Fig-sur-Yvette (S&O)
FRANCE

No. of Copies

Librarian
Colorado State University
Serials Section
Ft. Collins, CO 80521

Librarian
Commonwealth Scientific and Industrial Research Organization
314 Albert Street
P.O. Box 89
East Melbourne, Victoria
AUSTRALIA

Librarian
CSIRO
Rangelands Research Centre
Private Mail Bag, P.O.,
DENILIQUIN, N.S.W. 2710
AUSTRALIA

Librarian
ENEA (OECD) Health and Safety Office
38, Blvd. Suchet
Paris
FRANCE

Librarian
HCS/EHE
World Health Organization
CH-1211 Geneva 27
SWITZERLAND

Librarian
Health Sciences Library, SB-55
University of Washington
Seattle, WA 98195

Librarian
Kernforschungzentrum Karlsruhe
Institut für Strahlenbiologie
D-75 Karlsruhe 1
Postfach 3640
FEDERAL REPUBLIC OF GERMANY

No. of Copies

Librarian
Lawrence Radiation Laboratory
University of California
Technical Information Dept., L-3
P.O. Box 808
Livermore, CA 94550

Librarian
Los Alamos National Laboratory
P.O. Box 1663
Los Alamos, NM 87545

Librarian
Max-Planck-Institut für Biophysics
Forstkasstrasse
D-6000 Frankfurt/Main
FEDERAL REPUBLIC OF GERMANY

Librarian
Ministry of Agriculture, Fisheries and Food
Fisheries Laboratory
Lowestoft, Suffolk NR33 OHT
UNITED KINGDOM

Librarian
Tri-Cities University Center
100 Sprout Road
Richland, WA 99352

Library
Risø National Laboratory
DK-4000 Roskilde
DENMARK

Library
Atomic Energy Commission of Canada, Ltd.
Whiteshell Nuclear Research Establishment
Pinawa, Manitoba
CANADA

I. R. Linger
ER-63, GTN
Department of Energy
Washington, DC 20545

No. of Copies

O. R. Lunt
Laboratory of Nuclear Medicine and Radiation Biology
University of California
900 Veteran Avenue
West Los Angeles, CA 90024

Wei Luxin
Laboratory of Industrial Hygiene
Ministry of Public Health
2 Xinkang Street
Deshangmanwai, Beijing
THE PEOPLE'S REPUBLIC OF CHINA

J. N. Maddox
ER-73, GTN
Department of Energy
Washington, DC 20545

J. R. Maher
ER-65, GTN
Department of Energy
Washington, DC 20545

C. R. Mandelbaum
ER-32, GTN
Department of Energy
Washington, DC 20545

B. Manowitz
Energy and Environment Division
Brookhaven National Laboratory
Upton, Long Island, NY 11973

A. M. Marko, Director
Atomic Energy Commission of Canada, Ltd.
Biology and Health Physics Division
Chalk River Nuclear Laboratories
P.O. Box 62
Chalk River, Ontario K0J 1J0
CANADA

No. of Copies

D. D. Mayhew
ER-63, GTN
Department of Energy
Washington, DC 20545

H. M. McCammon
ER-75, GTN
Department of Energy
Washington, DC 20545

R. O. McClellan
Inhalation Toxicology Research Institute
Lovelace Foundation for Medical Education & Research
P.O. Box 5890
Albuquerque, NM 87115

T. F. McCraw
EH-132, GTN
Department of Energy
Washington, DC 20545

C. B. Meinhold
Instrumentation and Health Physics Department
Brookhaven National Laboratory
Upton, Long Lsland, NY 11973

M. L. Mendelsohn
Biomedical and Environmental Research Program
Lawrence Livermore National Laboratory, L-523
University of California
P.O. Box 808
Livermore, CA 94550

P. Michael
Brookhaven National Laboratory
Upton, NY 11973

M. L. Minthorn, Jr.
ER-72, GTN
Department of Energy
Washington, DC 20545

No. of Copies

D. R. Monti
ER-14, GTN
Department of Energy
Washington, DC 20545

B. Morgan
Safety Division
DOE - Savannah River Operations Office
P.O. Box A
Aiken, SC 29801

H. Moses
ER-74, GTN
Department of Energy
Washington, DC 20545

W. E. Mott
EH-12, GTN
Department of Energy
Washington, DC 20545

S. M. Nealey
Battelle - Seattle
4000 NE 41st Street
Seattle, WA 98105

N. Nelson
Environmental Protection Agency
Washington, DC 20460

J. C. Nénot, Deputy Director
Departement de Protection
Centre d' Etudes Nucléaires
B.P. No. 6
F-92260 Fontenay-Aux-Roses
FRANCE

W. R. Ney, Executive Director
National Council on Radiation Protection and Measurement
7910 Woodmont Avenue
Suite 1016
Washington, DC 20014

No. of Copies

Nuclear Regulatory Commission
Advisory Committee on Reactor Safeguards
Washington, DC 20555

G. Oertel
Deputy Assistant Secretary for Safety, Health and Quality Assurance
Department of Energy
Germantown, MD 20545

D. E. Olesen
Battelle Memorial Institute
505 King Avenue
Columbus, OH 53201

J. P. Oliver
ENEA (OECD) Health and Safety Office
38, Blvd. Suchet
Paris
FRANCE

B. Ottar
Director
Norwegian Institute for Air Research
Elvegaten 52
N-2000 Lillestrom
NORWAY

R. S. Paul
Battelle, Columbus Laboratories
505 King Avenue
Columbus, OH 43201

A. A. Pitrolo
Morgantown Energy Research Center
Department of Energy
P.O. Box 880
Morgantown, WV 26505

L. Prahm
National Agency of Environmental Protection
Risø National Laboratory
DK-4000 Roskilde
DENMARK

No. of Copies

V. Prodi
Department of Physics
University of Bologna
Via Irnerio 46
I-40126 Bologna
ITALY

R. G. Rader
ER-33, GTN
Department of Energy
Washington, DC 20545

D. P. Rall, Director
NIEHS
P.O. Box 12233
Research Triangle Park, NC 27709

C. R. Richmond
Oak Ridge National Laboratory
P.O. Box X
Oak Ridge, TN 37830

C. Riordan
Environmental Protection Agency
401 M St., S.W. (RD-676)
Washington, DC 20460

J. S. Robertson
ER-73, GTD
Department of Energy
Washington, DC 20545

H. Rodhe
Meteorological Institute
Stockholm University
S-10691 Stockholm
SWEDEN

Wang Ruifa, Associate Director
Laboratory of Industrial Hygiene
Ministry of Public Health
2 Xinkang Street
Deshangmanwai, Beijing
THE PEOPLE'S REPUBLIC OF CHINA

No. of Copies

J. M. Rusin
Battelle - Seattle
4000 NE 41st Street
Seattle, WA 98115

M. Rzekiecki
Commissariat à l'Energie Atomique
Centre d'Etudes Nucléaires de Cadarache
BP No. 13-St. Paul
Les Durance
FRANCE

R. A. Scarano
Nuclear Regulatory Commission
Mill Licensing Section
Washington, DC 20545

F. A. Schiermeier
Environmental Protection Agency
Atmospheric Sciences Research Laboratory (MD-80)
Research Triangle Park, NC 2771

M. Schulman
ER-70, GTN
Department of Energy
Washington, DC 20545

R. Setlow
Brookhaven National Laboratory
Upton, NY 11973

R. Shikiar
Battelle - Seattle
4000 NE 41st Street
Seattle, WA 98105

Sun Shi-quan, Head
Radiation-Medicine Department
North China Institute of Radiation Protection
Taiyuan, Shanxi
THE PEOPLE'S REPUBLIC OF CHINA

No. of Copies

Cao Shu-yuan, Deputy Head
Laboratory of Radiation Medicine
North China Institute of Radiation Protection
Taiyuan, Shanxi
THE PEOPLE'S REPUBLIC OF CHINA

W. K. Sinclair, President
NCRP
7910 Woodmont Avenue
Suite 1016
Bethesda, MD 20814

R. Skarin, Chief Librarian
Meteorological Institute
University of Stockholm
Arrhenius Laboratory
S106 91 Stockholm
SWEDEN

D. H. Slade
ER-74, GTN
Department of Energy
Washington, DC 20545

H. Smith, Head
Biology Department
National Radiological Protection Board
Chilton, Didcot
Oxon OX11 ORQ
ENGLAND

J. Snow
ER-6, FORS
Department of Energy
Washington, DC 20585

J. H. Spickard
DOE - Idaho Operations Commission
550 Second Street
Idaho Falls, ID 83401

R. J. Stern
EH-10, FORS
Department of Energy
Washington, DC 20585

No. of Copies

J. F. Stevens
Dayton Area Office
DOE - Albuquerque Operations Office
P.O. Box 66
Miamisburg, OH 45342

S. Stryker
Battelle, Washington Operations
2030 M Street, NW
Washington, DC 20036

F. Swanberg
Nuclear Regulatory Commission
Washington, DC 20545

J. Swinebroad
EH-12, GTN
Department of Energy
Washington, DC 20545

Technical Information Service
Savannah River Laboratory
Room 773A
E. I. duPont de Nemours & Company
Aiken, SC 29801

J. W. Thiessen
ER-71, GTN
Department of Energy
Washington, DC 20545

R. G. Thomas
ER-72, GTN
Department of Energy
Washington, DC 20545

M. Thorne
International Commission on Radiological Protection
Clifton Avenue
Sutton, Surrey
ENGLAND

C. Tiller
RG-30, FORS
Department of Energy
Washington, DC 20585

No. of Copies

A. W. Trivelpiece, Director
ER-1, FORS
Department of Energy
Washington, DC 20585

United Nations Scientific Committee on the Effects of Atomic Radiation
Vienna International Center
P.O. Box 500
A-1400 Vienna
AUSTRIA

U.S. Department of Energy
Environment, Safety and Health Division
P.O. Box 5400
Albuquerque, NM 87115

E. J. Vallario
PE-222, GTN
Department of Energy
Washington, DC 20545

C. R. Vest
Battelle Memorial Institute
Washington Operations
2030 M Street, NW
Washington, DC 20036

G. L. Voelz
Los Alamos National Laboratory
P.O. Box 1663
Los Alamos, NM 87545

H. L. Volchok
Environmental Measurements Laboratory
Department of Energy
375 Hudson Street
New York, NY 10014

B. W. Wachholz
Low Level Radiation Effects Branch
National Cancer Institute
Landow Bldg., Room 8C09
Rockville Pike
Bethesda, MD 20205

No. of Copies

M. L. Walker
EH-1, FORS
Department of Energy
Washington, DC 20585

M. E. Walsh
Battelle - Seattle
4000 NE 41st Street
Seattle, WA 98105

Yibing Wang
North China Institute
of Radiation Protection
P.O. Box 120
Taiyuan, Shanxi
THE PEOPLE'S REPUBLIC
OF CHINA

R. Watters
Los Alamos National
Laboratory
P.O. Box 5400
Albuquerque, NM 87115

R. L. Watters
ER-75, GTN
Department of Energy
Washington, DC 20545

C. G. Welty, Jr.
EH-123, GTN
Department of Energy
Washington, DC 20545

I. Wender
Dept. of Chemical
Engineering
1249 Benedum Hall
University of Pittsburgh
Pittsburgh, PA 15261

M. L. Wesely
Argonne National
Laboratory
Building 181, ER
Argonne, IL 60439

No. of Copies

W. W. Weyzen
Electric Power Research
Institute
3412 Hillview Avenue
Palo Alto, CA 92665

M. M. Williamson
DOE - Idaho Operations
Commission
550 Second Street
Idaho Falls, ID 83401

B. C. Winkler, Director
Licensing
Raad Op Atoomkrag
Privaatsk X 256
Pretoria 0001
REPUBLIC OF SOUTH AFRICA

M. T. Wood
Battelle - Seattle
4000 NE 41st Street
Seattle, WA 98105

R. W. Wood
ER-74, GTN
Department of Energy
Washington, DC 20545

Chen Xing-an, M.D.
Laboratory of Industrial
Hygiene
Ministry of Public Health
2 Xinkang Street
Deshangmanwai, Beijing
THE PEOPLE'S REPUBLIC
OF CHINA

Deng Zhicheng
North China Institute of
Radiation Protection
Taiyuan, Shanxi
THE PEOPLE'S REPUBLIC
OF CHINA

Z. Zhixian
Laboratory for Energy-
Related Health Research
University of California
Davis, CA 95616

No. of Copies

ONSITE

6 DOE Richland Operations Office

K. R. Absher
P. K. Clark
D. R. Elle
J. L. Rhoades
A. J. Rizzo
J. J. Sutey

Joint Center for Graduate Study

Director

2 Hanford Environmental Health

B. D. Breitenstein
R. D. Gilmore

Westinghouse Hanford Co.

R. O. Budd

137 Pacific Northwest Laboratory

O. B. Abbey
K. J. Allwine
R. W. Baalman (5)
J. F. Bagley
W. J. Bair (15)
W. R. Barchet
K. M. Busness
D. B. Cearlock
T. D. Chikalla
D. S. Daly
M. T. Dana
J. M. Davidson
W. E. Davis
G. W. Dennis
D. W. Dragnich
R. C. Easter
C. E. Elderkin (20)
R. M. Fleischman
J. J. Fuquay

No. of Copies		No. of Copies		No. of Copies	
	W. A. Glass		J. A. Mahaffey		D. S. Sharp
	D. W. Glover		S. Marks		C. L. Simpson
	R. H. Gray		R. P. Marshall		W. G. N. Slinn
	J. L. Gregory		L. N. McKenney		G. M. Stokes
	R. K. Hadlock		A. H. Miller		J. A. Stottlemyre
	J. M. Hales (5)		J. M. Nielsen		D. L. Strenge
	R. V. Hannigan		M. M. Orgill		J. M. Thorp
	L. C. Harrison		E. L. Owczarski		L. H. Toburen
	P. C. Hays		J. F. Park		B. E. Vaughan
	D. J. Hoitink		W. T. Pennell (5)		L. L. Wendell (5)
	T. W. Horst		R. W. Perkins		E. L. Wierman
	B. J. Kelman		A. M. Platt		R. E. Wildung
	N. S. Laulainen (5)		P. M. Potter		W. R. Wiley
	G. L. Laws		D. C. Powell		L. D. Williams
	R. N. Lee		D. S. Renne		R. K. Woodruff
	A. C. Leslie		W. D. Richmond		B. W. Wright
	R. C. Liikala		G. F. Schiefelbein		Life Sciences Library (2)
	C. G. Lindsey		L. C. Schmid		Publishing Coordination (2)
	F. D. Lloyd		R. I. Schreck		Technical Information (5)
	D. G. Luecken		G. A. Sehmel		

*GPO 692-959 (1986)